

WestminsterResearch

<http://www.westminster.ac.uk/westminsterresearch>

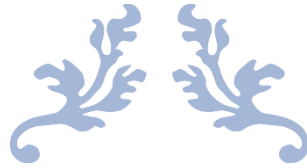
**The Effects of Quorum Sensing Molecules on Streptococcus
mutans Biofilm
Garner, Camille**

This is a PhD thesis awarded by the University of Westminster.

© Miss Camille Garner, 2022.

<https://doi.org/10.34737/vz7z6>

The WestminsterResearch online digital archive at the University of Westminster aims to make the research output of the University available to a wider audience. Copyright and Moral Rights remain with the authors and/or copyright owners.



The Effects of Quorum Sensing Molecules on *Streptococcus mutans* Biofilm

Elizabeth Camille Garner



May 9, 2022

A thesis submitted in the partial fulfilment of the requirements of the University of
Westminster for the degree of
Doctor of Philosophy.

Abstract

The use of quorum quenching (QQ) molecules to prevent biofilm formation has recently gained momentum. Interrupting the quorum sensing (QS) pathways of cariogenic bacteria like *Streptococcus mutans* could reduce the formation of dental plaque on teeth, lowering the incidences of caries and periodontitis.

This research studied the effects of three QQ molecules (p-coumaric acid, tyrosol, and farnesol) on *S. mutans* biofilm formation on biotic and abiotic surfaces. This research specifically studied the changes in eDNA, protein, carbohydrate, and viable cells in the extracellular matrix (ECM) of the biofilm. The gene expression of *gtfb* was studied to determine if the QQ molecules played a role in gene expression.

All three QQ molecules showed reduction on different components of the *S. mutans* biofilm. Tyrosol reduced the greatest amount of overall biomass when the biofilm was formed on examples of both biotic and abiotic surfaces. Tyrosol also had the highest reduction of proteins in biofilms formed on plastic and the total number of viable cells in biofilms formed on 20% porosity hydroxyapatite (HA) disks. p-Coumaric acid reduced the most eDNA and the number of viable cells in the biofilm when it was formed on plastic. p-Coumaric acid also decreased the eDNA and carbohydrate concentrations the most in biofilms formed on 20% porosity HA disks. Additionally, p-coumaric acid reduced the number of viable cells in the biofilm formed on full density HA disks. Farnesol decreased the most carbohydrates concentration on both plastic and full density HA disks. Farnesol decreased the most eDNA on full density HA disks. Farnesol was the only QQ molecule to lower the gene expression of *gtfb* in the biofilm.

All three QQ molecules decreased some individual components of the *S. mutans* biofilm, but tyrosol was the overall best QQ molecule for total lessening of biomass and components of the ECM.

Table of Contents

ABSTRACT.....	I
LIST OF FIGURES	VI
LIST OF TABLES	VIII
LIST OF ABBREVIATIONS	IX
ACKNOWLEDGMENTS.....	XII
AUTHOR’S DECLARATION.....	XIII
CHAPTER 1 INTRODUCTION	1
1.0 General Introduction	1
1.1 Significance of Bacterial Biofilms.....	2
1.2 Biofilm Formation.....	4
1.3 Introduction to Quorum Sensing.....	6
1.3.1 Quorum Sensing in Gram-negative Bacteria.....	9
1.3.2 Quorum Sensing in Gram-positive Bacteria.....	10
1.3.3 The Universal Quorum Sensing Pathway in Bacteria.....	12
1.4 Quorum Quenching	12
1.5 Extracellular Matrix and EPS Components.....	13
1.5.1 Extracellular polysaccharides.....	15
1.5.2 Extracellular Proteins.....	17
1.5.3 Extracellular DNA.....	18
1.5.4 Cells Within a Biofilm	19
1.6 Traditional Methods of Prevention and Eradication of Bacterial Biofilms	20
1.7 The Oral Cavity	21
1.8 Periodontium.....	25

1.9 Biofilm Formation in the Oral Cavity	26
1.10 <i>Streptococcus mutans</i>	31
1.11 Glucosyltransferases.....	35
1.12 Mechanisms of Dispersal for Prevention of Oral Biofilm Formation	37
1.13 Aim and Objectives.....	41
1.14 Contribution to Knowledge	42
CHAPTER 2 MATERIALS AND METHODS	43
2.0 Materials.....	43
2.1 Bacterial Strain	43
2.2 Cell Culture	43
2.3 Maintenance and Growth conditions of Bacterial and Cell Culture	44
2.3.1 Media Preparation for Bacterial Culture	44
2.3.2 Long Term Storage of <i>S. mutans</i> 25175	45
2.3.3 Media preparation for Cell Culture.....	46
2.3.4 Long Term Storage of HGF-1 cell line	47
2.4 Cell Culture Reagents	47
2.5 Quorum Quenching Molecule Stock Preparation	48
2.5.1 p-Coumaric Acid.....	49
2.5.2 Tyrosol	49
2.5.3 Farnesol	49
2.6 Methods for Microbiology Assays	50
2.6.1 Bacterial Inoculum	50
2.6.2 <i>S. mutans</i> 25175 Biofilm formation on various Surfaces.....	50
2.6.2.1 Bacterial Biofilm formation in 96-Well Plates.....	50
2.6.2.2 Bacterial Biofilm Formation in Test Tubes	51
2.6.2.3 Bacterial Biofilm Formation on HA Disks	51
2.6.3 Determining the MIC of the QQ molecules	52
2.6.4 Growth curve	53
2.6.5 Analysis of components of the extracellular matrix of <i>S. mutans</i> 25175 biofilm	53
2.6.6 Colony Forming Unit (CFU) method for cell viability	53
2.6.7 Qubit® dsDNA broad spectrum assay method for eDNA quantification	54
2.6.8 Phenol-sulfuric acid method for carbohydrate analysis	55
2.6.9 Bradford Assay for protein quantification	56
2.6.10 Crystal Violet Assay	57

2.7 Methods for Cell culture and co-culture assays.....	57
2.7.1 HGF-1 Cell Culture Methods.....	57
2.7.2 Passaging HGF-1 Cells.....	58
2.7.3 Seeding Cells in 96 and 12-well Plates.....	59
2.7.4 Treating HGF-1 Cells with QQ molecules.....	59
2.7.5 HGF-1 Cellular viability: 3-(4,5-Dimethylthiazol-2-yl)-2,5-diphenyltetrazolium bromide (MTT) Assay.....	60
2.7.6 Co-culture of <i>S. mutans</i> 25175 and HGF-1 Adherence assay.....	60
2.7.7 Co-culture of <i>S. mutans</i> 25175 and HGF-1 cell line biofilm assay.....	61
2.8 Molecular Biology Methods for RT-qPCR.....	62
2.8.1 Primers.....	62
2.8.2 RNA Extraction.....	63
2.8.3 Reverse Transcription.....	64
2.8.4 RT- qPCR Protocol.....	66
2.9 Statistical Analysis.....	67
CHAPTER 3 RESULTS.....	68
3.0 Introduction to the Results.....	68
3.1 Results Section 1: Microbiological Profile of <i>S. mutans</i> 25175 Biofilm.....	70
3.1.1 Introduction to Section 1 Results.....	70
3.1.2 <i>S. mutans</i> 25175 Growth Curve and Doubling Time.....	71
3.1.3 Optimisation of Sugar and Air for <i>S. mutans</i> 25175 Biofilm Formation.....	73
3.1.4 Minimum Inhibitory Concentration of QQ molecules on <i>S. mutans</i> 25175 Biofilm.....	75
3.1.5 Quantification of Total <i>S. mutans</i> 25175 Biofilm Biomass.....	76
3.1.6 CFU of Cells in the EPS of <i>S. mutans</i> 25175 Biofilm.....	78
3.1.7 Carbohydrates Quantification of the EPS of <i>S. mutans</i> 25175 Biofilm.....	80
3.1.8 eDNA Quantification of the EPS of <i>S. mutans</i> 25175 Biofilm.....	81
3.1.9 Protein Quantification of the EPS of <i>S. mutans</i> 25175 Biofilm.....	82
3.1.10 mRNA Expression of Glucosyltransferase B (<i>gtfb</i>) in <i>S. mutans</i> 25175.....	83
3.1.11 Section 1 Summary.....	86
3.2 Results Section 2: Study of <i>S. mutans</i> 25175 Biofilm Treated with QQ Molecules Formed on Full Density and 20% Porosity HA Disks.....	89
3.2.1 Introduction to Section 2 Results.....	89
3.2.2 CFU Enumeration in <i>S. mutans</i> 25175 Biofilm Formed on HA Disks.....	91
3.2.3 Carbohydrate Quantification of <i>S. mutans</i> 25175 Biofilm Formed on HA Disks.....	94
3.2.4 eDNA Quantification of <i>S. mutans</i> 25175 Biofilm Formed on HA Disks.....	97
3.2.5 Protein Quantification of <i>S. mutans</i> 25175 Biofilm Formed on HA Disks.....	100
3.2.6 Summary of Section 2 Results.....	104
3.3 Section 3 Cell Culture Results.....	108
3.3.1 Introduction to Section 3 Results.....	108
3.3.2 HGF-1 Cellular Viability Assay Results.....	109

3.3.3 <i>S. mutans</i> 25175 Cellular Adherence to HGF-1 Cell Line	112
3.3.4 Quantification of <i>S. mutans</i> 25175 Biofilm Formation on HGF-1 Cell Line	114
3.3.5 Summary of Section 3 Results	117
CHAPTER 4 DISCUSSION.....	89
CHAPTER 5 CONCLUSION.....	89
CHAPTER 6 FUTURE WORK	145
CHAPTER 7 REFERENCES.....	148
APPENDIX.....	167

List of Figures

FIGURE 1.1 BACTERIAL BIOFILM FORMATION.....	6
FIGURE 1.2 EXAMPLES OF QUORUM SENSING MOLECULES FROM GRAM-NEGATIVE AND GRAM-POSITIVE BACTERIA	8
FIGURE 1.3 AHL MODEL OF GRAM-NEGATIVE QUORUM SENSING	10
FIGURE 1.4 GRAM-POSITIVE QUORUM SENSING MODEL	11
Figure 1.5 Biofilm Formation and Components	15
FIGURE 1.6 THE ANATOMY OF THE ORAL CAVITY	222
FIGURE 1.7 THE ANATOMY OF THE SALIVARY GLANDS.....	233
FIGURE 1.8 THE STRUCTURE OF THE TOOTH AND PERIODONTIUM.....	255
FIGURE 1.9 THE LAYERS IN WHICH ORAL BIOFILMS EVOLVE ON THE SURFACE OF THE TOOTH	288
FIGURE 1.10 FACTORS INVOLVED IN DENTAL BIOFILM FORMATION.....	311
FIGURE 1.11 <i>STREPTOCOCCUS MUTANS</i>	322
FIGURE 1.12 CSP AND COMD/COME PATHWAY	34
Figure 1.13 Crystal Structure of Gtf.....	36
FIGURE 3.1 <i>S. MUTANS</i> 25175 GROWTH.....	72
FIGURE 3.2 <i>S. MUTANS</i> 25175 BIOFILM FORMATION AEROBIC VERSES ANAEROBIC.....	74
FIGURE 3.3 EFFECTS OF QQ MOLECULES ON <i>S. MUTANS</i> 25175 BIOFILM.....	77
FIGURE 3.4 LOG CFU/ML OF <i>S. MUTANS</i> 25175 CELLS FROM BIOFILM TREATED WITH QQ MOLECULES	79
FIGURE 3.5 CARBOHYDRATES (MG/L) OF <i>S. MUTANS</i> 25175 BIOFILM TREATED WITH QQ MOLECULES:	80
FIGURE 3.6 eDNA (μ G/ML) OF <i>S. MUTANS</i> 25175 BIOFILM TREATED WITH QQ MOLECULES:	81
FIGURE 3.7 PROTEIN (MG/ML) OF <i>S. MUTANS</i> 25175 BIOFILM TREATED WITH QQ MOLECULES	83
FIGURE 3.8 mRNA EXPRESSION OF <i>GTFB</i> IN <i>S. MUTANS</i> 25175 BIOFILM	86
FIGURE 3.9 THE LOG CFU/ML OF <i>S. MUTANS</i> 25175 CELLS IN BIOFILM	92

FIGURE 3.10 THE LOG CFU/ML OF <i>S. MUTANS</i> 25175 CELLS IN	93
FIGURE 3.11 THE LOG CFU/ML OF <i>S. MUTANS</i> 25175 CELLS IN BIOFILM	94
FIGURE 3.12 THE CARBOHYDRATE CONCENTRATION (MG/L) OF <i>S. MUTANS</i> 25175 BIOFILM	95
FIGURE 3.13 THE CARBOHYDRATE CONCENTRATION (MG/L) OF <i>S. MUTANS</i> 25175 BIOFILM	96
FIGURE 3.14 THE CARBOHYDRATE CONCENTRATION (MG/L) OF <i>S. MUTANS</i> 25175 BIOFILM	97
FIGURE 3.15 THE EDNA (μ G/ML) OF <i>S. MUTANS</i> 25175 BIOFILM	98
FIGURE 3.16 THE EDNA (μ G/ML) OF <i>S. MUTANS</i> 25175 BIOFILM	99
FIGURE 3.17 THE EDNA (μ G/ML) OF <i>S. MUTANS</i> 25175 BIOFILM	100
FIGURE 3.18 THE PROTEIN CONCENTRATION (MG/ML) OF <i>S. MUTANS</i> 25175 BIOFILM....	101
FIGURE 3.19 THE PROTEIN CONCENTRATION (MG/ML) OF <i>S. MUTANS</i> 25175 BIOFILM....	102
FIGURE 3.20 THE PROTEIN CONCENTRATION (MG/ML) OF <i>S. MUTANS</i> 25175 BIOFILM....	103
FIGURE 3.21 HGF-1 CELL VIABILITY AFTER QQ MOLECULE TREATMENTS	111
FIGURE 3.22 LOG CFU/ML OF <i>S. MUTANS</i> 25175 ATTACHMENT TO HGF-1 CELL LINE TREATED WITH QQ MOLECULES	114
FIGURE 3.23 <i>S. MUTANS</i> 25175 BIOFILM FORMATION ON HGF-1 CELL LINE	116

List of Tables

TABLE 2.1 BACTERIAL CULTURE MEDIA AND DESCRIPTION/COMPOSITION USED FOR <i>S. MUTANS</i> 25175 GROWTH AND MAINTENANCE.....	44
TABLE 2.2 CELL CULTURE MEDIA AND COMPOSITION/DESCRIPTION USED FOR HGF-1 CELL CULTURE.....	46
TABLE 2.3 CELL CULTURE REAGENTS AND THE SUPPLIERS USED FOR CELL CULTURE.....	48
TABLE 2.4 QQ MOLECULES, SOLVENTS, AND STOCK CONCENTRATIONS	48
TABLE 2.5 PRIMER SEQUENCES FOR <i>GTFB</i> , <i>GTFC</i> , AND <i>SM16S</i> USED FOR RT-QPCR.....	62
TABLE 2.6 DNA ELIMINATION REACTION COMPONENTS, VOLUMES, AND FINAL CONCENTRATION	64
TABLE 2.7 REVERSE TRANSCRIPTION MASTER MIX REACTION FOR 20 μ L FINAL WORKING VOLUME.....	65
TABLE 2.8 RT-QPCR REACTION MIXTURES.....	66
TABLE 3.1 THE GENERATION TIME (IN MINUTES), INITIAL CELL COUNT (CFU/ML), FINAL CELL COUNT (CFU/ML), AND THE TIME (IN HOURS) OF <i>S. MUTANS</i> 25175.....	73
TABLE 3.2 MIC OF QQ MOLECULES ON <i>S. MUTANS</i> 25175 BIOFILM FORMATION.....	76
TABLE 3.3 SUMMARY OF SECTION 1 RESULTS.....	87
TABLE 3.4 SUMMARY OF SECTION 2 RESULTS FOR 20% POROSITY HA DISKS.....	106
TABLE 3.5 SUMMARY OF SECTION 2 RESULTS FOR FULL DENSITY HA DISKS	107
TABLE 3.6 SECTION 3 SUMMARY OF RESULTS.....	119

List of Abbreviations

- μ – Micro
- μg – Microgram
- μL – Microlitres
- AHL – Acyl-homoserine lactones
- AI – Auto inducers
- AI-2 – Auto-inducer 2
- AIP – Autoinducing peptide
- AIP-1 – Autoinducing peptide 1
- ANOVA – Analysis of variance
- ATCC – American Type Culture Collection
- BSA – Bovine serum albumin
- BHI – Brain heart infusion
- BR – Broad range
- C – Celsius
- cDNA – Complimentary DNA
- CFU – Colony forming units
- cm – Centimetre
- CO₂ – Carbon dioxide
- CPS – Competence stimulating peptide
- CV – Crystal violet
- DMEM – Dulbecco's Modified Eagle's Medium
- DMSO – Dimethyl sulfoxide
- DNA – Deoxyribonucleic acid
- DPBS – Dulbecco's Phosphate Buffered Saline

dsDNA – Double stranded DNA

ECM – Extracellular matrix

eDNA – Extracellular DNA

EDTA – Ethylenediamine tetraacetic acid

EPS – Extracellular polymeric substances

FBS – Foetal bovine serum

g – Grams

gDNA – Genomic DNA

Gtf – Glucosyltransferase

HA – Hydroxyapatite

HGF-1 – Human gingival fibroblasts

IE – Infective endocarditis

L – Litre

M – Molar

MIC – Minimum inhibitory concentration

mL – Millilitre

mM – Millimolar

mol – Mole

mRNA – Messenger RNA

MTT – 3-(4,5-dimethylthiazol-2-yl)-2,5-diphenyl-2H-tetrazolium bromide

n – Total number

ng – Nanograms

NIH – National Institutes of Health

nm – Nanometre

OD – Optical density

p – P-value

PBS – Phosphate buffered saline

PDLs – Population doublings

Pen-strep – Penicillin-Streptomycin

pg – Picogram

QQ – Quorum quenching

QS – Quorum sensing

QSI – Quorum sensing inhibitor

® – Registered

RNA – Ribonucleic acid

rpm – Revolutions per minute

RT – Real time

RT-qPCR – Quantitative reverse transcription polymerase chain reaction

SAM – S-adenosylmethionine

™ – Trademark

U.K. – United Kingdom

U.S.A. – United States of America

v/v – Volume per volume

vs. – Versus

WIG – Water-insoluble glucans

WSG – Water-soluble glucans

X – times

Acknowledgments

It has been said that it takes a village to raise a child. I believe that the same can be said regarding the completion a PhD. Although I have put all my personal effort into this piece of work, it would have not been possible without the support and encouragement from the village that surrounds me.

I would like to express my gratitude for my Director of Studies, Taj, for the endless fountain of knowledge, suggestions, opinions, guidance, and direction that he so graciously offered me throughout my research.

I would also like to thank my two secondary supervisors: Amara and Godfrey. I recognise how lucky I am to have not one, but two secondary supervisors who are experts in their respective fields who have enriched my scientific curiosity and this thesis beyond what I could ever imagine.

This research would have not been possible without the amazing team of technical staff at the university. I would especially like to extend a gracious thank you to Umar, Vanita, Burak, and Kim.

I would like to thank all my colleagues for creating a positive and enjoyable learning environment in both the labs and the office. A special thanks to Nicola, Rhys, Leah, Calam, Kyle, Lucy, and Kurtis for their selfless advice and lending a helping hand throughout the years.

I would especially like to express my gratitude for my lab colleagues: Rachith, Ghazal, Zeynab, and Azita for the unconditional support, inspiration, and compassion whilst conducting research. You all made the lab a fun and exciting place and I will cherish all the memories as well as the well-earned *coffee* breaks.

I want to thank my parents for their limitless love and support.

Lastly, I want to thank my life-long, childhood friend Dr. Hunter Isbell. Your optimism, selflessness, and kindness encourage me to be a better person every day.

Author's Declaration

I declare that all the material contained in this thesis is my own work.

Chapter 1 Introduction

1.0 General Introduction

From the salty shores of the Dead Sea to the acidic insides of the gastrointestinal tract, from subzero temperatures in the Antarctic to scorching hot hydrothermal vents deep in the oceans, bacteria can be found in extreme habitats across the planet (di Lorenzo et al., 2020). Bacteria are microscopic, single cell organisms living in both biotic and abiotic settings in a variety of ecosystems, terrestrial as well as aquatic. Bacteria have been found in geysers, hot springs, hydrothermal vents, soil, in and on the human body, and just about every place imaginable where they often overcome difficult living conditions and thrive (Giordano, 2020). Bacteria were first described by the inventor of the microscope, Anton Von Leeuwenhoek in the 17th century. The Dutch scientist is universally known as the father of microbiology and is credited for discovering both bacteria and protists (Lane, 2015). Leeuwenhoek described his findings of 'animalcules' in a paper published in Philosophical Transactions in 1677. The famous paper 'letter on the protozoa' detailed the first description of protists and bacteria living in an assortment of environments (Lane, 2015). Bacteria are the most common and numerous living organisms on the planet. Some scientists have estimated that there are 5 million trillion trillion bacteria inhabiting the Earth (Whitman et al., 1998). Bacteria flourish and surmount obstacles largely by living in protective structures called biofilms.

Although Leeuwenhoek used his single lensed microscope to observe microscopic aggregates on samples of plaque he scraped from his teeth, it was not until 1978 that the term “biofilm” was coined by Bill Costerton (Banthia et al., 2011). Bacterial biofilms can be defined as assemblages of one or more species of surface-associated bacterial cells enclosed by a self-produced extracellular matrix (ECM) consisting primarily of polysaccharides, extracellular DNA (eDNA), and proteins that adhere to firm, sessile surfaces in sufficiently moist environments (Donlan, 2002). Biofilms provide an alternative lifestyle to independent, planktonic living by providing protection from external factors including changes in temperature and pH as well as shielding the bacterial cells from antimicrobial agents.

1.1 Significance of Bacterial Biofilms

Biofilm formation allows bacterial pathogens to colonise a wide range of host niches and persist in harsh environments, making their eradication particularly challenging (Kostakioti et al., 2013). Biofilms are magnificent strongholds for bacteria and once a biofilm has been established on a surface, it is difficult to remove it. Bacterial cells embedded within a biofilm are up to 1,000 times more resistant to antimicrobial compounds compared to their planktonic counterparts (Luo *et al.*, 2021). In biofilms, poor antibiotic penetration, nutrient limitation and slow growth, adaptive stress responses, and formation of persister cells are theorized to constitute a multi-layered defense mechanism (Stewart, 2002). The persistence of bacterial biofilms in both clinical and industrial settings are forcing researchers to better understand the implications of biofilm infections and

develop solutions for eradication of established biofilms in a system (Abu Khweek and Amer, 2018). Clinically, the reason for many human bacterial infections is due to bacteria's ability to form and live inside biofilms from where they are able to evade the host's immune system. Bacterial biofilms that colonise the human body can colonise both human tissues and prosthetics (Jamal et al., 2018). Bacterial biofilms are responsible for up to 75% of infectious diseases in humans according to the National Institutes of Health (NIH). Diseases associated with bacterial biofilms include bacterial otitis media, wound infections, lung infections, urinary tract infections, and most nosocomial infections to name a few (Yadav et al., 2020). For example, *Staphylococcus aureus* is a human commensal bacterium that persistently colonizes the anterior nares in healthy adults but can cause chronic infections if it is successful in colonising tissues or prosthetics in immunocompromised patients (Lister & Horswill, 2014) Bacterial biofilms are not only a problem for the human body. Biofilms can also be problematic in industry. Water fouling can be caused by an array of bacterial biofilms and causes water treatment plants to use costly chemicals to treat the contaminated water before it can be used (Nguyen et al., 2012). Although bacterial biofilms can be problematic like the ones previously described, they can also be beneficial and in some cases necessary. In agriculture, bacterial biofilms found in the rhizosphere of soil helps break down essential nutrients for plant growth such as nitrogen and phosphorus (Pandit et al., 2020). Additionally, wastewater treatment plants are turning to anaerobic biofilm filtration systems as a natural, eco-friendly way to clean and recycle wastewater (Yousra Turki et al., 2017). Whether

bacterial biofilms are harmful or beneficial, the overarching theme that makes them successful in the first place is their ability to form biofilms.

1.2 Biofilm Formation

Formation of the biofilm matrix produces a unique environment for bacteria that allows the dynamic biofilm lifestyle. Biofilms, and the resulting lifestyle, are built in specific, defined steps, producing a bacterial community that is mixed in space and time. (Flemming and Wingender, 2010). What was once described as the formation of a community of microorganisms attached to a firm, sessile surface has come to be recognized as a complex developmental process that is intricate and dynamic in nature (Kostakioti, Hadjifrangiskou and Hultgren, 2013). The transition from planktonic growth to biofilm formation occurs in response to environmental changes, and involves multiple regulatory networks, which translate signals to collaborative gene expression changes thereby mediating the spatial and progressive reorganization of the bacterial cell. This cellular reprogramming modifies the expression of surface molecules, nutrient exploitation, and virulence factors and equips bacteria with a collection of properties that enable their survival in harsh, unfavorable conditions (Kostakioti, Hadjifrangiskou and Hultgren, 2013).

There are five main stages of biofilm formation: (1) initial attachment, (2) irreversible attachment, (3) maturation I, (4) maturation II, and (5) dispersion. Each bacterium implements individual gene expression that contributes to the properties of the community-like environment that will become the biofilm (Pierrat and Persat, 2017). The first stage of biofilm formation is the initial attachment

stage where bacteria attempt to transition from a single, free-living planktonic state overcoming various obstacles such as hydrodynamic forces, repulsive forces, or response from nutrient and/or pH imbalances (Kostakioti *et al.*, 2013). Although there is no guarantee that the contact will be permanent, the motile bacterial cells use extracellular adhesive appendages such as flagellum, pili, fimbriae, curli fibers, and outer membrane proteins to adhere to firm, sessile surfaces. Once in contact with the desired surface (that is immersed in or in contact with the surface in an aqueous environment), the bacterial cells secrete adhesions that help to anchor the cell to the surface (Renner and Weibel, 2011). Stage two of biofilm formation involves the secretion of EPS which contain eDNA, lipids, lipopolysaccharides, and proteins that aid in facilitation of adhesion between the bacteria cell and the surface it intends to adhere to and creates the extracellular matrix (ECM) that protects the bacterial cells from toxic outside forces such as antibiotics and the host's immune responses (Renner and Weibel, 2011). The third stage of biofilm formation, commonly referred to as the first maturation phase, occurs when the cells that are attached on the surface begin to replicate forming micro-colonies (Renner and Weibel, 2011). Stage four, or the second maturation stage, occurs when the micro-colonies grow and mature into three dimensional structures and continue to replicate and secrete EPS to accumulate a sturdy ECM (Renner and Weibel, 2011). The fifth stage is the detachment phase. Bacterial cells near the outside regions of the biofilm are released from the mass and attempt to attach to other surfaces and begin the

formation of another biofilm in a new environmental niche (Renner and Weibel, 2011). Figure 1.1 depicts the five stages of bacterial biofilm formation.

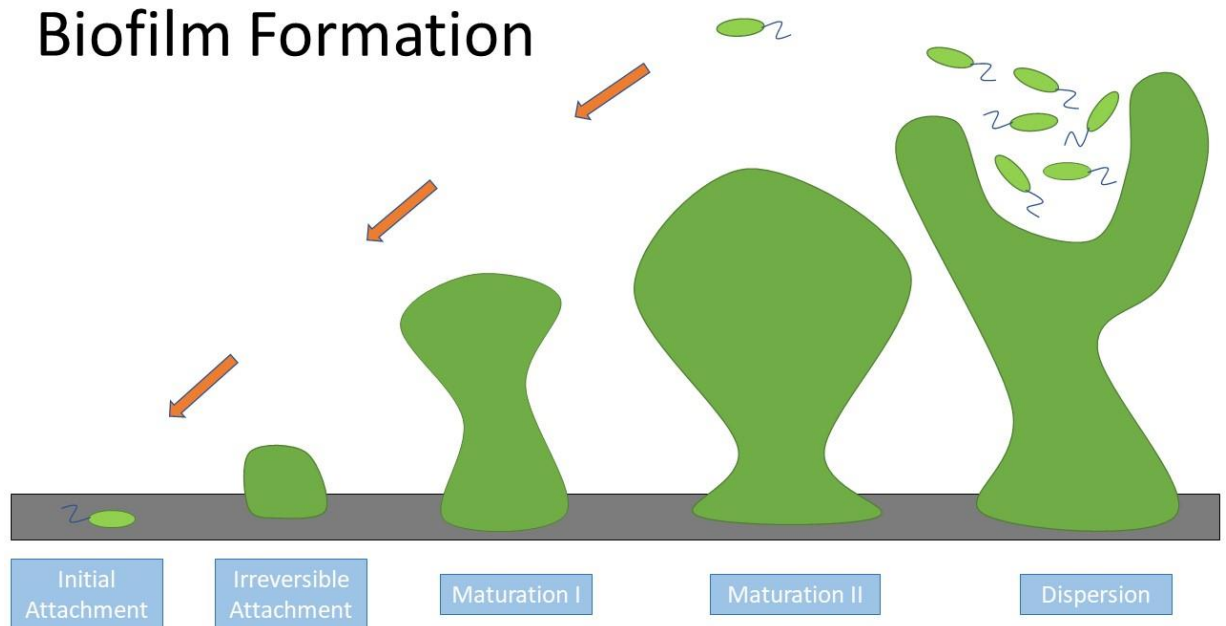


Figure 1.1 Bacterial Biofilm Formation: During biofilm formation, planktonic bacterial cells attach to sessile surfaces, adhere irreversibly and go through two stages of maturation. Once the biofilm is mature, cells on the outside of the biofilm can be released and become planktonic until they reach another surface to develop a new biofilm and begin the process again.

1.3 Introduction to Quorum Sensing

In the late 1960's while studying the bioluminescent marine bacteria *Vibrio harveyi* and *Vibrio fischeri*, Woody Hastings and Kenneth Nealson discovered a process that is today known as quorum sensing (QS). QS in biofilms is part of the regulation of gene expression in accordance to cell population density (Majumdar and Pal, 2016). Initial research focused on the bioluminescence regulation in *V. fischeri*, and lead to the discovery of extracellular influences that regulated the

light-producing enzyme luciferase. Hastings and Nealson observed that these excreted molecules increased the population density of *V. fischeri* and the bacteria would only emit light once they were at this high population density. These signalling molecules were called autoinducers (AI) and are now known to coordinate gene expression in biofilms (Fuqua, Parsek and Greenberg, 2001).

There are three main categories of QS mechanisms, and different sets of signalling molecules are attributed to each of the categories (Vadakkan et al., 2018). Gram-negative bacteria generally rely on small molecules known as acyl-homoserine lactones (AHLs). Gram-positive bacteria commonly rely on peptide-based molecules, often referred to as auto-inducing peptides (AIPs). These two broad classes tend to have limited crosstalk between the majority of species, with each species making a version of the signal that they will respond strongly to. Although there are general differences between AHLs and oligopeptides, there are also differences in AHLs and oligopeptides among bacteria of different species (Xu *et al.*, 2018). The third category of signalling molecules has been implicated as being largely used for interspecies communication and depend on a “universal” molecule known as auto-inducer 2 (AI-2) (McBrayer, Cameron and Tal-Gan, 2020). Some examples of QS molecules are shown in Figure 1.2 that was adopted from Whiteley, Diggle and Greenberg (2017).

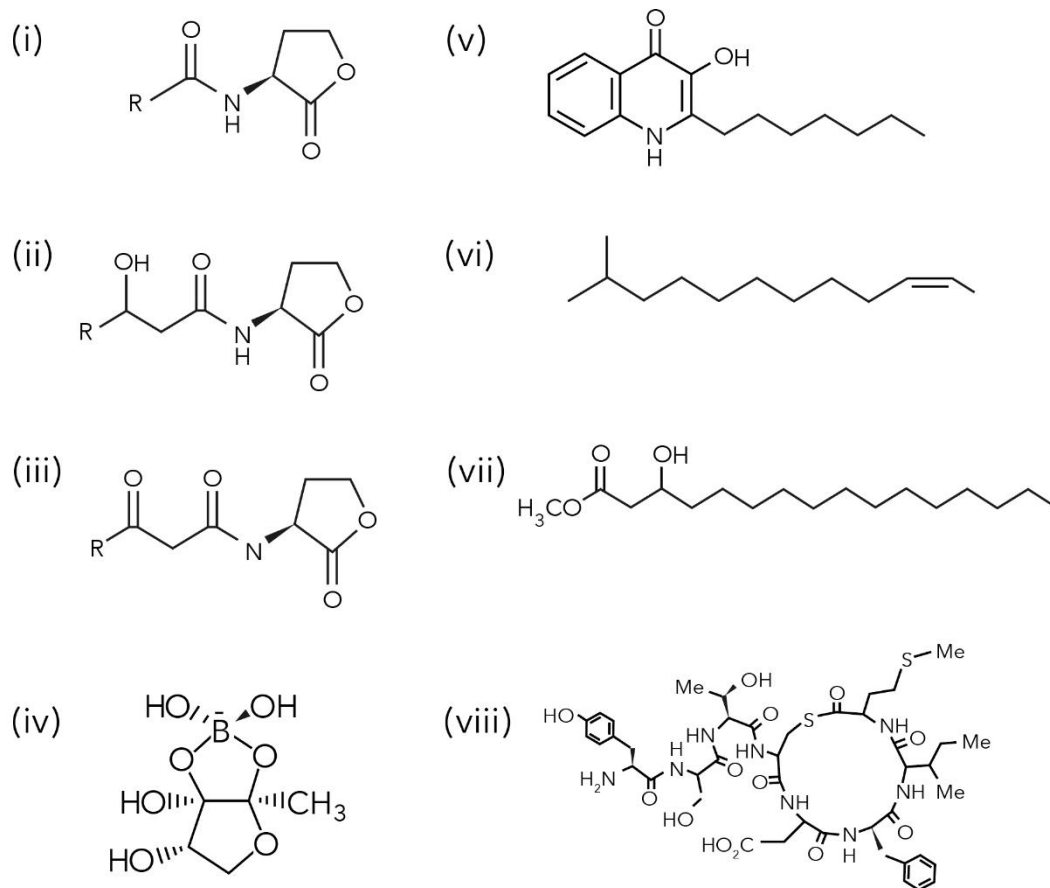


Figure 1.2 Examples of quorum sensing molecules from Gram-negative and Gram-positive bacteria. (i) AHL, N-acyl homoserine lactone; (ii) 3-Hydroxy-AHL, N-(3-hydroxyacyl)homoserine lactone; (iii) 3-oxo-AHL, N-(3-oxoacyl)-L-homoserine lactone. R can be a fatty acyl group of 4–18 carbons with or without one unsaturated carbon-carbon bond, the terminal carbon can be branched and some R groups are aromatic acids (p-coumaric acid or cinnamic acid); (iv) The *V. harveyi* AI-2, autoinducer-2, furanosyl borate ester form; (v) PQS, Pseudomonas quinolone signal, 2-heptyl-3-hydroxy-4(1H)-quinolone; (vi) DSF, diffusible factor, methyl dodecenoic acid; (vii) PAME, hydroxyl-palmitic acid methyl ester; (viii) Autoinducing peptide 1 (AIP-1) from *Staphylococcus aureus* (Whiteley, Diggle and Greenberg, 2017).

1.3.1 Quorum Sensing in Gram-negative Bacteria

QS in Gram-negative bacteria has been widely researched and the mechanisms are well understood. Gram-negative bacteria communicate using small molecules as autoinducers (AIs). These are either AHLs or other molecules whose production depends on *S*-adenosylmethionine (SAM) as a substrate. AIs are produced in the cell and freely diffuse across the cell membranes. When the concentration of AIs is sufficiently high in the extracellular environment, which occurs at high cell density, they bind to cytoplasmic receptors that are transcription factors. The AI-bound receptors regulate expression of the genes. In some cases of Gram-negative bacterial QS, AIs are detected by two-component histidine kinase receptors that function analogously to those described for Gram-positive QS bacteria (Rutherford and Bassler, 2012). The AHL-based QS system comprises three components: a cytoplasmic AHL synthase protein of the LuxI family, an AHL-responsive DNA-binding transcriptional regulator belonging to the LuxR family, and an AHL signal, which has a conserved homoserine lactone ring linked by an amide bond to side chains that vary depending upon the species and the system (Passos da Silva *et al.*, 2017). Although many Gram-negative bacteria use the AHL-based QS system, some species of Gram-negative bacteria lack any genes homologous to *luxI* despite having a *LuxR* homologue (SdiS) such as *Salmonella enterica* and *Escherichia coli* (Turovskiy *et al.*, 2007). The AHL-based QS system is illustrated in Figure 1.3.

AHL model of Gram-negative quorum sensing

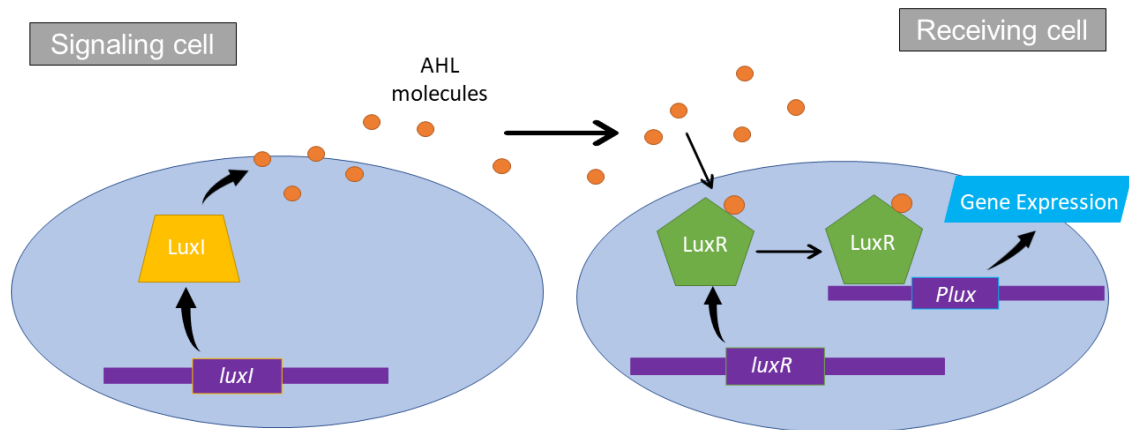


Figure 1.3 AHL model of Gram-negative quorum sensing: The signalling cell produces LuxI proteins via the *luxI* gene. The LuxI protein produces AHL molecules that passively diffuse across the cell membrane. The AHL molecules passively diffuse into neighboring receiving cells and bind to LuxR proteins in the cytoplasm that were produced via the *luxR* gene. The activated LuxR protein then binds to the *lux* promoter region on the DNA. The gene is transcribed and produces specific gene expression.

1.3.2 Quorum Sensing in Gram-positive Bacteria

Gram-positive bacteria typically employ the peptide-based QS system using oligopeptides or AIPs as their AI molecule (Abisado et al., 2018). QS in Gram-positive bacteria follow the principles common to all QS systems: production, detection, and cellular response (Rutherford and Bassler, 2012). Gram-positive bacteria produce pre-signalling molecules from *agrD* that undergo modification into AIPs by AgrB and then are transported across the cell membrane via AgrB. Once outside the cell, the AIPs attach to AgrC receptors on the cell surface when a high cell density is detected. AgrC is a cognate membrane-bound two-

component histidine kinase receptor that, upon binding with an AIP, activates the receptor's kinase activity (Rutherford and Bassler, 2012). ArgC autophosphorylates and passes phosphate to a similar cytoplasmic response regulator (usually ArgA). The final step, cellular response, happens when the phosphorylated ArgA attaches to the DNA and translates the specific gene and the coinciding product is produced (Mukherjee and Bassler, 2019). These bacteria are on a positive feedback loop where the more AIP produced stimulates more AIP production with no way to stop it except from external forces such as quorum sensing inhibitory molecules (Monnet and Gardan, 2015). Figure 1.4 illustrates the Gram-positive QS model.

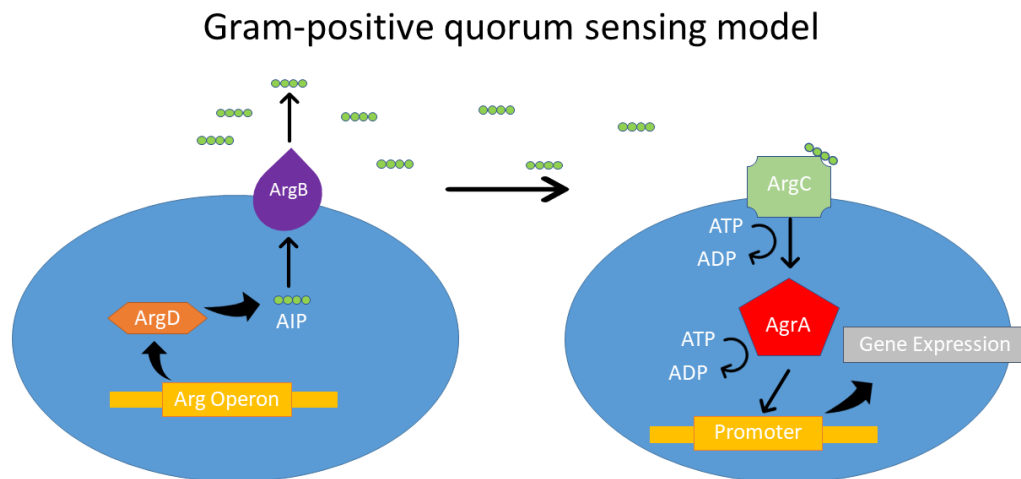


Figure 1.4 Gram-positive quorum sensing model: In Gram-positive QS, the Arg operon encodes ArgD cytoplasmic proteins that produce autoinducing peptides or AIPs. The AIPs are actively transported outside the cell via ArgB proteins embedded in the cellular membrane. The AIPs can then attach to ArgC receptors on the surface of neighboring cells. An activated ArgC then phosphorylates ArgA inducing activation. ArgA is phosphorylated again and can then bind to the promoter region of the DNA and gene transcription begins.

1.3.3 The Universal Quorum Sensing Pathway in Bacteria

Many bacterial biofilms exist as multi-species biofilms. For different types of bacteria within the biofilm environment to communicate effectively and induce coordinated behaviours, they employ the AI-2 QS pathway for interspecies communication. Curiously, the AI-2 molecule is not a single signalling molecule but a group of 4,5-dihydroxy-2,3-pentanedione (DPD) derivatives that can convert rapidly to one another (Zhang et al., 2020). AI-2 is synthesized by the S-ribosylhomocysteine lyase (LuxS) in both Gram-positive and -negative bacteria and used for inter- and intraspecies communication. The biosynthetic pathway for AI-2 in different bacterial species is highly conserved; AI-2 can be automatically converted from the precursor substance 4,5-dihydroxy-2,3-pentandione (DPD). The recognition of signals is as important as signal synthesis for coordinated behavioural responses. Homologous protein complexes can perceive and transduce signals and their regulation plays a key role in defining behaviours (Gu et al., 2020). Differential gene expression in response to AI-2 may cause bacterial behavioural modifications, such as biofilm formation or transition to a pathogenic state (Federle, 2009).

1.4 Quorum Quenching

In contrast to QS molecules, quorum quenching (QQ) molecules interrupt the communication or signalling between bacterial cells inhibiting the formation of a quorum and subsequent gene expression. A QQ molecule is a molecule that inhibits or reduces bacterial communication (Rehman & Leiknes, 2018). QQ

molecules act by blocking the main steps of quorum sensing such as generation, accumulation, and reception of signal molecules (Dong et al., 2007). These QQ molecules are frequently QS molecules in some microorganisms but act as quorum quenchers in other microbial species. For example, some bacteria produce different types of enzymes that can degrade or modify AHLs (AHL-lactonases hydrolyze the lactone moiety of AHLs, AHL-acylases hydrolyze the amide bond between lactone ring and acyl chain, and AHL-oxidoreductase oxidize or reduce the third carbon of the acyl chain of AHL molecules) which aids in reduction of biofilm formation in many Gram-negative species (Rehman & Leiknes, 2018). Potential mechanisms of how quorum quenchers may operate in bacterial biofilms was described by Mikłasińska-Majdanik *et al.*, (2018) where different mechanisms such as: multi-target action where each compound acts on a different site in the bacterial cell; pharmacokinetic or physicochemical properties such as an increase of solubility or bioavailability of the antibiotics; or aimed for a specific bacterial resistance mechanism were described. Amid rising antibiotic and antimicrobial resistance, it is vital to explore different methods of controlling bacterial biofilm infections such as QQ.

1.5 Extracellular Matrix and EPS Components

Within a biofilm, bacterial cells are surrounded by a self-generated extracellular matrix, which accounts for approximately 90% of the overall biomass (Kostakioti, Hadjifrangiskou and Hultgren, 2013). The ECM was once thought to be composed of mostly extracellular polysaccharides but in fact has been found to be made up of several other necessary extracellular polymeric substances (EPS)

including extracellular proteins, lipids, and eDNA (Kostakioti, Hadjifrangiskou and Hultgren, 2013). The EPS immobilizes cells in the biofilm, keeping them in long-term close proximity and allows powerful interactions to occur, including cell–cell communication, horizontal gene transfer, and formation of synergistic microconglomerates (Flemming and Wingender, 2010). Along with providing structural integrity to the biofilm, the ECM also hydrates the biofilm through its networks of channels that provide nutrients and water to even the most embedded cells of the biofilm. The ECM protects organisms in the biofilm from dehydration, biocides, antibiotics, heavy metals, ultraviolet radiation, host immune defences, and many protozoan grazers (Flemming and Wingender, 2010). Although individual components of the EPS differ in proportions in the ECM among different species of bacteria, the extracellular polysaccharides, proteins, and eDNA are important aspects to explore independently because they each play a vital role in the overall stability and survival of the biofilm. Elements of a microbial biofilm including the eDNA, cells, proteins, polysaccharides, and others along with mechanisms of possible disruption are depicted in Figure 1.5.

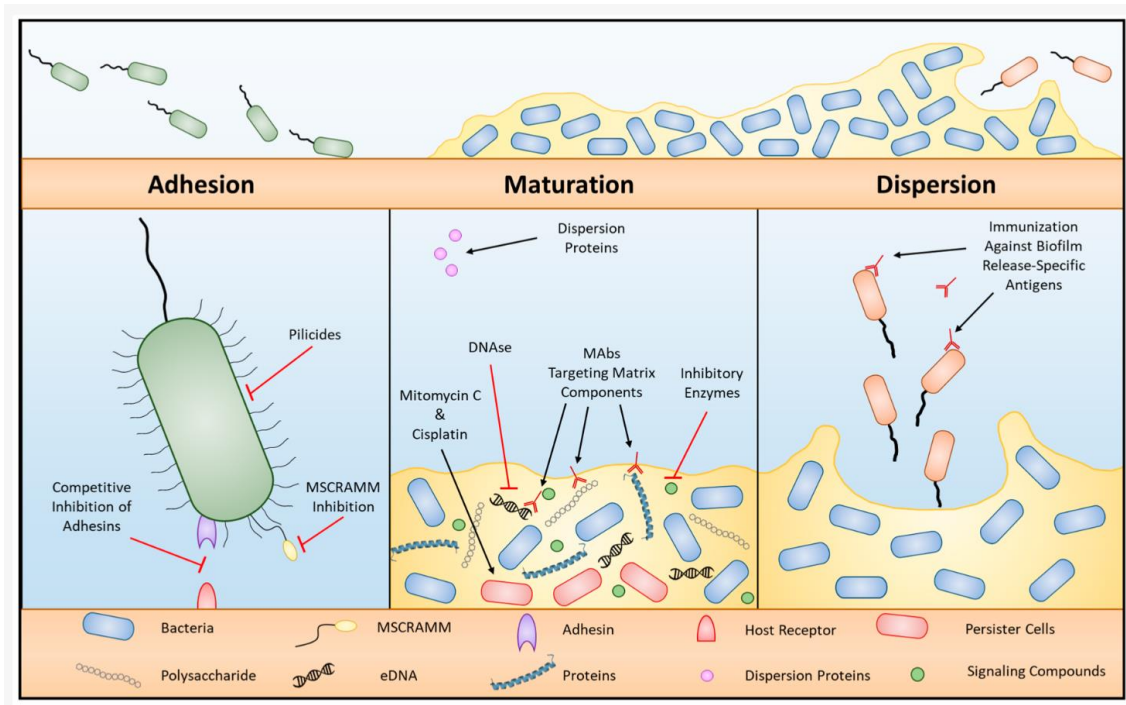


Figure 1.5 demonstrates the formation of a bacterial biofilm from planktonic cellular adhesion onto a surface, through maturation, and finally to dispersion. This figure also depicts various components of bacterial biofilms and potential avenues of disruption of the biofilm formation process (Beitelshees, Hill, Jones and Pfeifer, 2018).

1.5.1 Extracellular polysaccharides

Extracellular polysaccharides, or carbohydrates, in the ECM prescribe a framework for the biofilm landscape. Inhabitants of the biofilm need to be protected from external environmental factors (host cells, antimicrobials, dehydration, temperature, competing microbes, etc.) while maintaining access to nutrients and the ability to react to changes in the environment (Limoli, Jones and Wozniak, 2015). Bacteria generate numerous extracellular polysaccharides to cope with these needs in a variety of ways. Extracellular polysaccharides can aid in bacterial adherence to many different surfaces, hosts, and other bacterial cells,

provide protection from the onslaught of antimicrobials in the environment, provide reservoirs for nutrient acquisition, and aid in the creation of distinct architectures, which further potentiate an environment suitable for microbes to persist (Limoli, Jones and Wozniak, 2015). Extracellular polysaccharides can be divided into three functional categories to highlight their importance and diversity in biofilm biology: aggregative, protective, and architectural. (Limoli, Jones and Wozniak, 2015). The formation of biofilms occurs in several stages: initial attachment, irreversible attachment, maturation I, maturation II, and dispersion. Aggregative extracellular polysaccharides play essential roles in each of these steps: assisting in adhesion to surfaces, formation of complicated structures by promoting microbial connections, and relief of these interactions encouraging dissolution of the biofilm (Limoli, Jones and Wozniak, 2015). Microbial protection from the onslaught of host and environmental factors is a classical and frequently described characteristic of the biofilm mode of growth. Current criteria used to define infectious biofilms is increased resistance to antimicrobials and the host immune response. While several factors including metabolic heterogeneity, altered chemical microenvironments, and persister cell populations contribute to biofilm antimicrobial resistance, an important role for extracellular polysaccharides is evident (Limoli, Jones and Wozniak, 2015). Extracellular polysaccharides synthesised by oral bacteria constitute one of their major virulence factors. The extracellular polysaccharides, synthesised from sucrose, facilitate adhesion and colonisation by bacteria to tooth surfaces. (Steinberg, Poran and Shapira, 1999). Some of the first biofilm-related extracellular

polysaccharides identified were studied due to the role they play in oral (or tooth associated) biofilm structure. These extracellular polysaccharides have provided extensive insight into the regulation of biofilm formation and structure, primarily due to the readily observable phenotypes associated with mutants or overproducers of these products (Limoli, Jones and Wozniak, 2015).

1.5.2 Extracellular Proteins

Proteinaceous elements of the ECM include secreted extracellular proteins, cell surface adhesins, and protein subunits of cell appendages such as flagella and pili (Fong and Yildiz, 2015). Biofilm matrix proteins play varied roles in both biofilm formation and dissolution. Proteins are involved in attaching bacterial cells to surfaces, stabilizing the matrix via interactions with exopolysaccharide and eDNA components, developing three-dimensional biofilm architectures, and dissolving biofilm matrix via enzymatic degradation of polysaccharides, proteins, and nucleic acids (Zhang et al., 2015). Cell surface proteins, pili, and flagella contribute to initial attachment of cells to surfaces and can also be involved in migration along the surfaces, thus facilitating surface colonization (Fong and Yildiz, 2015). Proteins in the EMC contribute to biofilm structure and stability which have largely been identified by mutational studies that showed reduced biofilm formation and stability in the absence of certain protein (Zhang et al., 2015). One of the most studied groups of ECM proteins is the family of Bap proteins. Bap proteins are usually large and can function both as virulence factors involved in pathogenesis and as ECM proteins mediating abiotic surface adhesion and subsequent biofilm formation (Fong and Yildiz, 2015). In *S. mutans*,

some of the most notable matrix proteins are the extracellular Gtf proteins that synthesis sticky glucans from dietary sucrose leading to biofilm on tooth surfaces that if left untreated, can cause irreversible damage to the enamel surface (Ren et al., 2016)

1.5.3 Extracellular DNA

DNA is not found exclusively within cells. eDNA is an important component of the ECM and has long been known as one of the most abundant molecules in the matrixes of biofilms of different microorganisms (Ibáñez de Aldecoa, Zafra and González-Pastor, 2017). Several microorganisms release eDNA within their biofilms. For example, *Neisseria gonorrhoeae*, *P. aeruginosa*, and *Pseudomonas chlororaphis*, some *Staphylococcus* species such as *Staphylococcus epidermidis* or *Staphylococcus aureus*, *Streptococcus pneumoniae*, *Enterococcus faecalis*, *Helicobacter pylori*, and *Campylobacter jejuni*. Therefore, the presence of eDNA in biofilms is certainly a widespread feature (Castillo Pedraza et al., 2017). eDNA was first demonstrated as being an essential component of microbial biofilms in 2002 by Cynthia B. Whitchurch using DNase I to prevent *P. aeruginosa* biofilm formation (Whitchurch, 2002). While eDNA is an abundant polymer within the *P. aeruginosa* ECM, it is unclear whether it is essential for proper biofilm development because DNase I seemed to only affect early stages of biofilm formation, implying mature biofilms are immune, thus suggesting different functions of eDNA during the development of the biofilm (Whitchurch, 2002). Despite the unclear relevance of the eDNA for *P. aeruginosa* biofilm formation, it is considered as an adhesion compound that

enables cell-to-cell attachment, even in planktonic cultures, stabilizing the biofilm and providing resistance against degrading agents (Ibáñez de Aldecoa, Zafra and González-Pastor, 2017). Some proposed purposes for eDNA in bacterial biofilms are: (i) structural component within the biofilm that offers stability to the overall structure, (ii) a feature that promotes the formation of biofilm and the construction of the ECM and (iii) a role in gene transfer through transformation of competent sister bacteria (Ibáñez de Aldecoa, Zafra and González-Pastor, 2017). eDNA enters the EMC by active secretion or controlled cell lysis, occasionally linked to competence development (Montanaro et al., 2011). eDNA adsorbs to and extends from the cell surface, promoting adhesion to abiotic surfaces through acid–base interactions (Okshevsky and Meyer, 2015). The multifaceted role of eDNA makes it an alluring target to sensitise biofilms to traditional antimicrobial treatment or development of new strategies to combat biofilms (Okshevsky and Meyer, 2015).

1.5.4 Cells Within a Biofilm

Microorganisms have been characterized primarily as planktonic, freely suspended cells and described based on their growth characteristics in nutritionally rich culture media throughout the history of microbiology. Renewed interest in a microbiologic phenomenon that microorganisms adhere to and grow on exposed surfaces led to studies that uncovered surface-associated microorganisms within biofilms exhibited a distinct phenotype with respect to gene transcription and growth rate. These biofilm microorganisms have been shown to elicit specific mechanisms for initial attachment to a surface,

development of a community structure and ecosystem, and detachment (Donlan, 2002). Additionally, biofilms provide an ideal microenvironment for the exchange of plasmids with conjugation occurring at greater rates among cells within a biofilm than between their planktonic counterparts (Donlan, 2002). Although most cells within a biofilm have an accelerated growth rate, about 1% of bacterial cells in a biofilm are persister cells. Persister cells arise due to a state of dormancy, defined as a state in which cells are metabolically inactive and are increasingly associated with being the major cause of chronic infections (Wood *et al.*, 2013).

1.6 Traditional Methods of Prevention and Eradication of Bacterial Biofilms

Antibiotics are the preferred treatment approach for bacterial infections, but usually have little to no effect on established bacterial biofilms (Taylor, Stapleton and Paul Luzio, 2002). Methods of biofilm eradication include physical removal of the biofilm by scraping the biofilm from the surface or removing the surface occupied by the biofilm (for example, removing a catheter). Traditional antibiotics operate by either preventing bacterial cell division (bacteriostatic) or killing the cell (bactericidal) (Taylor, Stapleton and Paul Luzio, 2002). Over the years, antibiotics have proven critical in eliminating bacterial pathogens, mounting evidence indicates that they extensively harm the host microbiota, creating an environment where opportunistic pathogens can succeed, and they increase the selective pressure toward antibiotic resistance. Biofilm bacteria are particularly refractory to antibiotic treatments not only due to increased transmission of resistance markers within the biofilm community, but also because of diffusion

restrictions posed by the ECM, antibiotic inactivation by high metal ion concentration (heavy metals such as arsenic, copper, silver, lead and mercury) and low pH, and the presence of metabolically inactive persister cells that survive treatment (Kostakioti, Hadjifrangiskou and Hultgren, 2013) and (Uppsala University, 2014). Because of the ever-evolving nature of bacteria and the strength that comes with a biofilm lifestyle, the need for more effective biofilm eradication treatments becomes imperative. Therefore, novel strategies, designed to block a specific step in the biofilm formation process without killing the bacteria, such as the use of anti-adhesion agents, or using natural, bacterially produced signals to promote bacterial dispersal, are potential avenues for exploration and ultimately the development of fast-acting, potent, and bioavailable treatment and prevention strategies (Kostakioti, Hadjifrangiskou and Hultgren, 2013).

1.7 The Oral Cavity

In the human body, the oral cavity is an active, thriving environment composed of several different elements including the lips, hard palate, soft palate, retromolar trigone, front two-thirds of the tongue, gingiva, buccal mucosa, the floor of the mouth under the tongue, tonsils, uvula, and teeth (Cohen, 2013). All of these elements contribute to the ingestion and initial digestion of the foods necessary to fuel the human body, provide initial protection against foreign invaders that could cause harm to the body, and house one of the most diverse environments of microbes. One of the most important products produced in the oral cavity is saliva. The anatomy of the oral cavity is shown in Figure 1.6.

Anatomy of the Oral Cavity

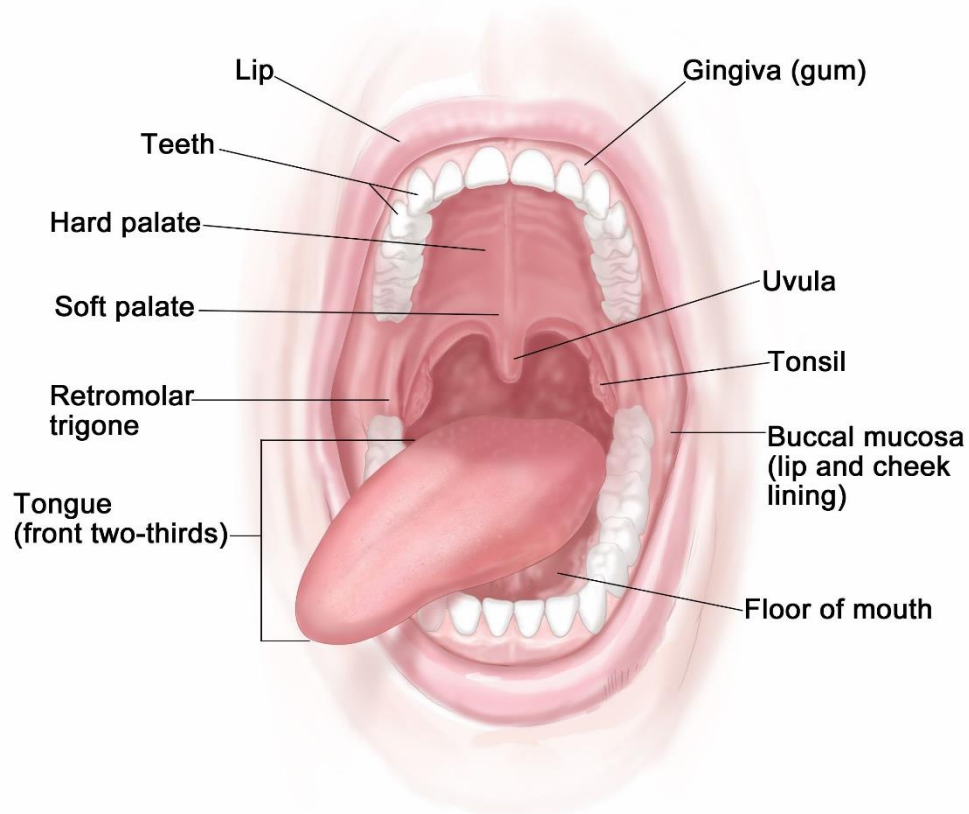


Figure 1.6 The anatomy of the oral cavity: the lip, teeth, hard palate, soft palate, retromolar trigone, tongue, gingiva, uvula, tonsil, buccal mucosa, and the floor of the mouth. This image was adopted from [<https://www.cancer.gov/publications/dictionaries/cancer-terms/def/oral-cavity>].

Saliva is a complex fluid that influences oral health through both its specific and nonspecific physical and chemical properties (Dave et al., 2020). Saliva is a very dilute extracellular fluid, consisting of more than 99% water with a variety of electrolytes, including sodium, potassium, calcium, magnesium, bicarbonate, and phosphates. Additionally, there are immunoglobulins, proteins, enzymes, mucins, and nitrogenous products, such as urea and ammonia found in saliva (Humphrey & Williamson, 2001). Saliva supports a host of functions in the oral

cavity including reducing biomass and providing mechanical cleansing of teeth, providing an optimal pH in which oral functions are efficiently carried out, and it contains an array of antimicrobial components (Tiwari, 2011). In the oral cavity, saliva is produced and excreted from the salivary glands. Essentially, salivary glands are clusters of cells called acini. These cell clusters secrete a fluid containing water, electrolytes, mucus, and enzymes that is collected in collecting ducts where the composition is further altered. Smaller collecting ducts within the network of salivary glands lead to larger ducts that eventually form a large duct that empties into the oral cavity (Tiwari, 2011). Figure 1.7 shows the anatomy of the salivary glands of humans.

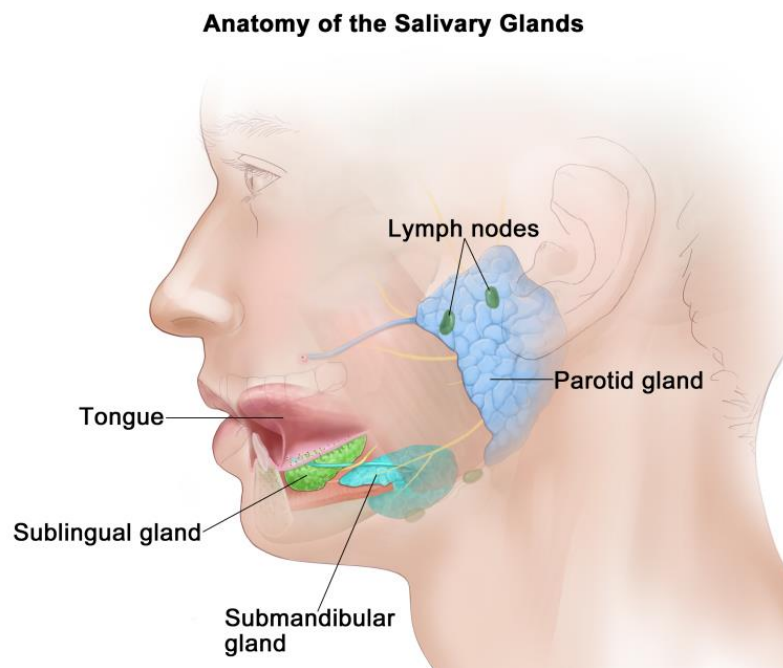


Figure 1.7 The anatomy of the salivary glands of humans is depicted in the figure above and includes the sublingual gland, the submandibular gland, and the parotid gland. The image was adopted from https://www.ncbi.nlm.nih.gov/books/NBK65749/figure/CDR0000258034__142/

Saliva serves many functions within the oral cavity and throughout species of saliva secreting animals. Some roles of saliva that are important to all species include but may not be limited to: aiding in lubrication and binding of food. The mucus in saliva is an effective binding agent that is able to create a slippery bolus of masticated food that can easily slid through the oesophagus. Saliva is the solvent necessary for solubilization of dry foods consumed. Saliva contributes to oral hygiene considerably because the oral cavity is almost constantly being flushed with a steady flow of saliva which allows food debris to flow away and helps keep the mouth relatively clean. Because salivary flow diminishes considerably during sleep, oral bacteria are allowed to build up overnight causing bad breath upon waking up. Luckily, saliva contains an enzyme called lysosome that is able to lyse many bacterial species and prevents the overgrowth of the oral microbiota. Saliva also aids in the initiation of dietary starch digestion into maltose by containing alpha amylase in most species (Tiwari, 2011). Although saliva's main function is to maintain homeostasis within the oral cavity, it also serves to be an excellent medium for microbes to flourish and build biofilms on the hard surfaces found in the oral cavity. The microbes in the oral cavity predominantly survive and flourish as harmless normal flora, but given the opportunity, some opportunistic pathogens will take advantage of lapses in the homeostasis of the oral cavity and attempt to colonise the moist surfaces including the teeth (Grande et al., 2015). The colonization of tooth surfaces by oral bacteria begin immediately after the teeth have been brushed and continue until the teeth are brushed again and the process repeats. Once the

hydroxyapatite (HA) surface of the tooth has been cleaned, the salivary pellicle begins to form, giving way to the perfect substrate for bacterial adhesion (Tiwari, 2011).

1.8 Periodontium

In the oral cavity, the teeth are anchored to bones via tissues of the periodontium. The periodontium is a connective tissue comprised of four parts: cementum, the periodontal ligament, alveolar bone, and gingival tissue (Torabi & Soni, 2022). A diagram depicting the interface between tooth and surrounding periodontium is shown in Figure 1.8.

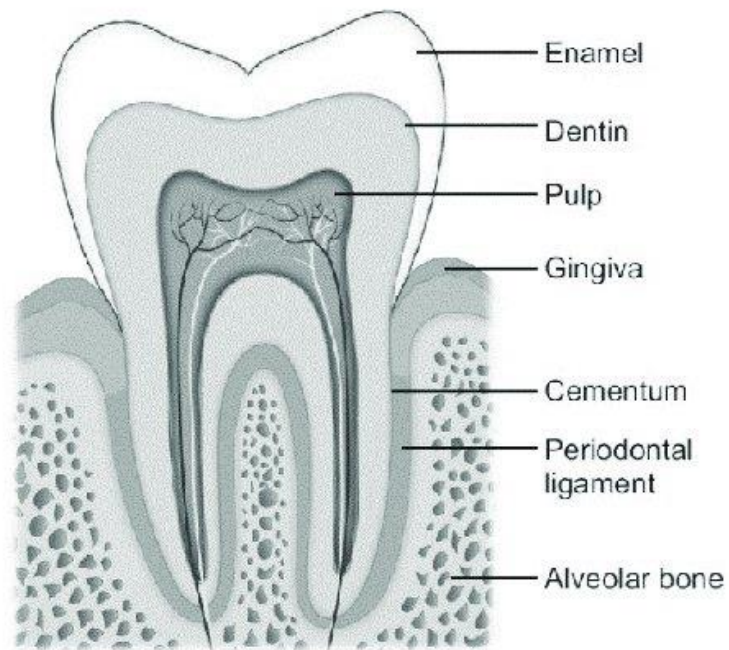


Figure 1.8 The structure of the tooth and periodontium tissues including: enamel, dentin, pulp, gingiva, cementum, periodontal ligament, and alveolar bone. (Wanasathop & Li, 2018).

Bacteria are found on all tissues in the oral cavity, and there is overlap in the bacteria found on each (Agnihotry, Fedorowicz and Nasser, 2016). The most copious bacteria in the oral cavity are *Streptococcus oralis*, *Streptococcus mitis*, and *Streptococcus peroris* (Graves *et al.*, 2019). Bacterial biofilm formation on the tooth surface initiated by a pellicle that promotes bacterial adhesion, with *Streptococcus* and *Actinomyces* as early colonizers, facilitates formation of a multispecies biofilm that is spatially organized and depends on coaggregation among bacterial taxa with subgingival biofilm typically more anaerobic than the supragingival biofilm (Graves *et al.*, 2019). Periodontal infections and diseases are initiated by bacteria accumulated in biofilms on the tooth surface and affect the adjacent periodontal tissues (Graves *et al.*, 2019). Because of the interconnected relationships among oral bacteria, understanding the oral cavity as a whole can lead to better research and understanding of individual bacterial behaviour and subsequent infections in the oral cavity.

1.9 Biofilm Formation in the Oral Cavity

The oral cavity has a rich and diverse microbiome. The oral microbiome consists of bacteria, fungi, archaea, viruses, and protozoa (Barbosa *et al.*, 2016). The formation of dental biofilms in infancy and early childhood is affected by the method of delivery (vaginal or caesarean), breast or bottle-feeding, and presence of siblings and pets (Graves *et al.*, 2019). Oral biofilms are primarily composed of microorganisms within an ECM of both organic and inorganic materials derived from saliva, gingival crevicular fluid, and bacterial products. The majority (50-95%) of the dry weight of the biofilm is the EPS produced by the bacteria which

play a crucial role in maintaining the integrity of the biofilm as well as protecting it from attack from harmful agents (Saini *et al.*, 2011). Although studies that have been conducted to characterize QS systems in oral biofilms have been mostly limited to a few species, some reports have also identified luxS homologous genes in other bacteria leading researchers to believe that biofilms of the oral cavity possess the AI-2 quorum sensing circuit that would allow interspecies communication within the oral biofilms, but AHL-mediated quorum sensing system has not been found in oral bacterial pathogens thus far (Majumdar and Pal, 2016). One distinguishable feature of oral biofilms is that many bacteria in the biofilms can both synthesize and degrade the EPSs (Saini *et al.*, 2011). There are thousands of different species of bacteria located in the oral cavity, but the composition of pathogenic oral biofilms (usually multispecies) are commonly composed of bacterial cells from the genera *Actinomyces*, *Streptococcus*, and *Fusobacterium* and are considered to be core periodontitis associated species (Chenicheri *et al.*, 2017). Although the microbial etiology of periodontitis is indisputable, there is now evidence to suggest the disease onset and progression is associated with the shift of population within the bacterial biofilm community (Majumdar and Pal, 2016). The bacterial species associated with periodontal diseases are overpopulated in the area of disease whereas they are considerably lower in number in healthy areas of the oral cavity. The complexity of these biofilms and their ability to shift the microbial community is the result of species association and intra- and inter-species quorum sensing abilities (Majumdar and Pal, 2016). In oral biofilms, the deeper levels are a dense layer of microbes bound

together in the ECM. The next layer is loose and tends to be irregular in appearance and shape and may extend into the surrounding aqueous medium. In the fluid layer bordering the biofilm and throughout the matrix, there is a presence of voids or water channels that permit the passage of nutrients and other materials throughout the biofilm acting like a primitive circulatory system. The bacterial species in the deeper levels tend to be anaerobic while bacterial species closer to the edges of the biofilm tend to be aerobic leading to customized living environments within a single biofilm (Saini *et al.*, 2011). Figure 1.9 shows the order of the layers that are involved in the formation of biofilm on the tooth surface.

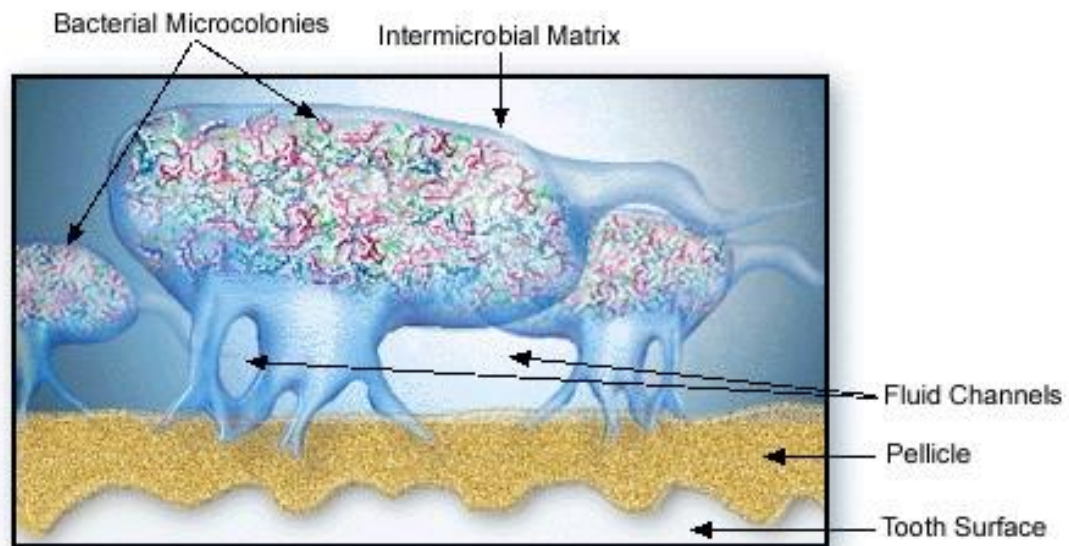


Figure 1.9 The layers in which oral biofilms evolve on the surface of the tooth. The bottom layer is the HA surface of the tooth, followed by the pellicle layer where the primary colonisers attach and begin producing microcolonies. Fluid channels as well as EPS can be seen in this figure. Image is adopted from <https://pdfs.semanticscholar.org/fbf3/c6fb6375c18f2db5e0a97a1c8ca1caac8c1c.pdf>

The formation of oral biofilms, commonly referred to as dental plaque, is comparable to the other biofilm formation steps mentioned earlier, but it can be more appreciated for its initial preparation given the activity of the oral cavity. The initial stages of oral biofilm formation begin immediately on a cleaned tooth surface. This initial biofilm formation is called pellicle formation. The salivary pellicle is a thin acellular organic film that forms on any type of surface upon contact with saliva. The role of the salivary pellicle is diverse, and it plays a crucial role in the maintenance of oral health. Its functions include not only serving as the base of protection and lubrication, but also remineralization and hydration of HA surfaces. Additionally, the salivary pellicle functions as a diffusion barrier and possesses buffering ability. Not only the function, but also the formation, composition and stability of the pellicle are known to be highly influenced by the physicochemical properties of both substrata and ambient media (Lindh et al., 2014). Once the salivary pellicle is formed, primary colonizers of dental biofilms begin to adhere. There are many key players in initiation of dental biofilm formation due to their anerobic metabolism and their ability to thrive in environments with a low pH. The primary colonizers include: *Streptococcus mutans*, *Streptococcus sanguis*, *Streptococcus oralis*, *Streptococcus gordonii*, and *Lactobacillus acidophilus* (Chenicheri et al., 2017). After the primary colonizers of dental biofilms become established, they are able to bridge the gap and provide an environment where other microorganisms can colonize other tissues within the oral cavity including the gum tissue and the pulp and root of the tooth. One of the most notable bacteria that swiftly move in to fill the available

niche made by the formation of the salivary pellicle is *S. mutans*. Single planktonic *S. mutans* cells will take advantage of the salivary pellicle on the tooth surface and adhere to moieties of proteins, such as sIgA, and start building micro colonies if there are no aversions to the attachment (Cukkemane, et al, 2014). *S. mutans* will bind to pellicle proteins via their adhesins proteins located on their cell membranes (Ito, Maeda, and Senpuku, 2012). This initial bacterial attachment begins via non-specific, long-range, physiochemical forces between bacteria and the pellicle-coated tooth surface including van der Waal attractive forces and repulsive negative electrostatic forces (Paluch et al., 2020). Hydrophobicity may also facilitate attachment. This monolayer grows and matures over the next 4 to 24 hours creating distinct microcolonies of both Gram-positive and Gram-negative bacterial species. As the biofilm continues to grow and mature (24+ hours), microbial succession occurs providing a pseudo-stable climax community. This is considered the stage of mature dental plaque formation. It is necessary for the stages of biofilm formation in the oral cavity and the doubling time of primary colonizers to be quick due to the daily practice of physically removing biofilm on the tooth surfaces via brushing and flossing if the biofilm stands a chance at becoming mature and dispersing. Figure 1.10 shows how all these steps come together to form a complex biofilm on the surface of the tooth.

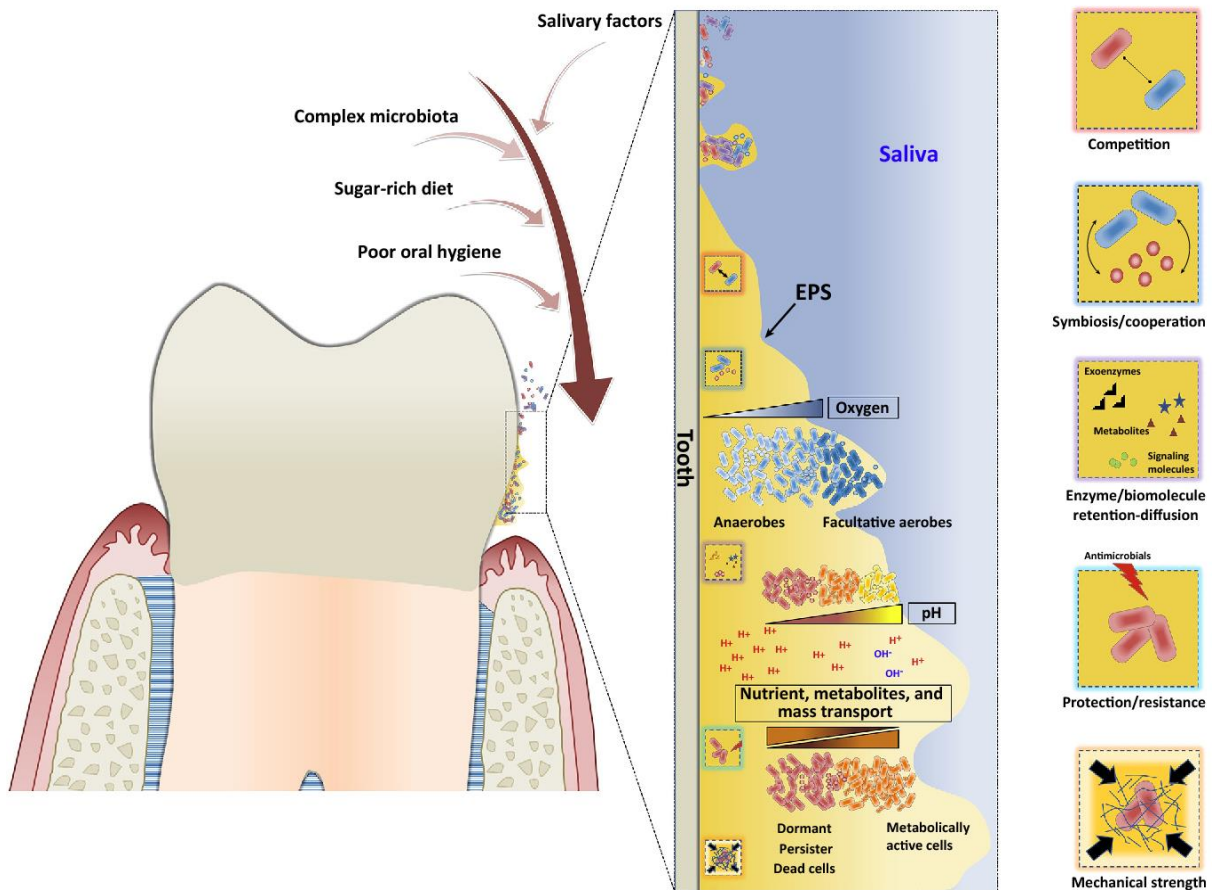


Figure 1.10 Factors involved in dental biofilm formation: This figure shows how many factors including salivary factors, a complex microbiota, a sugar rich diet, and poor oral hygiene techniques add up to produce an intricate bacterial biofilm on the surface of teeth within the oral cavity. The image above is adopted from (Bowen et al., 2018).

1.10 Streptococcus mutans

S. mutans is a facultatively anaerobic, Gram-positive, coccus shaped bacterium commonly found in the oral cavity where it opportunistically contributes to oral infections and diseases. *S. mutans* is an obligate human pathogen and an etiological agent in dental biofilms that lead to dental decay and formation of carious lesions and can be seen in Figure 1.11.

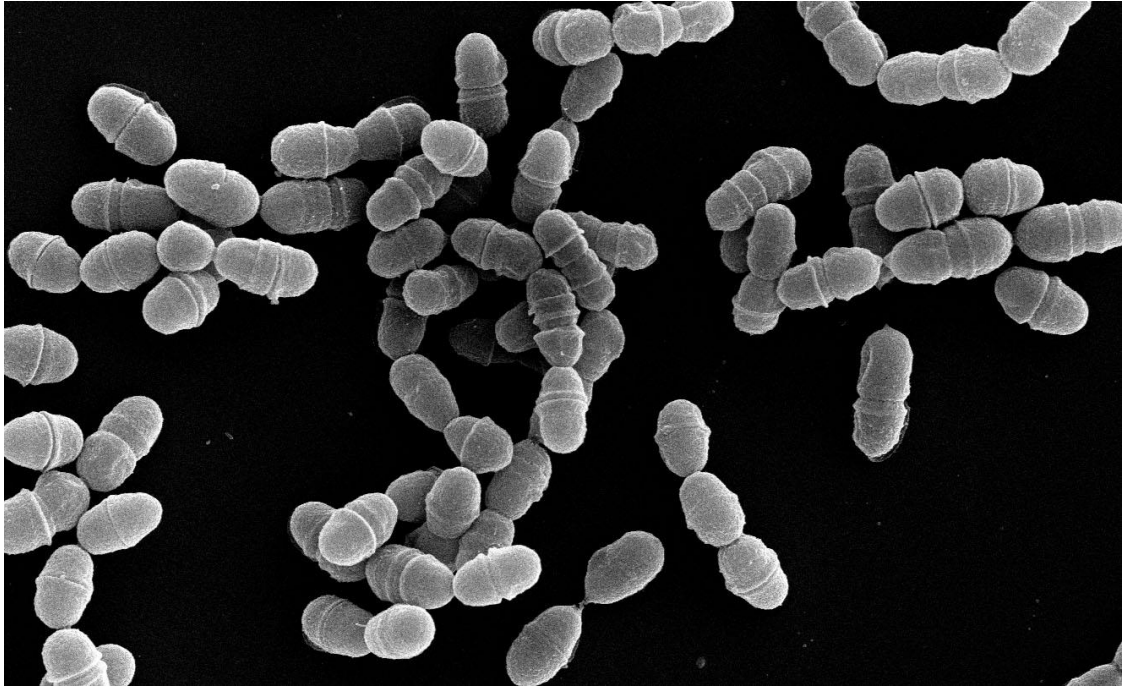


Figure 1.11 *Streptococcus mutans* adopted from <http://biochemistry.med.uky.edu/streptococcus-mutans>

S. mutans is considered a primary colonizer of dental biofilms due to it being one of the first species of bacteria to colonize the tooth surface (Lemos *et al.*, 2013). In 1924, J. Clarke attempted to isolate a specific organism or group of organisms responsible for creating dental caries. At the time, it was known that dental caries formed through the acidification of tooth surfaces by acid producing bacteria credit in part goes to Leeuwenhoek's discovery of bacteria in dental plaque taken from his own teeth in the 17th century. *Bacillus acidophilus* was the commonly accepted etiological agent responsible for dental caries because it appeared in nearly all advanced carious lesions. Although Clarke identified *B. acidophilus* in advanced carious lesions, he rarely found *B. acidophilus* in newly formed dental caries. Instead, he consistently found what he described as a slightly elongated

coccus that formed a small, greyish-white colony when grown on agar. Clarke called this mutant streptococcal bacterium *Streptococci mutans* (Clarke, 1924). Although *S. mutans* received greater attention in the late 1950's, it wasn't until the 1960's that *S. mutans*, after being recognized a major etiological agent of dental caries and tooth decay, was appreciated by the scientific community and scientists uncovered the pathophysiology of *S. mutans*. As the first tools for studying *S. mutans in vivo* and *in vitro* were being developed, early researchers described the three major virulence factors that made *S. mutans* so successful within the oral cavity: (i) the ability to produce large quantities of organic acids (acidogenicity) from metabolized carbohydrates; (ii) the ability to survive at low pH (aciduricity); and (iii) the ability to synthesize extracellular glucan-homopolymers from sucrose, which play a critical role in initial attachment, colonization and accumulation of biofilms on tooth surfaces (Lemos et al., 2013)

With the advances in molecular genetic techniques in the 1980's and 90's, the understanding of *S. mutans's* metabolic pathways enabled researchers to deduce how it evolved into a specialized, niche dental pathogen. Finally, in 2002, when the complete genome of *S. mutans* was released, the scientific community was able to take full advantage of the technologies that emerged during this era and were able to study the genetic code and understand further the virulence mechanisms that make *S. mutans* successful in colonising the oral cavity (Lemos et al., 2013). *S. mutans* utilises the quorum sensing pathway primarily comprised of the Competence Stimulating Peptide (CSP) and the ComD/ComE two-component signal transduction system for biofilm formation in the oral cavity

(Senadheera & Cvitkovitch, 2008). Figure 1.12 shows the CSP and ComD/ComE system.

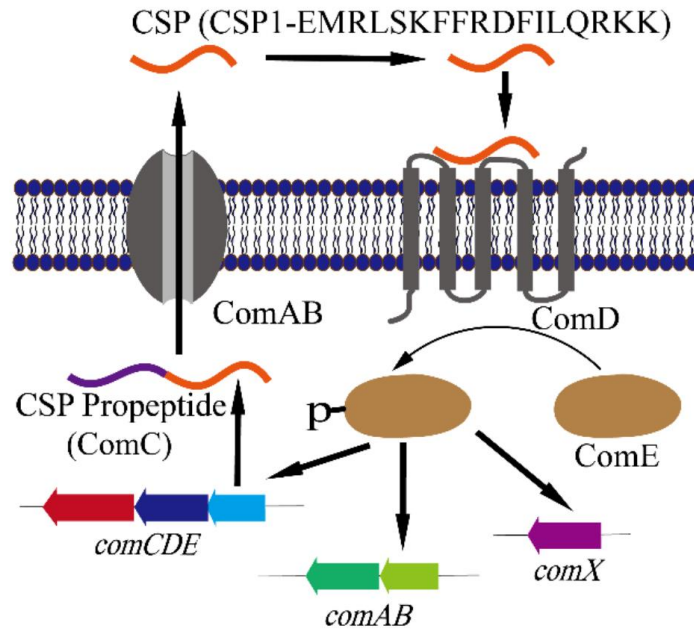


Figure 1.12 adapted from Yang and Tal-Gan (2019) shows the CSP-mediated quorum sensing circuit. CSP is created from a propeptide, ComC (encoded by the *comC* gene). An ABC transporter, ComAB, then cleaves the propeptide and exports the mature CSP out of the cell. When the concentration of CSP reaches a threshold, CSP can effectively bind and activate a transmembrane histidine kinase receptor, ComD. Upon activation, ComD activates the response regulator, ComE, through phosphorylation. Activated ComE then initiates the transcription of various genes including *comX*, which is responsible for the induction of competence (Yang and Tal-Gan, 2019).

S. mutans is most known for its role in dental caries formation, but it can also cause other infections including bacteraemia and infective endocarditis (IE) (Nomura et al., 2020). Bacteraemia occurs when oral bacteria are spread to the blood stream usually by professional dental treatment, daily oral hygiene routines including brushing and flossing, or even chewing food (Nakano et al., 2008) In healthy patients, bacteraemia usually clears up on its own, but for more

established infections or in immune suppressed/immunocompromised patients, symptoms can include fever, chills, and shaking or shivering. Treatment for bacteraemia caused by *S. mutans* is usually a course of intravenous antibiotics such as cefazolin or meropenem, as described in a case study by (Nomura et al., 2007) If left untreated, bacteraemia can lead to IE which is a more serious infection, especially in patients with heart conditions or implants (Li et al., 2000). IE is a multisystem disease that results from infection of the endocardial surface of the heart. Although rare, IE is a life-threatening disease that has long-lasting effects even among patients who survive and are cured and disproportionately affects those with underlying structural heart disease and is increasingly linked with healthcare contact, predominantly in patients who have intravascular prosthetic material (Holland et al., 2016). Treatment for IE is achieved with weeks of intravenous antibiotics and in some cases oral antibiotic (Al-Omari et al., 2014).

1.11 Glucosyltransferases

Glucosyltransferases (Gtfs) comprise a large group of enzymes involved in the biosynthesis of oligosaccharides, polysaccharides, and glycoconjugates. Gtf proteins are vastly diverse and facilitate a wide range of functions from structure and storage to signalling (Koo et al., 2002). Gtfs are found in both prokaryotes and eukaryotes and typically display excellent specificity for both the glycosyl donor and the acceptor substrates (Breton *et al.*, 2006). Many groups of oral microorganisms produce Gtfs; these include *Streptococcus sanguinis*, *Streptococcus mutans*, *Streptococcus*

sobrinus, *Actinomyces* spp., *Streptococcus salivarius* and *Lactobacillus* spp. (Bowen & Koo, 2011). Gtfs secreted by *S. mutans* are enzymatic proteins that synthesise adhesive glucans from dietary sucrose (Matsumoto-Nakano, 2018). Gtfs are comprised of three regions: an N-terminal variable region, a C-terminal glucan-binding region, and a highly conserved catalytic region in the middle shown in Figure 1.13 (Zhang et al., 2017).

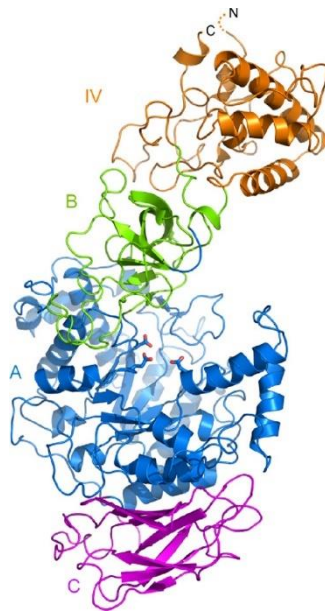


Figure 1.13 shows a crystal structure of Lr2613 GtfB- Δ N Δ V with the four domains A, B, C, and IV indicated. The active site is at the interface of domains A and B, with the three catalytic residues (D679, E717, and D788) shown in stick representation. The figure is prepared with PyMOL and adapted from Pijning et al., (2021).

S. mutans produces three genetically distinct Gtfs (GtfB, GtfC, and GtfD); each appears to play a different but overlapping role in the formation of virulent plaque (Bowen & Koo, 2011). After these Gtfs exit the *S. mutans* plasma membrane, they embed themselves into the salivary pellicle where they work to synthesise

glucans from dietary sucrose in addition to providing binding sites for bacterial cells in the developing biofilm (Veloz, Alvear and Salazar, 2019). Gtfs also adsorb to surfaces of other oral microorganisms converting them to glucan producers (Bowen & Koo, 2011). GtfB, which primarily synthesises adhesive, water-insoluble glucans (WIG) rich in α 1, 3-linkages, can adsorb onto the surfaces of *S. mutans* as well as other oral bacteria and stimulate the accumulation of bacterial cells in biofilm (Kawada-Matsuo, Oogai and Komatsuzawa, 2016). GtfC, on the other hand, demonstrates a high affinity to tooth enamel pellicles and substantially aids bacteria adhering onto tooth surfaces by synthesising a combination of WIG and water-soluble glucans (WSG), rich in α 1, 6-linkages. Additionally, both GtfB and GtfC are involved in focusing protons around *S. mutans* and pre-acclimatising of bacteria for the acidic conditions in biofilms. GtfD predominately synthesises water soluble glucans and serves as primers for GtfB to enhance the overall synthesis efficiency of glucans within a biofilm. In general, a biofilm matrix rich in WIG is more porous and favours polysaccharide diffusion through the matrix, permitting even the most embedded bacterial cells in the biofilm (nearest the tooth surface) to ferment sugars and release acids (Xu *et al.*, 2018).

1.12 Mechanisms of Dispersal for Prevention of Oral Biofilm Formation

Biofilm formation is the primary mode of growth for bacteria in most natural and clinical settings. For many pathogenic bacteria, biofilm dispersal plays a crucial role in the transmission of bacteria from environmental reservoirs to human hosts,

in the transmission of bacteria between hosts, and in the worsening and spread of infection within a single host (Kaplan, 2010). Biofilm dispersal can be divided into three distinctive stages: (1) cell detachment from the biofilm colony; (2) translocation of the cells to a new location; and (3) cellular attachment to a substrate in the new location (Kaplan, 2010). In the oral cavity, *S. mutans* cells that detach from dental plaque can be transported to the saliva of another person by direct contact or by means of a vector such as a shared utensil, and then attach to the tooth surface and initiate colonization of the new host (Kaplan, 2010). Commonly, mechanisms of biofilm dispersal can be separated into two broad categories: active and passive. Active dispersal refers to mechanisms that are instigated by the bacteria themselves, while passive dispersal refers to biofilm cell detachment that is facilitated by external forces such as fluid shear, abrasion, predator grazing, and human intervention. At least three distinct modes of biofilm dispersal have been identified: erosion, sloughing, and seeding. Erosion refers to the constant release of single cells or small bundles of cells from a biofilm in small numbers over the course of biofilm formation. Sloughing refers to the abrupt detachment of large segments of the biofilm, usually during the later stages of biofilm formation. Seeding dispersal, also known as central hollowing, refers to the rapid release of many single cells or small clusters of cells from hollow cavities that form inside the biofilm colony. Erosion and sloughing can be either active or passive practices, whereas seeding dispersal is always an active process (Kaplan, 2010) In multispecies biofilms like dental plaque, close relationships between species based on competition, mutualism, predation, or parasitism are

likely to have resulted in the development of several other passive dispersal mechanisms (Sahni and Khashai, 2016). These could include interspecific antimicrobial compounds, quorum-sensing signals, or matrix-degrading enzymes. Additionally, phagocytosis may also contribute to the passive dispersal of oral biofilms (Kaplan, 2010)

Given what is already known about biofilm growth, dispersal, and repopulation in the literature, there are several avenues of biofilm treatments for prevention or eradication that can be utilised. Generally, it is accepted that mechanical approaches such as tooth brushing and flossing are fundamental for the control of dental biofilms, because they can be applied without surgical involvement (Takenaka, Ohsumi and Noiri, 2019). However, even in well-trained patients, satisfactory cleaning of hard-to-reach areas and of the gingival margin is challenging. Brushing and interdental cleaning is especially tricky for elderly patients with physical or mental constraints, isolated teeth, bridge work, or orthodontic appliances. Additionally, even though flossing and interdental brushing have been essential to oral health, systematic reviews and meta-analyses indicate that flossing in addition to tooth brushing may be linked with a small reduction in dental biofilm (Takenaka, Ohsumi and Noiri, 2019). To supplement the effects of mechanical approaches, several antimicrobial agents are now integrated into oral hygiene products such as toothpastes and mouthwashes (Takenaka, Ohsumi and Noiri, 2019). Potential strategies that may overcome biofilm-related antibiotic resistance, focuses on targeting biofilm EPSs,

blocking quorum sensing signalling, and using recombinant phages (Luo et al., 2021).

1.13 Aim and Objectives

The aim of this research is to mitigate the formation of *S. mutans* 25175 biofilm on surfaces using three naturally occurring QQ molecules (p-coumaric acid, tyrosol, and farnesol) by investigating the effects the molecules have on individual components of the EPS while also studying the effect the molecules have on selected human tissue cells. These three molecules were chosen because of the characteristics that constitute them being QQ molecules including their ability to prevent biofilm formation without being bactericidal. In order to study the effects of these molecules on *S. mutans* biofilms, the following objectives have been set:

- determine the MIC of each QQ molecule on *S. mutans* 25175 biofilm
- investigate the effects of QQ molecules on CFU, eDNA, protein, and carbohydrate concentrations of the EPS of *S. mutans* biofilm formed on abiotic surfaces
- determine how QQ molecules effect co-culture interactions of *S. mutans* 25175 with HGF-1 cell line
- investigate the influence of the QQ molecules on gene expression of the water insoluble glucan gene, *gtfb*, from *S. mutans* 25175 biofilm

1.14 Contribution to Knowledge

QQ effects of in Gram-negative bacteria has been widely studied, but there is less research in QQ in Gram-positive bacteria. This research contributes knowledge to the study of QQ in Gram-positive bacteria, specifically *S. mutans* 25175 and QQ molecules naturally found in nature. Additionally, this study hopes to complement or provide an alternative to the current gold standard (chlorhexidine) for dental biofilm prevention.

Chapter 2 Materials and Methods

2.0 Materials

Materials used for the duration of this study were purchased from Thermo Fisher Scientific (U.K.), ATCC (U.K.), Sigma® Life Science (U.K.), Aldrich® (U.K.), Sigma-Aldrich (U.K.), QIAGEN (U.K.), Eurofins Scientific (U.K.), and Corning® (U.K.). All reagents were analytical grade products suitable for scientific research.

2.1 Bacterial Strain

Culti-Loops™ *Streptococcus mutans* ATCC® 25175™ (*S. mutans* 25175) was purchased from Thermo Fisher Scientific (U.K.). This culture comes in sealed foil packaging on dried loops. *S. mutans* 25175 was revived following the indirect (broth) method provided by Thermo Fisher Scientific. The loop was aseptically removed from the foil packaging and was swirled into warmed (37°C) brain heart infusion (BHI) medium until the gelatine film was completely dissolved. For initial revitalisation from the loop, the culture was incubated aerobically at 37°C and 180 rpm for 48 hours.

2.2 Cell Culture

Human gingival fibroblast (ATCC®CRL-2014™) (HGF-1) cells were purchased from ATCC culture collection, U.K. HGF-1 cells are primary adherent fibroblast cells obtained from a white, male *Homo sapiens* aged 28 years. The stocks are prepared with only 4-5 WIG

(PDLs) remaining under recommended culture conditions after cryopreservation. The HGF-1 cell line was maintained in complete Dulbecco's Modified Eagle's Medium- high glucose (DMEM) medium in a humidified 37°C incubator with 5% CO₂.

2.3 Maintenance and Growth conditions of Bacterial and Cell Culture

2.3.1 Media Preparation for Bacterial Culture

All media for bacterial cultures were prepared according to the manufacturer's instructions and sterilized by autoclaving at 121°C for 15 minutes. Sugar solutions were prepared separately in deionised water and autoclaved at 110 °C for 10 minutes. Media were supplemented with the sugar solutions under aseptic conditions after appropriate sterilisation procedures were complete. The media and its composition/description for bacterial culturing and maintenance are shown in Table 2.1.

TABLE 2.1 BACTERIAL CULTURE MEDIA AND DESCRIPTION/COMPOSITION USED FOR *S. MUTANS* 25175 GROWTH AND MAINTENANCE

<i>Bacteria Culture Media</i>	<i>Composition/Description</i>
<i>BHI</i>	Brain infusion solids 12.5 g/L, beef heart infusion solids 5.0 g/L, proteose peptone 10.0 g/L, glucose 2.0 g/L, sodium chloride 5.0 g/L, di-sodium phosphate 2.5 g/L
<i>BHI Agar</i>	Brain infusion solids 12.5 g/L, beef heart infusion solids 5.0 g/L, proteose peptone 10.0 g/L, glucose 2.0 g/L, sodium chloride 5.0 g/L, di-sodium phosphate 2.5 g/L, agar 15.0 g/L

Brain heart infusion (BHI) medium was made by dissolving 37 g BHI powder into deionised water for a final volume of 1 L. BHI agar was made by first making BHI medium then dissolving 15 g/L agar into the BHI medium while being continuously stirred on a magnetic hot plate until the agar was completely melted. Both the BHI medium and the BHI agar were then sterilised by autoclaving at 121°C for 15 minutes. A 0.5 g/mL sucrose solution was made by dissolving 50 g sucrose into a final volume of 100 mL deionised water. The sucrose solution was sterilised by autoclaving it at 110°C for 10 minutes. To make BHI medium supplemented with sucrose, 1% of the total volume of BHI medium was removed and discarded from the sterile BHI medium and replaced with the same volume of the sterile sucrose solution under aseptic conditions. The final concentration of the sucrose supplemented BHI was 1 g/L. All media were stored at room temperature.

2.3.2 Long Term Storage of *S. mutans* 25175

S. mutans 25175 was grown in BHI medium overnight (~18 to 24 hours) at 37°C at 180 rpm. One loopful of inoculum was streaked onto BHI agar plates and incubated overnight at 37°C. A single colony was selected from a plate, inoculated into fresh BHI medium, and incubated overnight at 37°C and 180 rpm. To prepare working stocks, 1 loopful of the liquid culture was streaked onto BHI agar slants, incubated overnight at 37°C, and placed in 4°C storage. To prepare stocks for -80°C storage, 20% (v/v) glycerol was added to the overnight grown liquid culture and vortexed until thoroughly mixed. The glycerol stocks were aliquoted into 1

mL cryovials and stored at -80°C. The working stocks were refreshed every 6 months by culturing stocks from -80°C storage.

2.3.3 Media preparation for Cell Culture

The HGF-1 cell line was maintained using complete high glucose (4.5 g/L) Dulbecco's Modified Eagle Medium (DMEM) with phenol red, 10% foetal bovine serum, and 1% (v/v) pen-strep in Corning® 75 cm² Cell Culture Flasks. The culture media and their components/description are shown in Table 2.2.

TABLE 2.2 CELL CULTURE MEDIA AND COMPOSITION/DESCRIPTION USED FOR HGF-1 CELL CULTURE

<i>Cell Culture Media</i>	<i>Composition/Description</i>
<i>Incomplete DMEM</i>	High glucose (4.5 g/L) Dulbecco's Modified Eagle Medium (DMEM) with phenol red
<i>Complete DMEM</i>	High glucose (4.5 g/L) Dulbecco's Modified Eagle Medium (DMEM) with phenol red, 10% foetal bovine serum, and 1% (v/v) pen-strep
<i>Co-culture medium</i>	High glucose (4.5 g/L) Dulbecco's Modified Eagle Medium (DMEM) with phenol red, and 1 g/L sucrose

HGF-1 cells were maintained using DMEM from Sigma® Life Science Lot # RNBH4642. The medium was supplemented with 50 mL of foetal bovine serum (FBS) and 5 mL Pen-Strep. The cell line was maintained in Corning® 75 cm² Cell Culture Flasks. Trypsin-EDTA (1X, 0.25%) Gibco® by Life Technologies™, U.K. was used to detach cells from the surface. Dulbecco's Phosphate Buffered Saline (DPBS) 1X by Corning®, U.K. Lot # 08519006 was used to wash cells. Before

starting any experiment, all media and reagents were warmed in a 37°C incubator for 30 minutes and all materials were sterilised with 70% ethanol before being placed under the biological safety hood. Additionally, all cells were inspected for contamination and allowed to reach between 70-90% confluency before seeding or passaging.

2.3.4 Long Term Storage of HGF-1 cell line

HGF-1 cells were stored cryopreserved in liquid nitrogen for long term storage. Cryovials of HGF-1 cells (5.0×10^5 per mL) were prepared in freezing medium (DMEM with 20% FBS, 1% pen-strep, and 10% DMSO) and allowed to freeze by reducing the temperature by approximately 1°C per minute before submersion into liquid nitrogen.

2.4 Cell Culture Reagents

Trypsin-EDTA (1X, 0.25%) was used to detach the adherent cells from the bottom of T-75 flasks for passaging and seeding. Trypan Blue Solution 0.4% by Sigma® Life Science Lot # RNBH1006 was used to detect live cells from dead cells in solution and was used in tandem with Countess II FL Invitrogen automatic cell counter by Thermo Fisher Scientific which was used to automatically determine the number of cells in solution. Dulbecco's Phosphate Buffered Saline (DPBS) (1X) was used for washing cells. 3-(4,5-Dimethylthiazol-2-yl)-2,5-diphenyltetrazolium bromide (MTT) was used for detecting cellular viability after treatment. Foetal bovine serum (FBS) and pen-strep were used to create

complete DMEM for HGF-1 cell line growth and maintenance. The cell culture reagents and the suppliers used for cell culture are shown in Table 2.3.

TABLE 2.3 CELL CULTURE REAGENTS AND THE SUPPLIERS USED FOR CELL CULTURE

<i>Cell Culture Reagents</i>	<i>Supplier</i>
<i>0.25% Trypsin-EDTA (1X)</i>	Gibco Thermofisher (U.K.)
<i>Trypan Blue Solution 0.4%</i>	Sigma® Life Science (UK)
<i>MTT</i>	Thermofisher Scientific (U.K.)
<i>Dulbecco's Phosphate Buffered Saline (DPBS) (1X)</i>	Gibco Thermofisher (UK)
<i>Penicillin-Streptomycin</i>	Thermofisher Scientific (U.K.)
<i>Foetal Bovine Serum (FBS)</i>	Sigma® Life Science (UK)

2.5 Quorum Quenching Molecule Stock Preparation

The QQ molecules in this study were prepared fresh on each day of an experiment. Each QQ molecule was dissolved in a solvent to obtain the desired stock concentration as described in Table 2.4.

TABLE 2.4 QQ MOLECULES, SOLVENTS, AND STOCK CONCENTRATIONS

<i>QQ Molecule</i>	<i>Solvent</i>	<i>Stock Concentration</i>
<i>p-Coumaric acid</i>	Ethanol	250 mM
<i>Tyrosol</i>	Ethanol	1 M
<i>Farnesol</i>	Methanol	2 M

2.5.1 p-Coumaric Acid

p-Coumaric acid, purchased from Sigma® Life Science U.K., stock was prepared by dissolving 41 mg powdered p-coumaric acid into 1 mL absolute ethanol for a final concentration of 250 mM. Further dilutions of p-coumaric acid were made from the stock using the appropriate media for the experiment. Both the p-coumaric acid stock and the diluted solutions were made fresh on the day of use.

2.5.2 Tyrosol

A 1 M tyrosol (purchased from Aldrich®, U.K.) stock solution was prepared by dissolving 138 mg of concentrated tyrosol in 1 mL of ethanol. The 1 M stock solution was diluted in media to attain appropriate concentrations for each experiment. The tyrosol 1 M stock solution as well as all dilutions were prepared on the day of use.

2.5.3 Farnesol

Farnesol has a density of 886 g/L with a molecular weight of 222.37 g/mol. It is commercially available in a 4 M concentration, and was purchased from Sigma-Aldrich, U.K. Farnesol was diluted to 2 M stock concentrations using methanol. Further dilutions were prepared fresh with media using the 2 M stock. The farnesol 2 M stock solution as well as all dilutions were prepared on the day of use. QQ stock concentrations and their solvents are shown in Table 2.4.

2.6 Methods for Microbiology Assays

2.6.1 Bacterial Inoculum

S. mutans 25175 inoculum was made fresh for each experiment. Using a flame sterilised loop, a culture of *S. mutans* 25175 was taken from streaked stock slants in the fridge and gently swirled into 12 mL BHI medium in a 50 mL Falcon tube using aseptic techniques. The liquid culture was incubated aerobically overnight (~18 to 24 hours) at 37°C at 180 rpm. After overnight growth, the inoculum was normalised to 0.100 OD at 600 nm by adding 38 mL fresh BHI medium. This protocol was used for the entirety of the research and ensured approximately the same number of *S. mutans* 25175 cells per mL in liquid culture.

2.6.2 *S. mutans* 25175 Biofilm formation on various Surfaces

S. mutans 25175 biofilm was formed on a variety of surfaces including both biotic and abiotic surfaces. *S. mutans* 25175 inoculum was prepared and normalised as described in 2.2.1. A 20% (v/v) inoculum was used for each biological replicate to ensure unbiased results throughout the study. When *S. mutans* 25175 biofilm formation was desired, the appropriate medium was supplemented with 1 g/L of sucrose.

2.6.2.1 Bacterial Biofilm formation in 96-Well Plates

S. mutans 25175 biofilms were formed in Costar 96-well plates purchased from Corning®, U.K. Fresh BHI medium supplemented with 1 g/L sucrose was inoculated with 20% (v/v) of *S. mutans* 25175 inoculum as previously described (2.2.1) for a total volume of 200 µL per well. The plates were incubated

aerobically overnight (~18 to 24 hours) at 37°C in a stationary incubator. Spent medium was removed from the wells, and the wells were gently washed with 1 X PBS. The *S. mutans* 25175 biofilms formed in 96-well plates were then used for various analytical assays.

2.6.2.2 Bacterial Biofilm Formation in Test Tubes

S. mutans 25175 biofilm formed in 15 mL Falcon tubes were used to analyse various components of the EPS. Fresh BHI medium supplemented with 1 g/L sucrose was inoculated with 20% (v/v) of *S. mutans* 25175 inoculum as previously described (2.2.1) for a total volume of 3 mL per tube. The tubes were incubated aerobically overnight (~18 to 24 hours) at 37°C in a stationary incubator. Spent medium was gently aspirated from the tubes, and the biofilm was gently washed with 1 X PBS. To remove the biofilm from the surface of the test tube, 3 mL PBS was added to the test tube and vortexed until all biofilm was suspended in the PBS. The homogenate was then used to analyse various elements of the *S. mutans* 25175 biofilm.

2.6.2.3 Bacterial Biofilm Formation on HA Disks

Hydroxyapatite disks (1cm thickness; 5 cm diameter) (acquired from Himed NY, USA) of either full density or 20% porosity (calcium deficient) were used as a surface for biofilm growth. HA disks (sterilised at 121°C for 15 minutes) were carefully and aseptically placed in the centre of wells of a 6-well plate using sterilised forceps. BHI medium supplemented with 1 g/L sucrose plus 20% (v/v) *S. mutans* 25175 inoculum prepared as previously described (2.2.1) for a total

volume of 3 mL was placed in each well so that the HA disk was fully submerged in liquid. The plates were then placed in a stationary, aerobic incubator at 37°C (~18 to 24 hours). After incubation, the spent medium was carefully removed from the wells. The HA disks were gently washed with PBS to remove any loosely attached cells. The disks were then aseptically collected and placed into a 50 mL Falcon tube with 3 mL PBS. The HA disks were vortexed vigorously until the biofilm was detached. The HA disks were carefully removed from the Falcon tubes and the *S. mutans* 25175 biofilm homogenate was used for further analysis.

2.6.3 Determining the MIC of the QQ molecules

To determine the MIC of the QQ molecules, the microdilution method was used as described by Andrews (2001). *S. mutans* 25175 inoculum was grown and normalised as described in section 2.2.1. Stock solutions of the QQ molecules were prepared as described in section 2.6 and serially diluted in BHI medium supplemented with 1 g/L sucrose. In each column of a 96-well plate, 125 µL of each QQ molecule dilution was added to 125 µL of normalised *S. mutans* 25175 inoculum. The plates were serially diluted from left to right (250 mM to 0.5 mM) so that higher concentrations of the QQ molecules were on the left and decreased as it moved to the right. The plate was incubated overnight (~18 to 24 hours) at 37°C in air allowing the bacterial biofilm to form in the presence of the QQ molecules. The results were determined via visualization: the first column where there was no visible growth before a column with visible growth was determined to be the MIC for that QQ molecule. The MIC was determined independently three times to ensure repeatability.

2.6.4 Growth curve

Calculating the number of cells in a suspension as per unit of time can be determined by performing a growth curve experiment. The number of cells and doubling times can be determined in liquid culture. In a sterile 500 mL conical flask, 25 mL (10% of total working volume) of *S. mutans* 25175 inoculum (grown and normalised as described in section 2.2.1) was added to 225 mL of BHI medium. The flask was incubated aerobically at 37°C at 180 rpm. Samples (1 mL) were taken every hour for 12 hours. The OD₆₀₀ was taken in triplicate in a microtiter plate for each sample. The sample was also serially diluted and spot plated in triplicate onto BHI agar plates to enumerate the live cells per mL. The plates were incubated aerobically overnight at 37°C and the visible colonies were counted the following day. Each experiment was done independently three times (n=9).

2.6.5 Analysis of components of the extracellular matrix of *S. mutans* 25175 biofilm

To study various components of the *S. mutans* 25175 biofilm, microbiological, colorimetric, and fluorometric tests were done on either the *S. mutans* 25175 biofilm formed directly on the surfaces or when the biofilm was removed and homogenated.

2.6.6 Colony Forming Unit (CFU) method for cell viability

The Colony Forming Unit (CFU) method is a sensitive and broadly accepted method in microbiology that is utilized for testing the effect of antimicrobial

substances. In the CFU method, the number of living cells (cells able to reproduce) present in a suspension is counted on a nutrient agar surface. Bacterial cells were collected and suspended in PBS. The cell suspension was then diluted in a series of 10-fold dilutions in order to obtain plates with a countable number of bacterial colonies. Then 10 μ L of the diluted cell suspension from each dilution was spot plated in replicates of 3 on BHI agar plates. The plates were incubated at 37°C overnight (~18 to 24 hours). Each visible colony is termed a colony forming unit (CFU), and the number of CFUs is related to the viable number of bacteria in the sample. The number of bacteria in the original sample was calculated mathematically, factoring in the volume plated and its dilution factor. The results are presented as log CFU/mL.

2.6.7 Qubit® dsDNA broad spectrum assay method for eDNA quantification

The eDNA of the *S. mutans* 25175 biofilm was quantified using the Qubit® dsDNA broad spectrum assay method. The Qubit® dsDNA broad range (BR) assay is a highly selective assay for double-stranded DNA (dsDNA) over RNA and is designed to be accurate for initial sample concentration in the range 100 pg/ μ L – 1,000 ng/ μ L. Common contaminants, such as salts, free nucleotides, solvents, detergents, or protein are well tolerated in the assay. *S. mutans* 25175 biofilm samples were collected and suspended in PBS and then aliquoted into 1 mL Eppendorf tubes. A Qubit® working solution was prepared by diluting the Qubit® dsDNA BR Reagent 1:200 in Qubit® dsDNA BR Buffer at room

temperature. Then, 10 μL of each sample was added to 190 μL of Qubit[®] working solution. The solution was vortexed for 2 - 3 seconds and incubated at room temperature for 2 minutes. The samples were then inserted into the Qubit[®] Fluorometer and the values were recorded. This experiment was done independently three times and each sample was analysed in triplicate.

2.6.8 Phenol-sulfuric acid method for carbohydrate analysis

The amount of carbohydrates in *S. mutans* 25175 biofilm was measured using the phenol-sulfuric acid assay adopted from Masuko *et al.*, (2005). Among several colorimetric methods for carbohydrate analysis, the phenol-sulfuric acid method is one of the easiest and most reliable methods. The carbohydrate analysis was done in Costar 96-well microtiter plates. Samples of *S. mutans* 25175 biofilm suspended in PBS (50 μL) were placed in the wells. Then 150 μL of concentrated sulfuric acid was added to the sample immediately followed by 30 μL of 5% phenol. The plate was then placed in a 90°C water bath for 5 minutes and then allowed to cool to room temperature for 5 minutes before the absorbance was measured at 490 nm. Each sample was tested in triplicate and each test was done independently 3 times for reproducibility. The standard curve for carbohydrates was done using a range from 0 to 100 $\mu\text{g}/\text{mL}$ of glucose. The equation from the standard curve was used to determine the quantity of carbohydrates in each sample.

2.6.9 Bradford Assay for protein quantification

The Bradford protein assay, developed by Marion M. Bradford in 1976, is a protein determinant method widely used due to its rapid and convenient protocol as well as its relative sensitivity (Ernst and Zor, 2010). The assay involves the stable binding of Coomassie Brilliant Blue G-250 to proteins in a sample (Bradford, 1976). The Bradford assay is able to detect protein concentrations in a linear range between 0 - 10 mg/mL in samples based on a range of standards using bovine serum albumin (BSA) (Ernst and Zor, 2010). Samples with protein concentrations higher than the linear range must be diluted with deionized water to fall within the linear range and re-assayed for accurate results (Bio-rad.com, 2019). Each sample of *S. mutans* 25175 biofilm homogenate in PBS (150 μ L) was placed in a well followed by 150 μ L of the Bradford reagent (room temperature) and allowed to incubate at room temperature for 5 minutes before the results were read with a spectrophotometer. The absorbance was read at 595 nm. The standard curve was determined using the Bio-Rad Quick Start™ Bovine Serum Albumin Standard Set #5000207. Dilutions for the standard curve were carried out using distilled water as the diluent and followed the microassay protocol in the provided instruction manual. The assay was performed in a Costar 96-well microtiter plate. The absorbance was read at 595 nm using a SPECTROstar Nano spectrophotometer by BMG Labtech. The Bradford assay was repeated independently 3 times with 3 biological repeats for each sample.

2.6.10 Crystal Violet Assay

The crystal violet (CV) assay is a preferred method for quantifying microbial biofilms formed in 96-well flat bottom microtiter plates because of the ease, low cost, and flexibility that it offers. The microtiter plate assay has made it a critical tool for the study of biofilms (O'Toole, 2011). Following this technique, *S. mutans* 25175 biofilm was quantified using the microtiter plate protocol. *S. mutans* 25175 biofilm was formed in 96-well flat bottom wells as described in section 2.7.2.1. After overnight incubation, the contents of the wells were gently removed and the plates were gently washed with water three times to remove any unattached biomass. Crystal violet (1%) was then added to each well for 15 minutes at room temperature. After incubation, the crystal violet was removed and the wells were gently washed with water until the water ran clear. The plates were then allowed to completely dry in a 37°C incubator. Once dry, acetic acid was added to each well and incubated at room temperature for 15 minutes. After incubation, the contents of the wells were transferred to a new 96-well plate and the absorbance was determined at OD₅₉₅. Each CV assay was done three times with three biological replicates each time.

2.7 Methods for Cell culture and co-culture assays

2.7.1 HGF-1 Cell Culture Methods

All media and reagents were warmed to 37°C in a water bath prior to the cell culture. A static 37°C with 5% CO₂ incubator was used for cell culture incubation.

Work was done in a biological safety hood to avoid contaminations. The work surfaces and tools were sanitised with 70% ethanol prior to use.

2.7.2 Passaging HGF-1 Cells

HGF-1 cells were maintained in Corning® 75 cm² Cell Culture Flasks (T-75 flasks). When 80 - 100% confluency was achieved, the HGF-1 cells were passaged. All media and reagents were warmed to 37°C in a water bath prior to passaging. All spent media were removed and discarded. The cells were gently washed with 10 mL of sterile 1X DPBS. The cells were then detached from the T-75 flask by adding 1 mL of trypsin and incubated for 5 to 7 minutes at 37°C and 5% CO₂. The T-75 flask was firmly tapped on a flat surface to encourage detachment if necessary. Once the cells were detached, 9 mL of fresh medium was added to the flask to deactivate the trypsin and brought the final volume to 10 mL. The detached cells were carefully removed and placed into a sterile 15 mL falcon tube. The cell suspension was centrifuged for 5 to 7 minutes at 125 X g. The supernatant was carefully aspirated and discarded while making sure the pellet was not disturbed. The pellet was resuspended in 10 mL of fresh DMEM and carefully mixed by pipetting up and down gently. To determine the cell concentration, 20 µL of the cell suspension was mixed with 20 µL of Trypan Blue Solution and then 10 µL of the mixed cell suspension and Trypan Blue Solution was added to either side of the chambers of an automatic cell counter slide. Each side of the automatic cell counter slide was inserted into the automatic cell counter and the average of the number of live cells per mL was recorded. The average number of live cells per mL was used for calculating the number of cells

to seed. New T-75 flasks were seeded with 5×10^5 HGF-1 cells and enough fresh DMEM to reach a total volume of 10 mL. The HGF-1 cells were allowed to reach 80 - 100% confluency before further seeding or passaging and spent medium was replaced twice a week.

2.7.3 Seeding Cells in 96 and 12-well Plates

To seed HGF-1 cells for experimentation, the HGF-1 cells were detached, collected, and counted as described in section 2.8.2. The average number of cells per mL was used to determine the volume of the cell suspension needed for seeding 5,000 cells per cm^2 . Fresh DMEM was used to dilute the cell suspension for the required experiments. For cell seeding in 96-well plates, 5,000 cells per cm^2 were aliquoted to a total volume of 100 μL to each well and incubated at 37°C in 5% CO_2 until a visible monolayer of cells was formed (about 48 hours). For cell seeding in 12-well plates, 5,000 cells per cm^2 were aliquoted to a total volume of 500 μL to each well and incubated at 37°C in 5% CO_2 until a monolayer of cells was formed (about 48 hours).

2.7.4 Treating HGF-1 Cells with QQ molecules

HGF-1 cells were allowed to reach 100% confluency after seeding (about 48 hours) in either 96-well plates or 12-well plates before experimentation. On the day of treatment, the spent medium was removed, and the cells were washed with equal volumes of 1 X DPBS. The QQ molecules were prepared in DMEM and warmed to 37°C prior to application. The QQ preparations were applied to the cells and allowed to incubate for 10, 20, or 30 minutes at 37°C in 5% CO_2 .

The treatments were carefully aspirated from the wells and the HGF-1 cells were ready for further analysis.

2.7.5 HGF-1 Cellular viability: 3-(4,5-Dimethylthiazol-2-yl)-2,5-diphenyltetrazolium bromide (MTT) Assay

After treatment with QQ molecules for 10, 20, or 30 minutes, the spent medium was gently aspirated and discarded. The cells were then gently washed with 100 μ L of 1X DPBS. Fresh DMEM medium (100 μ L) was added to each well along with 10 μ L of MTT. Then the plate was covered with foil and incubated for 4 hours at 37°C in 5% CO₂. After 4 hours incubation, all the contents of the wells were aspirated and discarded. DMSO (100 μ L) was added to each well and thoroughly mixed by gently pipetting up and down. The plate was covered with foil and incubated on an orbital shaker for 15 minutes at 75 rpm. The absorbance was read at 570 nm using a spectrophotometer.

2.7.6 Co-culture of *S. mutans* 25175 and HGF-1 Adherence assay

HGF-1 cells were grown until 100% confluence in 12-well tissue culture plates and a monolayer was formed. The spent medium was carefully aspirated, and the cells were washed with 1X DPBS. The QQ treatments were prepared in non-complete DMEM (no antibiotics and no FBS) and warmed to 37°C before application. *S. mutans* 25175 inoculum was prepared in BHI medium and incubated overnight at 37°C. The inoculum was centrifuged and the supernatant was discarded. The pellet was resuspended in 50 mL 1 X DPBS to achieve the correct cellular density. The *S. mutans* 25175 cells were added at 20% (v/v). Each

treatment was applied to the HGF-1 cells for either 10, 20, or 30 minutes before being removed and washed with 1X DPBS 5 times to ensure any unattached bacteria were removed from the cells. The HGF-1 cells and any adherent *S. mutans* 25175 cells were then detached using 1x Trypsin EDTA (100 μ L). The reaction was stopped after 5 minutes by adding DMEM (900 μ L). Each sample was then spot plated on BHI agar plates in triplicate and incubated at 37°C for 24 hours. The number of visible colonies of *S. mutans* 25175 arose from viable cells attached to HGF-1 cells and were counted. The total number of cells per mL was determined mathematically and analysed as log CFU/mL. The co-culture of *S. mutans* 25175 and HGF-1 adherence assay was done independently three times with three biological replicates each time.

2.7.7 Co-culture of *S. mutans* 25175 and HGF-1 cell line biofilm assay

HGF-1 cells were seeded into 96-well plates and grown to 100% confluency at 37°C and 5% CO₂. The *S. mutans* 25175 inoculum was normalized to the cell density equivalent to 0.1 OD_{600 nm} in 1 x DPBS. The QQ molecules were prepared in incomplete DMEM supplemented with 1% (v/v) sucrose. The QQ molecules (160 μ L) and *S. mutans* 25175 inoculum (40 μ L) were gently pipetted into the wells with the monolayer of HGF-1 cells and was incubated for 20 minutes before being aspirated and discarded. The wells were gently washed 5 times with PBS to remove any remaining QQ molecules and any unattached *S. mutans* 25175 cells. Fresh incomplete DMEM supplemented with 1% (v/v) sucrose (200 μ L) was added to each well and incubated overnight at 37°C and 5% CO₂. The following day, the spent medium was carefully removed, and the wells were

gently washed with PBS and the biofilm was analysed via the crystal violet assay as previously described in section 2.7.12. The co-culture biofilm assay was done independently three times and three replicates were tested for each test.

2.8 Molecular Biology Methods for RT-qPCR

2.8.1 Primers

Table 2.5 shows the primers for *gtfb*, *gtfc*, and *16Ss* genes for *S. mutans* 25175. These primers were obtained from Eurofins Scientific and used for reverse transcriptase quantitative polymerase chain reaction (RT-qPCR).

TABLE 2.5 PRIMER SEQUENCES FOR *GTFB*, *GTFC*, AND *SM16S* USED FOR RT-QPCR

Primer	Sequence	Source
<i>gtfb</i> (forward)	5'-ACTACACTTTTCGGGTGGCTTGG-3'	Villhauer, A., Lynch, D. and Drake, D., (2017)
<i>gtfb</i> (reverse)	5'-CAGTATAAGCGCCAGTTTCATC-3'	
<i>gtfc</i> (forward)	5'-ACA ACA AAC CAG TCT ACA-3'	Yoshida, A. and Kuramitsu, H., (2002)
<i>gtfc</i> (reverse)	5'-CGG ACT GGT TGC TGT ATT-3'	
<i>sm16s</i> (forward)	5'-CCG GTG ACG GCA AGC TAA-3'	Yoshida, A. and Kuramitsu, H., (2002)
<i>sm16s</i> (reverse)	5'-TCA TGG AGG CGA GTT GCA-3'	

The MIC of p-coumaric acid, tyrosol, and farnesol for *S. mutans* 25175 biofilm were determined to be 31 mM, 125 mM, and 1 mM respectively. The MICs of these QQ molecules were used as a reference point for RT-qPCR. For RT-qPCR, the MIC and subinhibitory concentrations (1/2 of the MIC and 1/4 of the MIC) of each QQ molecule were used as treatments for *S. mutans* 25175 biofilms formed in test tubes. The cells were harvested via centrifugation. The supernatant was discarded, and the pellet was used for RNA extraction and followed the protocols for RNA extraction using the QIAzol® Lysis Reagent method.

2.8.2 RNA Extraction

RNA was extracted from *S. mutans* 25175 cells using QIAzol® Lysis Reagent as described by the manufacturer's instructions. Overnight liquid cultures (1 mL) were harvested via centrifugation for 5 minutes at 14,000 rpm in 1.5 mL Eppendorf tubes. The supernatant was discarded, and the pellet was resuspended in 1 mL QIAzol® by gently pipetting up and down until a homogeneous mixture was attained and was allowed to incubate at room temperature for 5 minutes. Following incubation, 0.2 mL chloroform per 1 mL QIAzol was added to the homogenate and shaken vigorously for 15 seconds. The homogenate was then incubated at room temperature for 2 - 3 minutes. After incubation, the homogenate was centrifuged at 12,000 x *g* for 15 minutes at 4°C. Upon completion of centrifugation, the upper aqueous layer was transferred to a new Eppendorf tube taking care to avoid the interface to which 0.5 mL isopropanol per 1 mL QIAzol Lysis Reagent pipetted in step 1 was added and thoroughly vortexed. The tube was incubated at room temperature for 10 minutes

and then centrifuged at 12,000 x g for 10 minutes at 4°C. The supernatant was carefully aspirated and discarded. Then 1 mL of 75% ethanol per 1 mL QIAzol Lysis Reagent pipetted in step 1 was added and centrifuged at 7,500 x g for 5 minutes at 4°C. The supernatant was discarded, and the RNA pellet was dried using a heating block at 37°C for 5 minutes. Once all the ethanol was evaporated, the RNA was dissolved in 50 µL of nuclease-free water and incubated at 37°C for 15 minutes. Nanodrop was done on 1 µL of the final RNA product. The RNA was stored in -80°C until it was used for reverse transcription.

2.8.3 Reverse Transcription

Complimentary DNA (cDNA) was synthesised from the extracted RNA using the QuantiTect Reverse Transcription Kit by Qiagen and no modifications were made from the manufacturer’s protocol. The template RNA was thawed on ice along with gDNA Wipeout Buffer, Quantiscript Reverse Transcriptase, Quantiscript RT Buffer, RT Primer Mix, and RNase-free water. The genomic DNA elimination reaction was prepared according to Table 2.6 and then stored on ice.

TABLE 2.6 DNA ELIMINATION REACTION COMPONENTS, VOLUMES, AND FINAL CONCENTRATION

Component	Volume/reaction	Final concentration
gDNA Wipeout Buffer, 7X	2 µL	1X
Template RNA	Variable (up to 1 µg)	-
RNase-free Water	Variable	-
Total Volume	14 µL	-

The reaction mix was then incubated for 2 minutes at 42°C and immediately placed on ice. The reverse-transcription master mix was prepared on ice according to Table 2.7.

TABLE 2.7 REVERSE TRANSCRIPTION MASTER MIX REACTION FOR 20 μ L FINAL WORKING VOLUME

Component	Volume/reaction	Final concentration
Reverse-transcription master mix	-	-
Quantiscript Reverse Transcriptase	1 μ L	-
Quantiscript RT Buffer, 5X	4 μ L	1X
RT Primer Mix	1 μ L	-
Template RNA	-	-
Entire genomic DNA elimination reaction	14 μ L (add at step 5)	-
Total Volume	20 μL	-

The template RNA from the third step (14 μ L) was added to each tube containing the reverse-transcription master mix and stored on ice. The reactions mixtures were then incubated for 15 minutes at 42°C. Subsequently, the reaction mixtures were incubated at 95°C for 3 minutes to inactivate the Quantiscript Reverse Transcriptase. The synthesised cDNA was then stored at -20°C until it was needed for RT-qPCR.

2.8.4 RT- qPCR Protocol

The RT-qPCR experiments were done using a Bio Rad CFX96™ Real-Time System in Bio Rad Hard-Shell® 96-Well Microplates. The method required by PowerUp™ SYBR™ Green Master Mix from Applied Biosystems by Thermo Fisher Scientific was used to amplify the cDNA. The protocol from the PowerUp™ SYBR™ Green Master Mix was used and no changes were made. The required number of reactions (plus 10% to account for pipetting errors) was prepared using Table 2.8.

TABLE 2.8 RT-QPCR REACTION MIXTURES

Component	Volume (10 µL/well)	Volume (20 µL/well)
PowerUp™ SYBR™ Green Master Mix (2X)	5 µL	10 µL
Forward and Reverse Primers	Variable	Variable
DNA template + Nuclease-Free Water	Variable	Variable
Total	10 µL	20 µL

The components were mixed thoroughly by centrifuging briefly to spin down the contents and eliminate any air bubbles. The reaction mixture (10 µL) was transferred to each well of the optical plate. The plate was sealed with an optical adhesive cover and centrifuged briefly to spin down the contents of the wells and eliminate any air bubbles. The method used to amplify the reactions was the Fast Cycling Mode and followed the steps as listed in Table 2.9.

Table 2.9 Rt-qPCR fast cycling mode protocol

Step	Temperature	Duration	Cycles
UDG activation	50°C	2 minutes	Hold
Dual-Lock™ DNA Polymerase	95 °C	2 minutes	Hold
Denature	95 °C	1-3 seconds	40
Anneal/extend	60 °C	30 seconds	40

Data from qPCR were analysed using the $2^{-\Delta\Delta CT}$ method with the *sm 16s* gene as the reference gene for normalisation (Rao, Lai and Huang, 2013).

2.9 Statistical Analysis

All experiments were done in triplicate with three biological repeats (n=9) unless otherwise stated. Data were analysed using GraphPad Prism 9.2.0 (San Diego, U.S.A.). Differences between groups (>2) of means were analysed using one-way ANOVA followed by Dunnett's multiple comparison test to investigate the differences among samples when compared to a control. Statistical significance was achieved when $p < 0.05$. Calculations of concentrations in samples were determined from a standard curve using linear regression.

Chapter 3 Results

3.0 Introduction to the Results

The focus of this research is to mitigate *S. mutans* 25175 biofilm formation on different surfaces, particularly oral, and determine the effect of three naturally occurring QQ molecules (p-coumaric acid, tyrosol, and farnesol) on specific components of the EPS in the ECM of the biofilm. Due to several virulence factors, *S. mutans* is a primary colonizer of dental biofilms in the oral cavity and a model organism for dental biofilm research (Díaz-Garrido et al., 2020). *S. mutans* is routinely present as part of normal flora in the human oral cavity but, under the right conditions, is an opportunistic pathogen (Phumat et al., 2018). The use of QQ molecules to prevent or eradicate bacterial biofilms is being studied as possible treatment options for biofilm related infections (Roy et al., 2018). P-coumaric acid, tyrosol, and farnesol are the QQ molecules used in this study. This research investigates *S. mutans* 25175 biofilm formation in the presence of the QQ molecules on both biotic and abiotic surfaces mimicking those found in the oral cavity. This research focused on certain individual components of the *S. mutans* 25175 biofilm including the proteins, carbohydrates, eDNA, and bacterial cells imbedded within the matrix of the biofilm because these specific components are known to provide support and protection to the *S. mutans* cells within the biofilm from outside influences (Rainey et al., 2019) The efficacy of the QQ molecules to prevent adherence of *S. mutans*

25175 to tissue cells (HGF-1) and biofilm formation was also examined to better understand how these QQ molecules interact with human tissues cells.

This chapter is divided into three sections. Section 1 investigates the effects of p-coumaric acid, tyrosol, and farnesol on *S. mutans* 25175 biofilm formation on polystyrene plastic surfaces such as test tubes and microtiter plates in the presences of the MIC and subinhibitory concentrations of the QQ molecules. Section 2 examines the effects the QQ molecules have on *S. mutans* biofilm formation on HA surfaces, mimicking the tooth surface in the oral cavity where dental biofilm formation of *S. mutans* can lead to the formation of dental caries. This section also explores the differences between 'healthy' and 'unhealthy' HA surfaces by using full density and 20% porosity HA disks. Section 3 of this study focuses on how the QQ molecules interact with soft tissue like the gingiva in the oral cavity. This section describes the toxicity of the QQ molecules on the HGF-1 cell line as well as the ability for the QQ molecules to prevent the adherence of *S. mutans* 25175 to the HGF-1 cells. This section further studies the effects of different treatment times of the QQ molecules on HGF-1 cells to determine the optimal outcome where the fewest number of *S. mutans* 25175 cells adhere to and form biofilms on the cell tissue monolayer.

3.1 Results Section 1: Microbiological Profile of *S. mutans* 25175 Biofilm

3.1.1 Introduction to Section 1 Results

The formation of dental caries occurs when bacteria adhere to and colonize tooth surfaces and subsequently form biofilms. Bacteria metabolize dietary sugar to form glucans that provide support and structure to the biofilm while at the same time produce acids that demineralize the HA surface of the tooth exposing the soft tissues of the inside of the tooth (like the dentin and pulp) to bacterial infections. *S. mutans* is the etiological agent for dental caries in humans. *S. mutans*' virulence factors including biofilm formation, acidogenicity, and acid tolerance allows it to thrive in the oral cavity (Guan et al., 2020). If tooth decay is identified before carious lesions form, fluoride treatments at a dental practice can potentially strengthen the enamel and reverse the decaying process. However, if a carious lesion is formed, filling the cavity with composite materials can prevent the infection from spreading further. In incidences where the infection has spread deeper into the tooth, crowns, root canals, and tooth extraction may be necessary to prevent the spread of infection to other teeth. Therefore, prevention of oral biofilm formation is the recommended course of action to deter later consequences imposed by dental biofilms. Brushing the teeth twice a day in addition to flossing once a day are the current recommendations for prevention of dental biofilm formation, but despite a person's best efforts, cavity formation can still occur. Antibiotics treat bacterial infections but are unable to penetrate the matrix of biofilms to kill the embedded bacterial cells and therefore is not an

acceptable treatment for dental biofilms. One suggestion of bacterial biofilm prevention is the use of QQ molecules. QQ molecules are small molecules that are similar to quorum sensing molecules that bacteria use to communicate in biofilm formation. By disrupting the communication process, bacteria cannot adequately form biofilms. Because of this, QQ molecules as a preventative treatment for biofilm formation has been proposed (Muras et al., 2018).

In this section, different aspects of *S. mutans* 25175 was studied including the growth curve in liquid culture, the determination of the generation time of a planktonic culture, and the media and air conditions required for *S. mutans* 25175 biofilm formation including optimum sugar supplementation. Once the optimum biofilm growth conditions for maximum biomass accumulation were achieved, the MIC of three QQ molecules was determined. Based on the MIC results, the impact of the three QQ molecules (p-coumaric acid, tyrosol, and farnesol) on various components of the EPS, namely the viable cells, proteins, carbohydrates, and eDNA of *S. mutans* 25175 biofilm formation on plastic surfaces was studied *in vitro*.

3.1.2 *S. mutans* 25175 Growth Curve and Doubling Time

If bacteria are introduced to fresh medium in a closed environment, like a conical flask, the population of cells will increase exponentially until all the available nutrients are exhausted and exhibits growth phases including lag phase, log phase, stationary phase, and death phase. During the lag phase, bacteria adjust to the new environment. They may not appear to replicate but instead the cells

may increase in volume. Bacterial cells replicate and grow exponentially in the log phase. During the log phase, the culture reaches the maximum growth rate, which could be estimated by generation time or doubling time. The culture arrives at stationary phase when the number of dividing cells appear to equal to the number of dead cells due to the exhaustion of nutrients. The final phase of bacterial growth is the death phase where bacteria lose the ability to divide and the number of dead cells exceeds that of live cells (Wang et al., 2015). Figure 3.1 shows the growth curve of *S. mutans* 25175 over a period of 12 hours and the absorbance measured at 600 nm every hour.

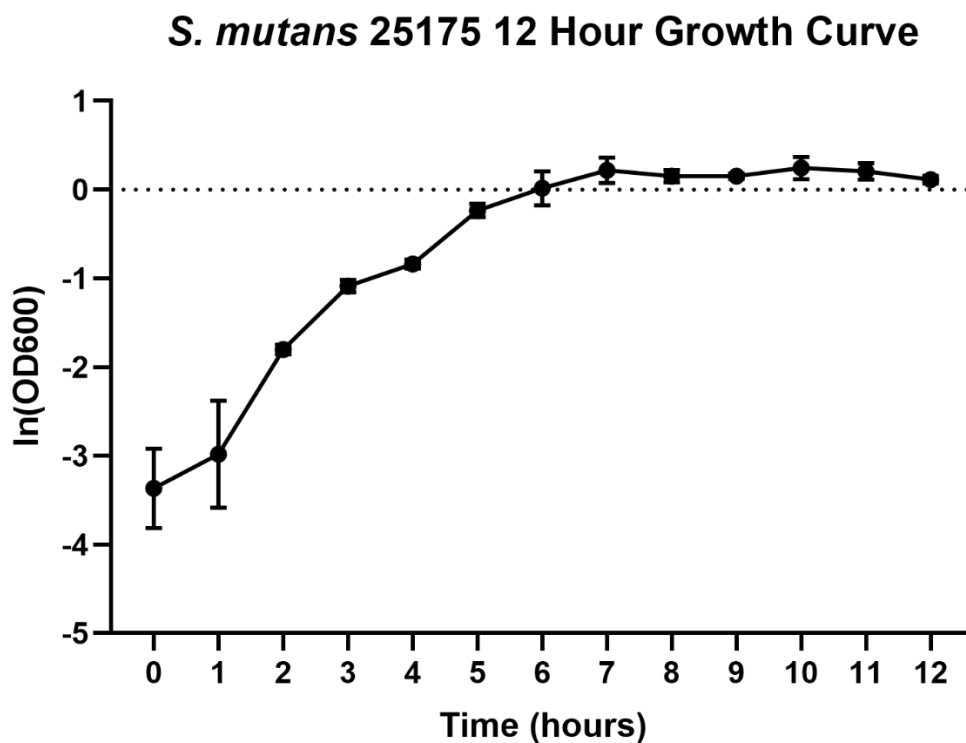


Figure 3.1 *S. mutans* 25175 growth curve plotted as $\ln(\text{OD}_{600\text{nm}})$ as a function of time (in hours) over the course of 12 hours. The error bars indicate the mean \pm the SD. The growth curve was done independently three times with three biological replicates (n=9).

Based on the graph of *S. mutans* 25175 growth curve in Figure 3.1, the values for the time point 0 to the time point 7 appear to be linear and was used to determine the specific growth rate by graphing the values between these two time points and calculating the slope of the line (graph not shown). This graph does not show the three phases of bacterial growth typically seen in liquid cultures but does show that *S. mutans* 25175 exhibits exponential growth and a death phase after 12 hours.

TABLE 3.1 THE GENERATION TIME (IN MINUTES), INITIAL CELL COUNT (CFU/ML), FINAL CELL COUNT (CFU/ML), AND THE TIME (IN HOURS) OF *S. MUTANS* 25175.

	Generation Time (minutes)	Initial Cell count (CFU/mL)	Final Cell count (CFU/mL)	Time between points in Log Phase (hours)
<i>S. mutans</i> 25175	65	3.1×10^8	4.06×10^9	4

According to the data in Table 3.1, the doubling time or generation time of *S. mutans* 25175 was determined to be about 1.1 hours or about 65 minutes using both the OD method and the CFU plating method to correlate the number of cells at a given OD at A_{600} .

3.1.3 Optimisation of Sugar and Air for *S. mutans* 25175 Biofilm Formation

In the literature, there are different growth conditions for successful *S. mutans* growth. *S. mutans* is a facultative anaerobe so it can grow in the presence, as well as in the absence, of oxygen. In order to study individual components of the

S. mutans 25175 biofilm, a high amount of biomass was desired. Additionally, *S. mutans* 25175 formation of biofilm relies on the synthesis of glucans from dietary sucrose. To determine the optimal conditions for *S. mutans* 25175 biofilm formation, sucrose supplementation as well as air conditions were optimised until the greatest quantity of biofilm was achieved. A CV assay (as described in Chapter 2) was done on the biofilms after overnight (~18 to 24 hours) incubation at 37°C in a stationary incubator. Each experiment was done independently three times in triplicates. The results are shown in Figure 3.2.

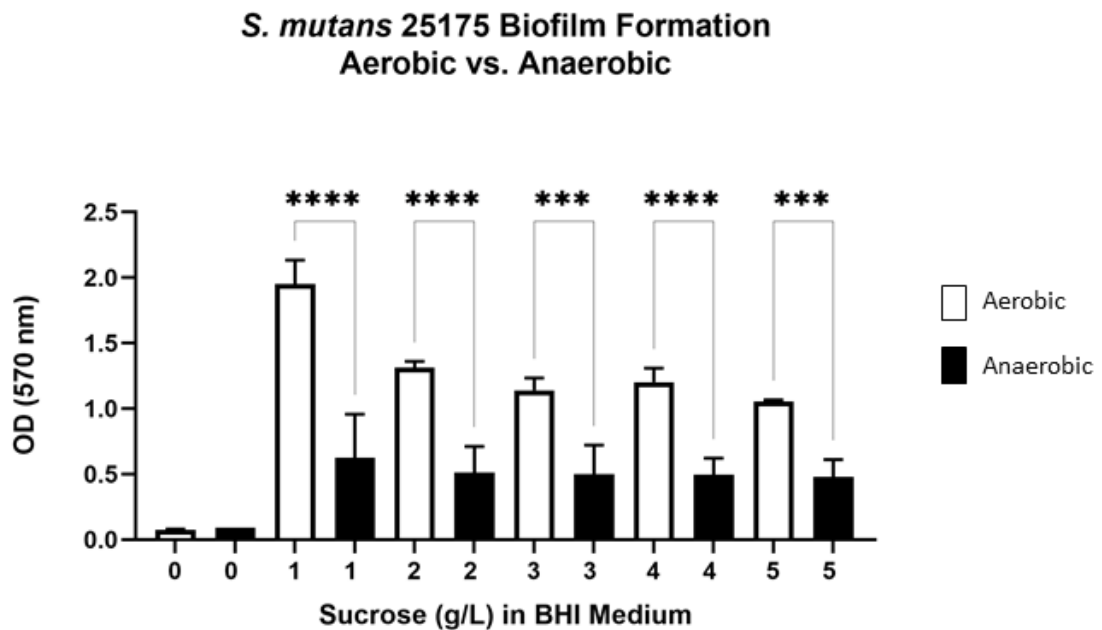


Figure 3.2 *S. mutans* 25175 biofilm formation aerobic versus anaerobic: *S. mutans* 25175 was formed in wells of microtiter plates aerobically (white) or anaerobically (black) at 37°C in BHI medium supplemented with sucrose (0 to 5 g/L). The experiment was repeated 3 times with 3 replicates (n=9). p < 0.0001 = ****, p (0.0001 to 0.001) = ***, p (0.001 to 0.01) = **, p (0.01 to 0.05) = *.

From the data, it was determined that *S. mutans* 25175 formed more biofilm when the BHI medium was supplemented with sucrose between 1 g/L and 5 g/L as opposed to no sucrose supplementation. Furthermore, it was determined that *S. mutans* 25175 produced a statistically significant more ($p < 0.05$) amount of biofilm in aerobic air conditions as opposed to anaerobic conditions. Based on this set of data, all further experiments involving the formation of *S. mutans* 25175 biofilm were done under these conditions and nutrient supplementation.

3.1.4 Minimum Inhibitory Concentration of QQ molecules on *S. mutans* 25175 Biofilm

p-Coumaric acid, tyrosol, and farnesol QQ molecules were used in this study to investigate their ability to inhibit biofilm formation by *S. mutans* 25175. To determine the effective concentration of each QQ molecule to be used to inhibit *S. mutans* 25175 biofilm formation, their MICs were determined using the microdilution protocol described by Andrews (2001). *S. mutans* 25175 biofilm was grown in 96-well plates as described in Chapter 2. Each experiment contained a negative control (media only), a positive control (20% v/v inoculum in medium with no QQ molecules), and the test comprising serial dilutions of each of the QQ molecules. The initial concentrations were based on literature research using these QQ molecules including Esteban-Fernández et al., (2018) for p-coumaric acid, Arias et al., (2016) for tyrosol, and Cao Li et al., (2017) for farnesol. For each of the QQ molecules, 8 separate replicate experiments were used to ensure reproducibility. The MIC for each QQ molecule was determined independently

three times. Table 3.2 shows the results of each QQ molecule's MIC on *S. mutans* 25175 biofilm formation.

TABLE 3.2 MIC OF QQ MOLECULES ON *S. MUTANS* 25175 BIOFILM FORMATION
 The MIC of p-coumaric acid (31.25 mM), tyrosol (125 mM), and farnesol (1 mM) on overnight (~18 to 24 hours) *S. mutans* 25175 biofilm formation at 37°C. The MIC was done three times in triplicates (n=9).

Quorum Quenching Molecule	MIC of QQ Molecules on <i>S. mutans</i> 25175 Biofilm
p-Coumaric acid	31.25 mM
Tyrosol	125 mM
Farnesol	1 mM

The MICs for each QQ molecule were experimentally determined to be 31 mM, 125 mM, and 1 mM for p-coumaric acid, tyrosol, and farnesol respectively. The MICs determined in this set of experiments established the concentrations that would be used for all other experiments and determined the subinhibitory concentrations (1/2 and 1/4 of the MICs) of each QQ molecule.

3.1.5 Quantification of Total *S. mutans* 25175 Biofilm Biomass

Once the MICs of each QQ molecule were determined, quantification of *S. mutans* 25175 biofilm when treated with the QQ molecules at their respective MICs and subinhibitory concentrations (1/2 and 1/4 of their respective MICs) was done using the CV assay method for biofilm quantification. Briefly, stocks of the QQ molecules were made the day of use in their respective solvents and then diluted to the respective MICs in BHI + 1 g/L sucrose medium in triplicate and

inoculated. The plates were incubated overnight (~18 to 24 hours) aerobically at 37 °C. The following day, the spent medium and any unattached cells were discarded from the wells by inversion and gently tapping and a CV assay was done (as described in Chapter 2). The data were analysed by a one-way ANOVA using GraphPad Prism. Each CV assay was done independently three times and the results are shown in Figure 3.3. ($p < 0.0001 = ****$, $p (0.0001 \text{ to } 0.001) = ***$, $p (0.001 \text{ to } 0.01) = **$, $p (0.01 \text{ to } 0.05) = *$).

Effects of QQ Molecules on *S. mutans* 25175 Biofilm

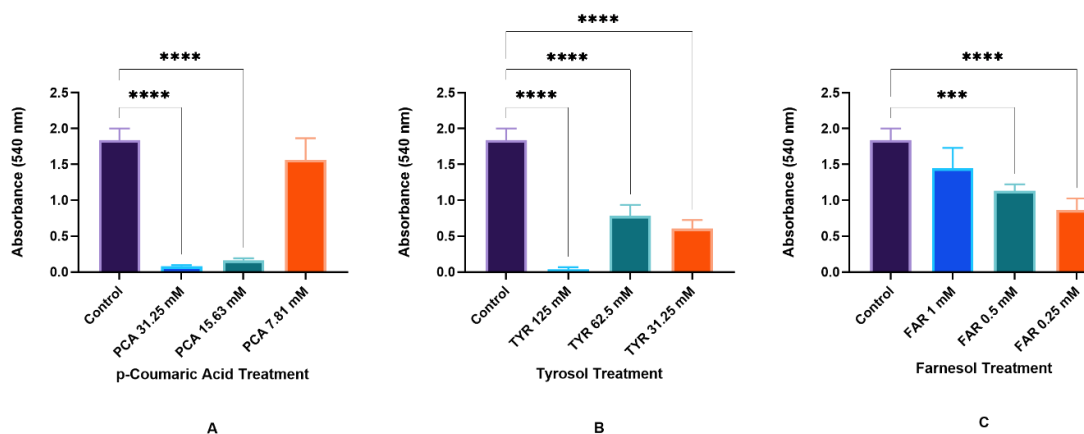


Figure 3.3 Effects of QQ molecules on *S. mutans* 25175 biofilm: Quantification of the whole *S. mutans* 25175 biofilm when treated with p-coumaric acid, tyrosol, and farnesol at their respective MICs and subinhibitory (1/2 and 1/4) MICs as determined by CV assay. Results were analysed by a one-way ANOVA with multiple comparisons using GraphPad Prism. The tests were done in 3 biological replicates with three repeats each time (n=9). ($p < 0.0001 = ****$, $p (0.0001 \text{ to } 0.001) = ***$, $p (0.001 \text{ to } 0.01) = **$, $p (0.01 \text{ to } 0.05) = *$).

The CV assay for quantifying the whole *S. mutans* 25175 biofilm treated with the QQ molecules at their respective MICs and subinhibitory concentrations showed a statistically significant decrease in *S. mutans* 25175 biofilm formation with p-

coumaric acid at 31.25 mM and 15.63 mM but not p-coumaric acid at 7.81 mM. There was a statistically significant decrease in *S. mutans* 25175 biofilm formation by tyrosol at each concentration tested (MIC, 1/2 of the MIC, and 1/4 of the MIC). *S. mutans* 25175 biofilm formation was reduced by farnesol at subinhibitory concentrations, but not at farnesol's MIC.

3.1.6 CFU of Cells in the EPS of *S. mutans* 25175 Biofilm

The *S. mutans* 25175 biofilms formed in test tubes were analysed for the cellular component by serial diluting the biofilm mixture that was collected (described in section 3.1) in PBS and spot plating the samples on BHI agar plates in triplicate. The plates were placed in a stationary, aerobic incubator overnight (~18 to 24 hours) at 37°C. The number of colonies that grew on the plate were counted and recorded. The data was analysed using GraphPad Prism. The results are shown as Log CFU/mL in Figure 3.4.

Log CFU/mL of *S. mutans* 25175 cells from biofilm treated with QQ molecules

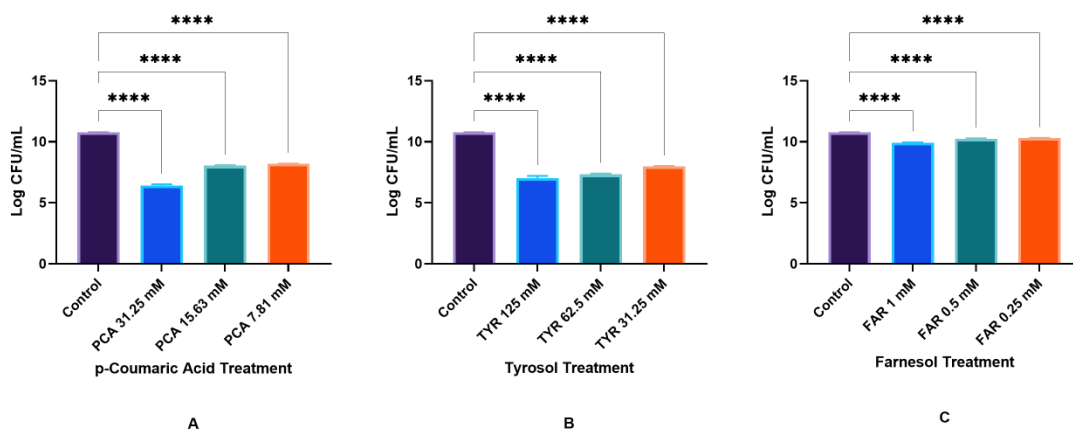


Figure 3.4 Log CFU/mL of *S. mutans* 25175 cells from biofilm treated with QQ molecules: The log CFU/mL of *S. mutans* 25175 biofilm when treated with p-coumaric acid, tyrosol, and farnesol at their respective MICs and subinhibitory (1/2 and 1/4) MICs as determined by spot plating. Results were analysed by a one-way ANOVA with multiple comparisons using GraphPad Prism. The tests were done in 3 biological replicates with three repeats each time (n=3). (p < 0.0001 = ****, p (0.0001 to 0.001) = ***, p (0.001 to 0.01) = **, p (0.01 to 0.05) = *).

There was a statistically significant decrease in the number (log CFU/ mL) of *S. mutans* 25175 cells within the biofilm formed in test tubes when treated with the QQ molecules at their respective MICs and subinhibitory concentrations by each QQ molecule at their respective MICs and subinhibitory concentrations.

3.1.7 Carbohydrates Quantification of the EPS of *S. mutans* 25175 Biofilm

To quantify the carbohydrate component of the *S. mutans* 25175 biofilm, the phenol-sulfuric acid assay was done on overnight *S. mutans* 25175 biofilms formed in test tubes. This experiment was done independently three times and each sample was analysed in triplicate (n=9) as shown in Figure 3.5.

Carbohydrates (mg/L) of *S. mutans* 25175 Biofilm treated with QQ

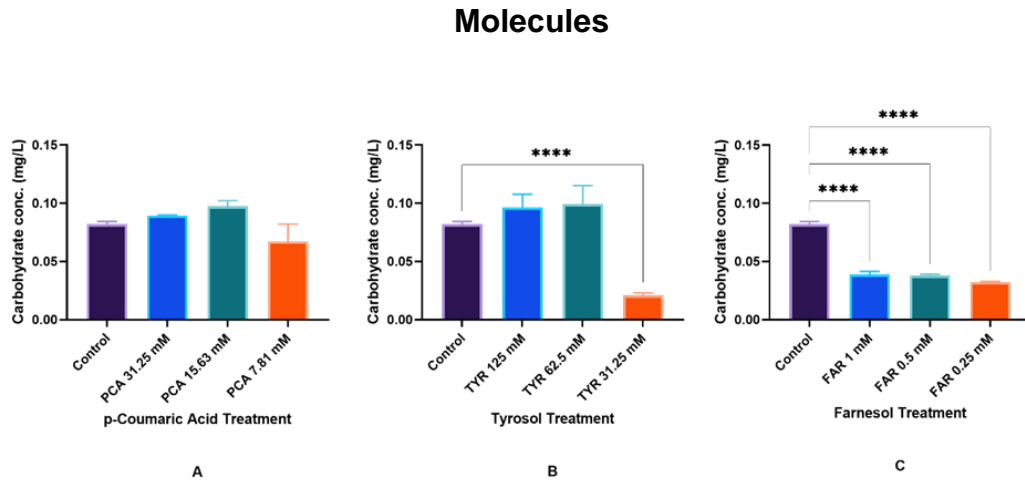


Figure 3.5 Carbohydrates (mg/L) of *S. mutans* 25175 Biofilm treated with QQ Molecules: The carbohydrate concentration (mg/L) of *S. mutans* 25175 biofilm when treated with p-coumaric acid, tyrosol, and farnesol at their respective MICs and subinhibitory (1/2 and 1/4) MICs as determined by spot plating. Results were analysed by a one-way ANOVA with multiple comparisons using GraphPad Prism. The tests were done in 3 biological replicates with three repeats each time (n=9). ($p < 0.0001 = ****$, $p (0.0001 \text{ to } 0.001) = ***$, $p (0.001 \text{ to } 0.01) = **$, $p (0.01 \text{ to } 0.05) = *$).

The amount of carbohydrates (mg/L) in the *S. mutans* 25175 biofilm formed in test tubes was not a statistically significant change when treated with p-coumaric

acid at the MIC and subinhibitory concentrations. Additionally, the amount of carbohydrates (mg/L) in the *S. mutans* 25175 biofilm formed in test tubes was only reduced by tyrosol at 1/4 of the MIC, but not at the MIC or 1/2 of the MIC. There was, however, a statistically significant reduction in the amount of carbohydrates (mg/L) in the *S. mutans* 25175 biofilm formed in test tubes by farnesol at all the tested concentrations (MIC, 1/2 of the MIC, and 1/4 of the MIC).

3.1.8 eDNA Quantification of the EPS of *S. mutans* 25175 Biofilm

The eDNA of the *S. mutans* 25175 biofilm formed in test tubes was quantified using the Qubit® dsDNA broad spectrum assay method previously described in Chapter 2. The *S. mutans* 25175 biofilm samples collected as described in section 3.1 were aliquoted into 1 mL Eppendorf tubes, ready for use in the assay. This experiment was done independently three times and each sample was analysed in triplicate. The results are displayed in Figure 3.6.

eDNA ($\mu\text{g/mL}$) of *S. mutans* 25175 Biofilm treated with QQ Molecules

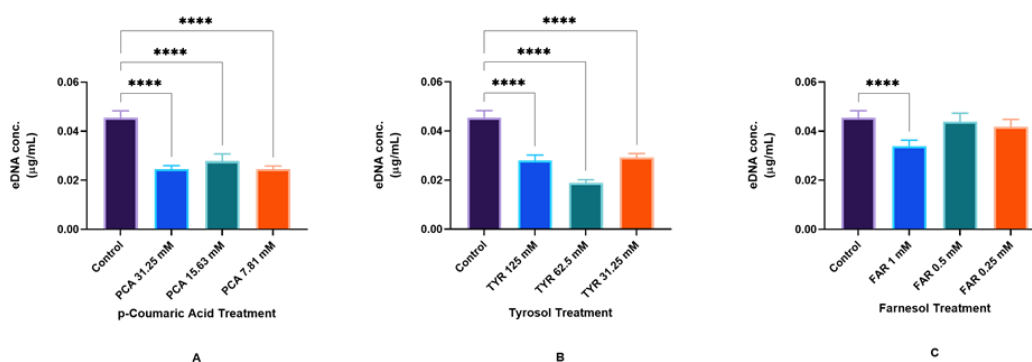


Figure 3.6 eDNA ($\mu\text{g/mL}$) of *S. mutans* 25175 Biofilm treated with QQ Molecules: The eDNA of *S. mutans* 25175 biofilm when treated with p-coumaric acid, tyrosol, and farnesol at their respective MICs and subinhibitory (1/2 and 1/4) MICs as determined by Qubit®. Results were analysed by a one-way ANOVA

with multiple comparisons using GraphPad Prism. The tests were done in 5 biological replicates with three repeats each time (n=15). ($p < 0.0001 = ****$, $p (0.0001 \text{ to } 0.001) = ***$, $p (0.001 \text{ to } 0.01) = **$, $p (0.01 \text{ to } 0.05) = *$).

The amount of eDNA in *S. mutans* 25175 biofilm formed in test tubes was reduced by both p-coumaric acid and tyrosol at their respective MICs and the subinhibitory concentrations. However, farnesol only reduced the amount of eDNA in *S. mutans* 25175 biofilm formed in test tubes at the MIC (1 mM).

3.1.9 Protein Quantification of the EPS of *S. mutans* 25175 Biofilm

Proteins of the *S. mutans* 25175 biofilm formed in test tubes were quantified using the Bradford assay described in Chapter 2. Figure 3.7 shows the amount of protein in each sample. This experiment was repeated independently three times with three replicates each time.

Protein (mg/mL) of *S. mutans* 25175 Biofilm treated with QQ Molecules

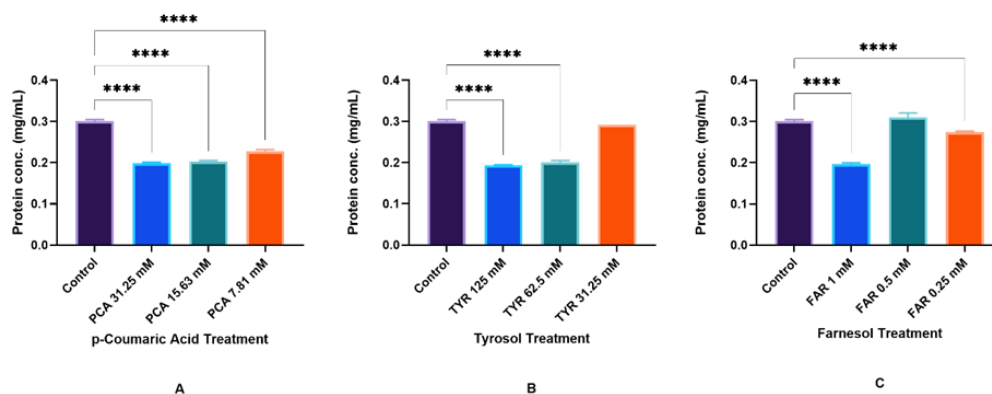


Figure 3.7 Protein (mg/mL) of *S. mutans* 25175 Biofilm treated with QQ Molecules: The total protein concentration of *S. mutans* 25175 biofilm when treated with p-coumaric acid, tyrosol, and farnesol at their respective MICs and subinhibitory (1/2 and 1/4) MICs as determined by the Bradford assay. Results were analysed by a one-way ANOVA with multiple comparisons using GraphPad Prism. The tests were done in three biological replicates with three repeats each time (n=3). ($p < 0.0001 = ****$, $p (0.0001 \text{ to } 0.001) = ***$, $p (0.001 \text{ to } 0.01) = **$, $p (0.01 \text{ to } 0.05) = *$).

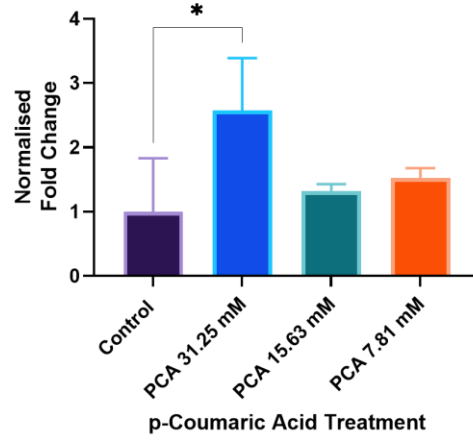
The amount of protein in *S. mutans* 25175 biofilm formed in test tubes was reduced by all the tested concentrations of p-coumaric acid (31.25 mM, 15.63 mM, and 7.81 mM). Tyrosol reduced the protein concentration of *S. mutans* 25175 biofilm formed in test tubes at the MIC and 1/2 of the MIC. Farnesol reduced the protein concentration of *S. mutans* 25175 biofilm formed in test tubes at the MIC and 1/4 of the MIC but not at 1/2 of the MIC.

3.1.10 mRNA Expression of Glucosyltransferase B (*gtfb*) in *S. mutans* 25175

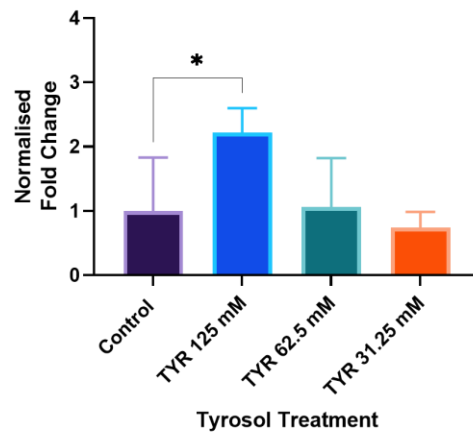
Glucosyltransferases (Gtfs) are proteins that are known to synthesise glucans from dietary sugars. In *S. mutans*, there are three Gtfs (*Gtfb*, *Gtfc*, and *Gtfd*) that

are secreted from the cells and are embedded within the biofilm matrix. In the matrix, these Gtfs synthesise chains of glucans primarily from dietary sucrose whereafter the glucans provide structure and support for the biofilm. The gene expression of *gtfb* was investigated when *S. mutans* biofilm was treated with p-coumaric acid, tyrosol, and farnesol at their respective MIC and subinhibitory concentrations (1/2 and 1/4 of the MIC). The normalized fold change for *gtfb* is shown in Figure 3.8 after treatment with the quorum quenchers. ($p < 0.0001 = ****$, $p (0.0001 \text{ to } 0.001) = ***$, $p (0.001 \text{ to } 0.01) = **$, $p (0.01 \text{ to } 0.05) = *$).

A mRNA Expression of *gffb* in *S. mutans* 25175



B mRNA Expression of *gffb* in *S. mutans* 25175



C mRNA Expression of *gffb* in *S. mutans* 25175

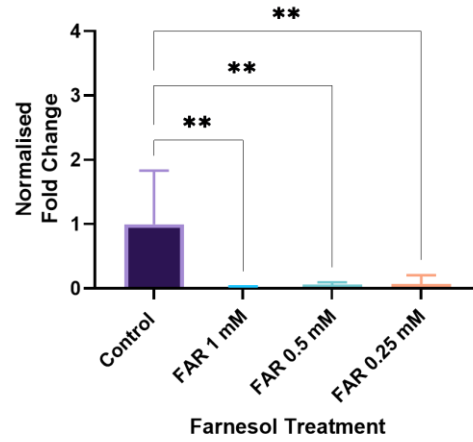


Figure 3.8 mRNA expression of *gtfb* in *S. mutans* 25175 biofilm when treated with (A) p-coumaric acid, (B) tyrosol, and (C) farnesol at respective MIC, 1/2 the MIC, and 1/4 the MIC overnight (~18 to 24 hours). Results are presented as normalized fold change where the untreated control is 1. The error bars represent the SEM (n=9). ($p < 0.0001 = ****$, $p (0.0001 \text{ to } 0.001) = ***$, $p (0.001 \text{ to } 0.01) = **$, $p (0.01 \text{ to } 0.05) = *$).

The results from RT-qPCR showed a statistically significant increase in fold change in *gtfb* of *S. mutans* 25175 when treated with p-coumaric acid at 31.25 mM and tyrosol at 125 mM, but a statistically significant decrease in fold change when treated with farnesol at all concentrations (1 mM, 0.5 mM, and 0.25 mM).

3.1.11 Section 1 Summary

In summary, Section 1 of the results investigated the microbiological profile of *S. mutans* 25175 including the generation time and the optimum sugar requirements for biofilm formation. Section 1 determined the effect of the MIC of the QQ molecules p-coumaric acid, tyrosol, and farnesol on *S. mutans* 25175 biofilm. Furthermore, this section studied the effects that p-coumaric acid, tyrosol, and farnesol at their respective MICs and subinhibitory concentrations have on the eDNA, carbohydrate, and protein concentrations of the EPS and the number of viable cells of *S. mutans* 25175 biofilm when formed on plastic surfaces (test tubes and microtiter plates). To determine the overall, collective effect the QQ molecules had on the biofilm, the data were normalised using mathematical techniques of multiplying all data values together and creating a new unit 'X'. Table 3.2 shows the summary of results for the amounts of protein, carbohydrate, eDNA, CFUs, and total biomass of *S. mutans* 25175 biofilm formed on plastic

surfaces and treated with QQ molecules at their respective MICs and subinhibitory concentrations while also ranking the treatments from 1 to 9 based on a normalized cumulative score as seen in Table 3.3.

TABLE 3.3 SUMMARY OF SECTION 1 RESULTS

A summary and ranking of the protein concentration, carbohydrate concentration, eDNA, CFUs, and total biomass of *S. mutans* 25175 biofilm grown on polystyrene (test tube) surfaces and treated with QQ molecules at their respective MICs and subinhibitory concentrations.

***S. mutans* 25175 biofilms formed on Plastic Surfaces**

Treatment	Protein (mg/mL)	Carbohydrate (mg/L)	eDNA (µg/mL)	CFU (Log CFU/mL)	Total Biomass (OD @ 570 nm)	Score (X)	Rank
PCA 31.25 mM	0.20	0.089	0.025	6.4	0.083	0.00023	2
PCA 15.63 mM	0.20	0.098	0.028	8.0	0.16	0.00073	3
PCA 7.81 mM	0.23	0.067	0.025	8.2	1.6	0.0048	8
TYR 125 mM	0.19	0.096	0.028	7.0	0.037	0.00014	1
TYR 62.5 mM	0.20	0.099	0.019	7.3	0.78	0.0022	5
TYR 31.25 mM	0.29	0.021	0.029	8.0	0.61	0.00086	4
FAR 1 mM	0.20	0.039	0.034	9.9	1.4	0.0037	7
FAR 0.5 mM	0.31	0.038	0.044	10	1.1	0.0060	9
FAR 0.25 mM	0.27	0.032	0.042	10	0.86	0.0033	6

Reduction of *S. mutans* 25175 biofilm formed on polystyrene plastic surfaces using QQ molecules was investigated in this section. Each treatment of QQ molecule exhibited different effects on the various components of the EPS of *S. mutans* 25175 biofilm. The overall effect of the QQ molecules can be summed up mathematically by multiplying the data together to create a new term 'X'. For this data,

$$X = \text{protein concentration (mg/mL)} * \text{carbohydrate concentration (mg/L)} * \text{eDNA } (\mu\text{g/mL}) * \text{CFU (Log CFU/mL)} * \text{total biomass (OD@A}_{570}\text{)}.$$

The treatment with the lowest term (or score X) indicated the best overall treatment since the goal was to reduce the total amount of *S. mutans* 25175 biofilm formed on polystyrene (test tube) surfaces. Interestingly, based on the overall combined data, tyrosol at a concentration of 125 mM (the MIC) was the most efficient at reducing the amount of overall biofilm compared to all the other treatments. Tyrosol at 125 mM did not statistically significantly reduce the amount of carbohydrates in the biofilm but did have statistically significant reduction of the other components of the biofilm measured in this study (proteins, eDNA, CFU, and the overall biomass). There is a good correlation between *gtfb* gene expression and carbohydrate concentrations in this study. p-Coumaric acid and tyrosol at their MICs resulted in no statistically significant change in carbohydrate concentration when compared to the control but increased the fold change of *gtfb*. Farnesol, at all concentrations, reduced the carbohydrate component of the *S. mutans* 25175 biofilm while also decreasing the *gtfb* expression at all concentrations.

3.2 Results Section 2: Study of *S. mutans* 25175 Biofilm Treated with QQ Molecules Formed on Full Density and 20% Porosity HA Disks

3.2.1 Introduction to Section 2 Results

Like many organisms, bacteria have a greater chance of survival when they live in community settings. Bacteria form biofilms for protection from external influences. The self-formed biofilm not only provides protection from external forces, but also houses the bacterial cells and keeps them in close proximity to one another for necessary tasks such as gene and nutrient transfer. As the biofilm matures, bacterial cells near the outermost part of the biofilm will break away and attempt to form new biofilms on other available surfaces. *S. mutans* is considered one of the etiological agents of dental caries and is found in nearly all cases of caries formation. Without the ability to attach to the HA surface of the tooth to form a biofilm, *S. mutans* would persist planktonically in the oral cavity as normal flora. This section of results investigated the components of the EPS of the ECM of *S. mutans* 25175 biofilm formed on full density and 20% porosity HA surfaces in the presence of QQ molecules (p-coumaric acid, tyrosol, and farnesol) at the MIC and subinhibitory concentrations determined in Section 2.

In this section, *S. mutans* 25175 was allowed to form on full density HA disks as well as HA disks with 20% porosity. The differences in porosity represent different aspects of tooth surfaces within the oral cavity where there are some healthy teeth with no enamel erosion (full density) and where there may be some enamel erosion (20% porosity). It was interesting to investigate if *S. mutans* 25175 biofilm was more adapted to form on healthy or damaged surfaces and if there are

differences in the composition of the components of the EPS of the ECM when treated with QQ molecules at their respective MICs and subinhibitory concentrations. The EPS components studied were the protein, carbohydrate, eDNA, and viable cells from the *S. mutans* 25175 biofilm.

The experimental set up for Section 2 was identical for each portion of the EPS that was studied. Briefly, *S. mutans* 25175 inoculum was grown overnight at 37°C and 180 rpm in an aerobic incubator. After overnight incubation the inoculum was normalized to 0.100 OD at A₆₀₀ using BHI medium supplemented with sucrose (1 g/L). The QQ molecule stocks were prepared the day of use as described in Chapter 2. The QQ molecules treatments at their MIC and subinhibitory concentrations were prepared in BHI medium supplemented with sucrose (1 g/L) from the stocks. The HA disks (sterilised at 121°C for 15 minutes) were carefully and aseptically placed in the centre of wells of a 6-well plate. The QQ molecules prepared in the BHI medium were added to each well with the HA disk followed by *S. mutans* 25175 inoculum at 20% (v/v) for a total volume of 3 mL. The plates were placed in a stationary, aerobic incubator at 37°C (~18 to 24 hours). After incubation, the spent medium was carefully removed from the wells. The HA disks were gently washed with PBS to remove any unattached cells. The HA disks were aseptically collected and placed into a 50 mL Falcon tube with 3 mL PBS. The Falcon tubes were vortexed vigorously until the biofilm was removed from the HA disks. The HA disks were carefully removed from the Falcon tubes using sterilised forceps, and the biofilm homogenate was used for analysis.

3.2.2 CFU Enumeration in *S. mutans* 25175 Biofilm Formed on HA Disks

In order to gain a better understanding of the number of viable *S. mutans* cells in the biofilm formed on a HA surface, the CFU was determined. The biofilm formed on the HA disks was analysed for its cellular component by serial diluting the homogenate that was collected and spot plating the samples on BHI agar plates in triplicate. The plates were placed in a stationary, aerobic incubator overnight (~18 to 24 hours) at 37°C. The number of colonies that grew on the plate were counted and recorded.

There was a statistically significant decrease in the number of viable cells in the biofilm when treated with the MIC of each QQ molecule. Similar results were collected regardless of the type of HA disks the biofilm formed on as shown in Figure 3.9.

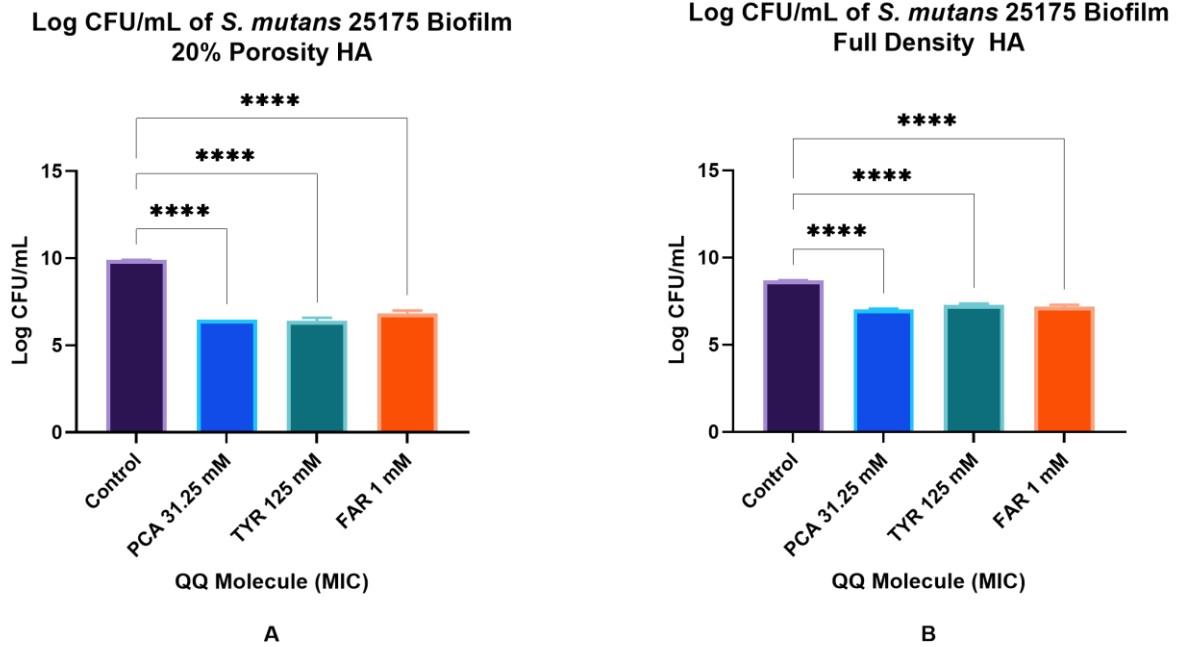


Figure 3.9 The Log CFU/mL of *S. mutans* 25175 cells in biofilm formed on A) 20% porosity HA disks or B) full density HA disks when treated with QQ molecules at their MIC. Results are representative of three biological replicates. ($p < 0.0001 = ****$, $p (0.0001 \text{ to } 0.001) = ***$, $p (0.001 \text{ to } 0.01) = **$, $p (0.01 \text{ to } 0.05) = *$).

Like the MIC QQ molecule treatments, there was a statistically significant decrease in the number of viable cells in the biofilm when treated with 1/2 of the MIC of each QQ molecule. Similar results were collected regardless of the type of HA disks the biofilm formed on as shown in Figure 3.10.

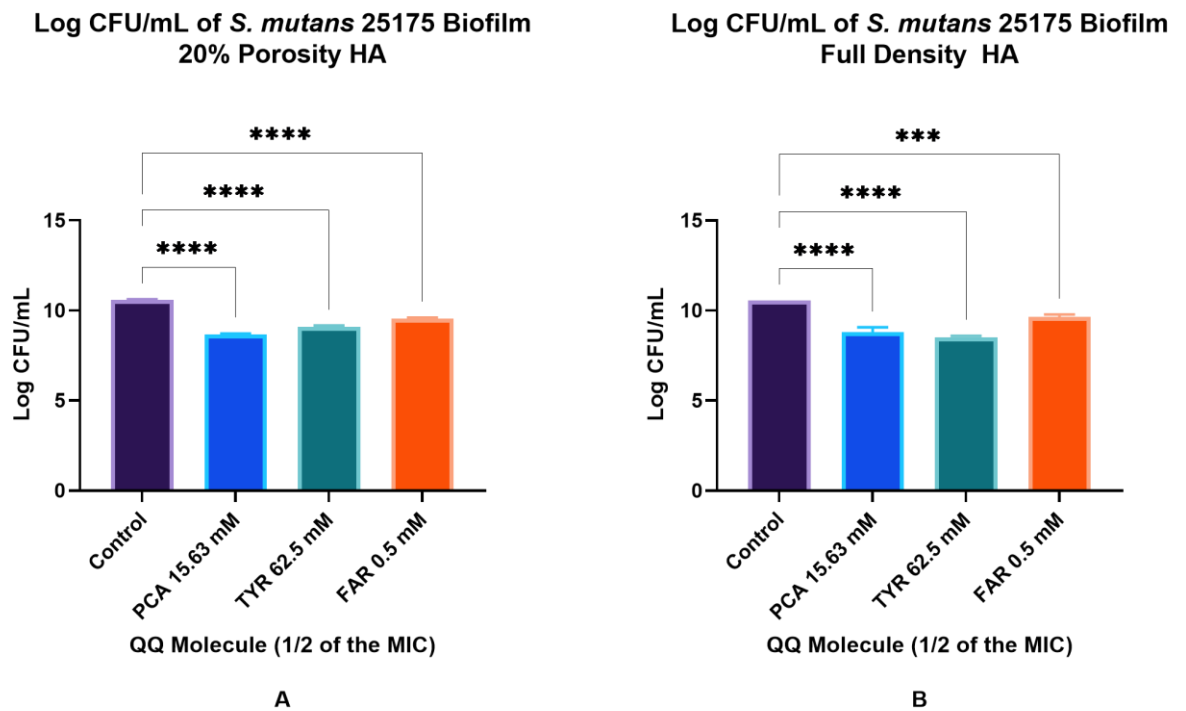


Figure 3.10 The Log CFU/mL of *S. mutans* 25175 cells in biofilm formed on A) 20% porosity HA disks or B) full density HA disks when treated with QQ molecules at 1/2 of the MIC. Results are representative of three biological replicates. ($p < 0.0001 = ****$, $p (0.0001 \text{ to } 0.001) = ***$, $p (0.001 \text{ to } 0.01) = **$, $p (0.01 \text{ to } 0.05) = *$).

At 1/4 of the MIC of each QQ molecule, there was a statistically significant reduction in the number of viable cells in the biofilm when formed on HA disks (either 20% porosity or full density) only with p-coumaric acid. Like the MIC and 1/2 of the MIC, there was no discrepancy in the results between the two types of HA disks the biofilm was formed on. There was no statistically significant reduction of viable cells with 1/4 of the MIC of tyrosol or farnesol as shown in Figure 3.11.

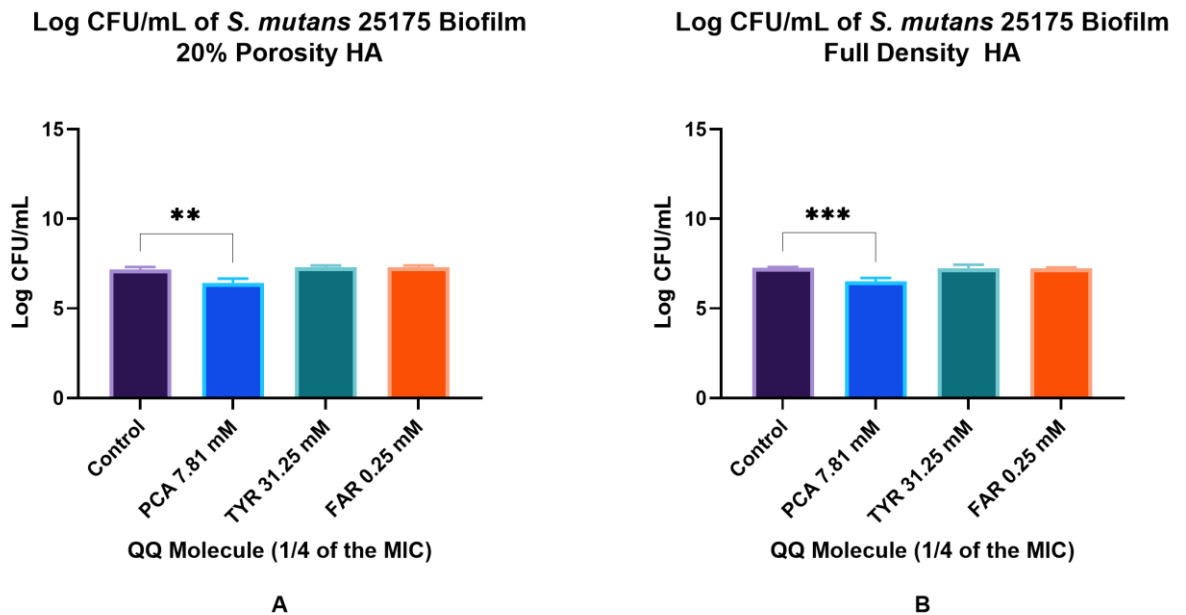


Figure 3.11 The Log CFU/mL of *S. mutans* 25175 cells in biofilm formed on A) 20% porosity HA disks or B) full density HA disks when treated with QQ molecules at 1/4 of their MIC. Results are representative of three biological replicates. ($p < 0.0001 = ****$, $p (0.0001 \text{ to } 0.001) = ***$, $p (0.001 \text{ to } 0.01) = **$, $p (0.01 \text{ to } 0.05) = *$).

3.2.3 Carbohydrate Quantification of *S. mutans* 25175 Biofilm Formed on HA Disks

S. mutans forms biofilms on surfaces in the oral cavity by converting dietary sugars, such as sucrose, into glucans which combine to form chains. These glucan chains provide support and structure to the biofilm. The concentration of carbohydrates in the *S. mutans* 25175 biofilm formed on HA disks were measured using phenol-sulfuric acid assay adopted from Masuko et al., (2005) as described in Chapter 2. This experiment was done independently three times and each sample was analysed in triplicate.

The *S. mutans* 25175 biofilm formed on HA disks, both full density and 20% porosity, comprised higher concentrations of carbohydrates when compared to the control among all three of the QQ molecules at their MICs as shown in Figure 3.12.

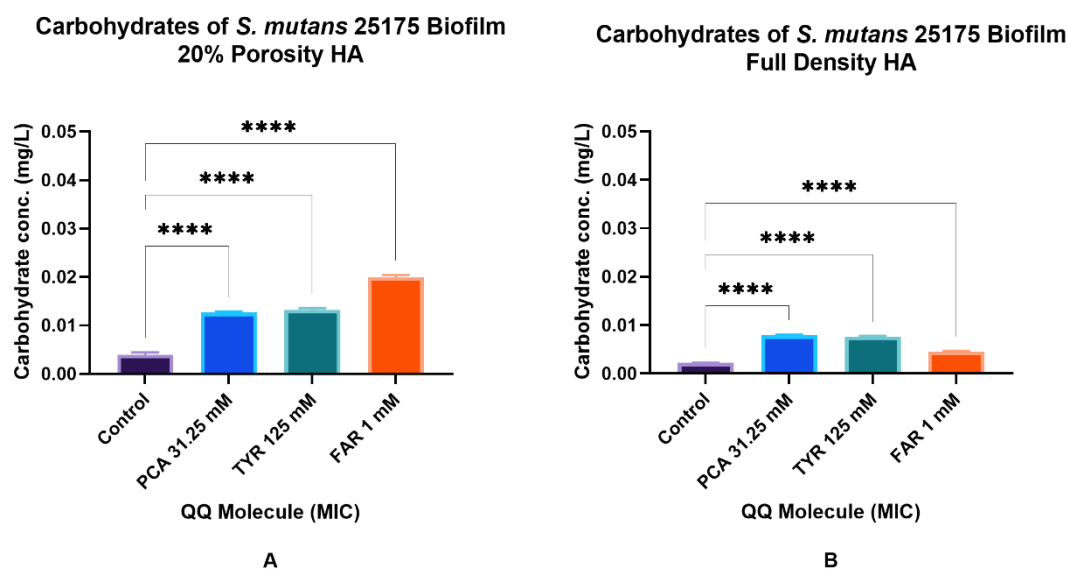


Figure 3.12 The carbohydrate concentration (mg/L) of *S. mutans* 25175 biofilm formed on A) 20% porosity HA disks or B) full density HA disks when treated with QQ molecules at their MIC. Results are representative of three biological replicates. ($p < 0.0001 = ****$, $p (0.0001 \text{ to } 0.001) = ***$, $p (0.001 \text{ to } 0.01) = **$, $p (0.01 \text{ to } 0.05) = *$).

The concentration of carbohydrates in the biofilm formed on the HA disks varied in the presence of the QQ molecules at 1/2 of their respective MICs. At 1/2 MIC, p-coumaric acid increased the concentration of carbohydrates from *S. mutans* 25175 biofilm formed on HA disks of 20% porosity, but decreased the concentration of carbohydrates when formed on the full density HA disks. Similar results were observed for tyrosol at 1/2 of the MIC. Unlike p-coumaric acid and

tyrosol, farnesol (at 1/2 of the MIC) decreased carbohydrate concentrations in *S. mutans* 25175 biofilm formed on the 20% porosity HA disks and increased the concentration of carbohydrates on the full density HA disks.

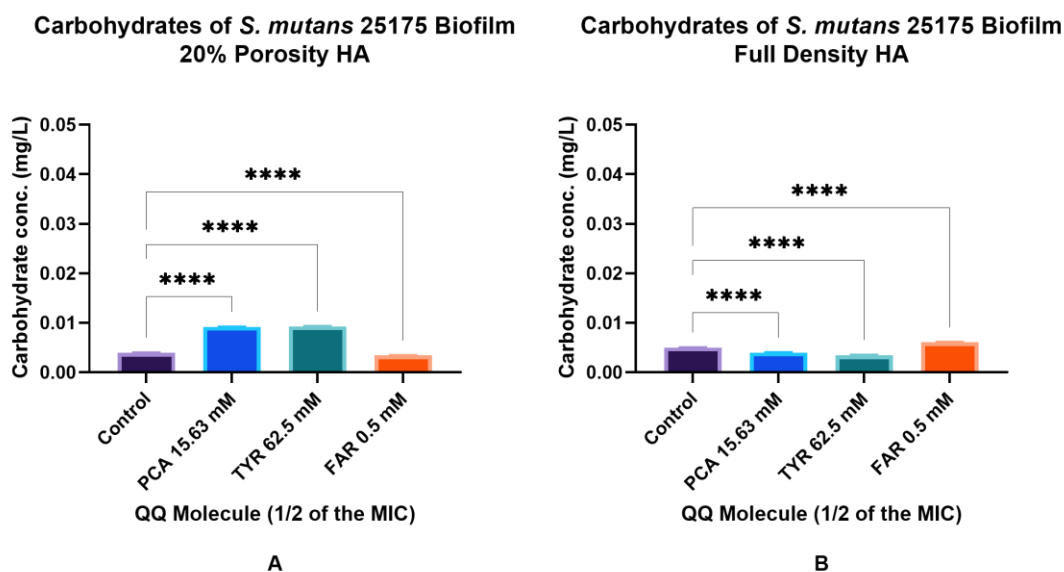


Figure 3.13 The carbohydrate concentration (mg/L) of *S. mutans* 25175 biofilm formed on A) 20% porosity HA disks or B) full density HA disks when treated with QQ molecules at 1/2 of their MIC. Results are representative of three biological replicates. ($p < 0.0001 = ****$, $p (0.0001 \text{ to } 0.001) = ***$, $p (0.001 \text{ to } 0.01) = **$, $p (0.01 \text{ to } 0.05) = *$).

When the concentrations of the QQ molecules were 1/4 of their respective MICs, a similar pattern was observed among the carbohydrate concentrations of the biofilm formed on either type of the HA disks. P-coumaric acid and tyrosol increased the carbohydrate concentration in the biofilm formed on the HA disks although p-coumaric acid increased the carbohydrate concentration of the biofilm more than tyrosol. Farnesol decreased the concentration of carbohydrates from the biofilm formed on the HA disks as shown in Figure 3.14.

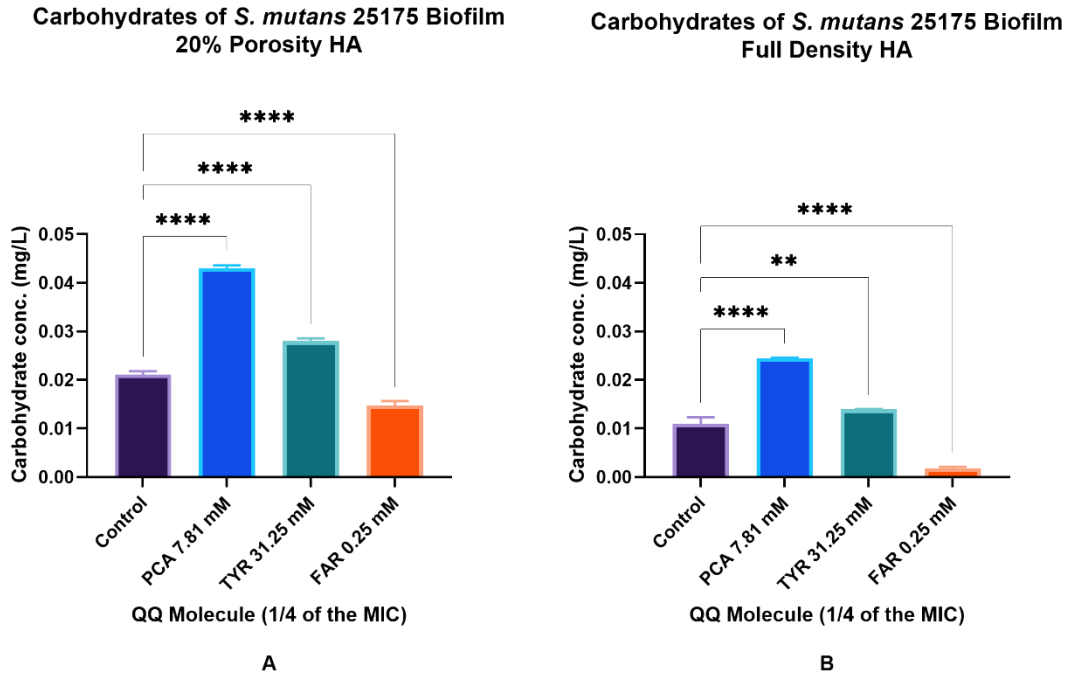


Figure 3.14 The carbohydrate concentration (mg/L) of *S. mutans* 25175 biofilm formed on A) 20% porosity HA disks or B) full density HA disks when treated with QQ molecules at 1/4 of their MIC. Results are representative of three biological replicates. ($p < 0.0001 = ****$, $p (0.0001 \text{ to } 0.001) = ***$, $p (0.001 \text{ to } 0.01) = **$, $p (0.01 \text{ to } 0.05) = *$).

3.2.4 eDNA Quantification of *S. mutans* 25175 Biofilm Formed on HA Disks

The concentration of eDNA in the *S. mutans* 25175 biofilm formed on HA disks was quantified using the Qubit® dsDNA broad spectrum assay method previously described in Chapter 2. The *S. mutans* 25175 biofilm samples collected (as described in section 3.1) were aliquoted into 1 mL Eppendorf tubes and centrifuged and the supernatant was used for eDNA analysis. This experiment was repeated independently three times and each sample was analysed in triplicate.

The concentration of eDNA ($\mu\text{g/mL}$) in the *S. mutans* 25175 biofilms formed on HA disks differed among the treatments of QQ molecules at their MICs and subinhibitory concentrations and between types of HA disks demonstrating no obvious pattern.

The concentration of eDNA in the biofilm formed on the HA disks of 20% porosity were all decreased by the QQ molecules at their MICs. The concentration of eDNA of the biofilm formed on the full density HA disks was not statistically significantly changed by p-coumaric acid at 31.25 mM, whereas there was a statistically significant increase by tyrosol and a statistically significant decrease by farnesol by their MICs as shown in Figure 3.15.

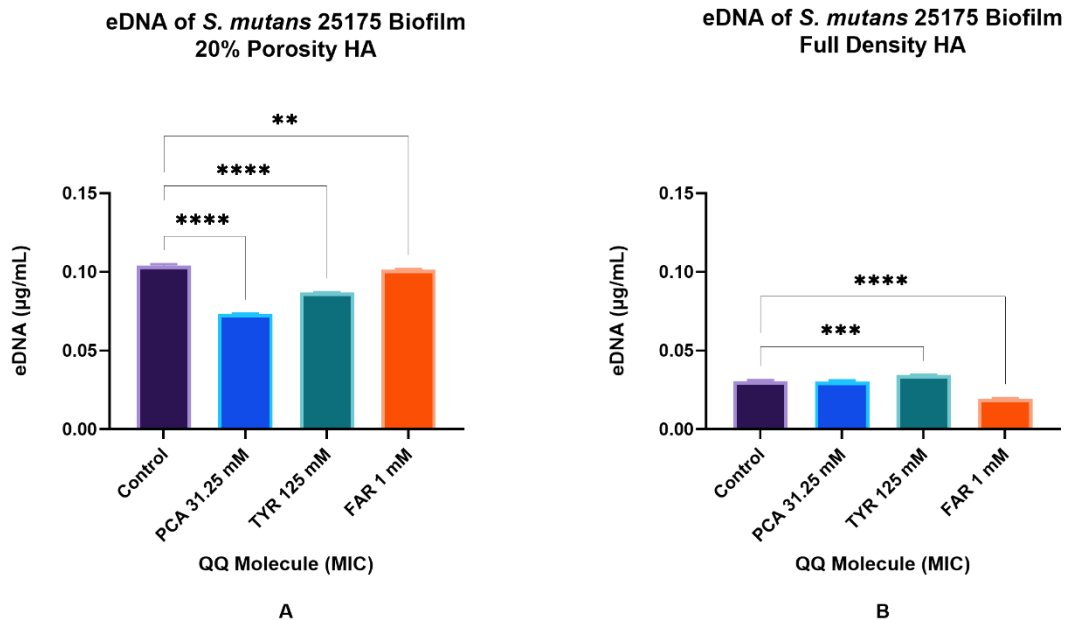


Figure 3.15 The eDNA ($\mu\text{g/mL}$) of *S. mutans* 25175 biofilm formed on A) 20% porosity HA disks or B) full density HA disks when treated with QQ molecules at their MIC. Results are representative of three biological replicates. ($p < 0.0001 = ****$, $p (0.0001 \text{ to } 0.001) = ***$, $p (0.001 \text{ to } 0.01) = **$, $p (0.01 \text{ to } 0.05) = *$).

At 1/2 of the MIC of the QQ molecules, the concentration of eDNA in the biofilm formed on the 20% porosity HA disks decreased with p-coumaric acid but did not change with tyrosol when compared to the untreated control. The concentration of eDNA in the biofilm formed on full density HA disks decreased with p-coumaric acid and tyrosol at 1/2 of their MICs. Farnesol increased the eDNA concentration of the biofilm formed on both types of HA disks.

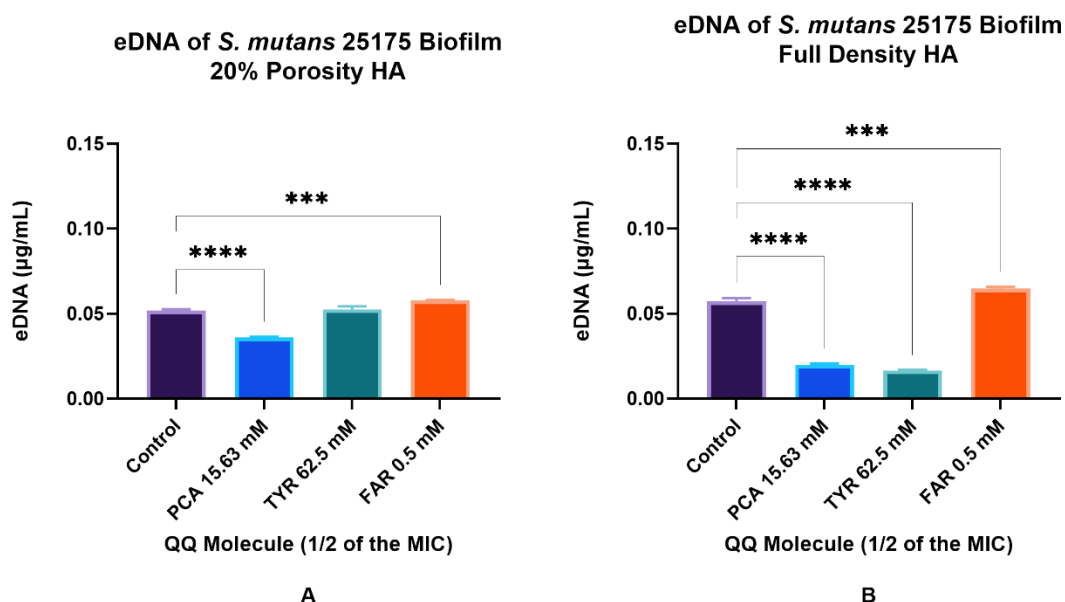


Figure 3.16 The eDNA ($\mu\text{g/mL}$) of *S. mutans* 25175 biofilm formed on A) 20% porosity HA disks or B) full density HA disks when treated with QQ molecules at 1/2 of their MIC. Results are representative of three biological replicates. ($p < 0.0001 = ****$, $p (0.0001 \text{ to } 0.001) = ***$, $p (0.001 \text{ to } 0.01) = **$, $p (0.01 \text{ to } 0.05) = *$).

At 1/4 of the MICs of the QQ molecules, p-coumaric acid and tyrosol increased the concentration of eDNA in the biofilm formed on 20% porosity HA disks while

there were no statistically significant changes with farnesol. The concentration of eDNA in the biofilm formed on the full density HA disks increased with the treatment of tyrosol at 31.25 mM while there were no statistically significant changes measured with p-coumaric acid and farnesol at 1/4 of their MICs as shown in Figure 3.17.

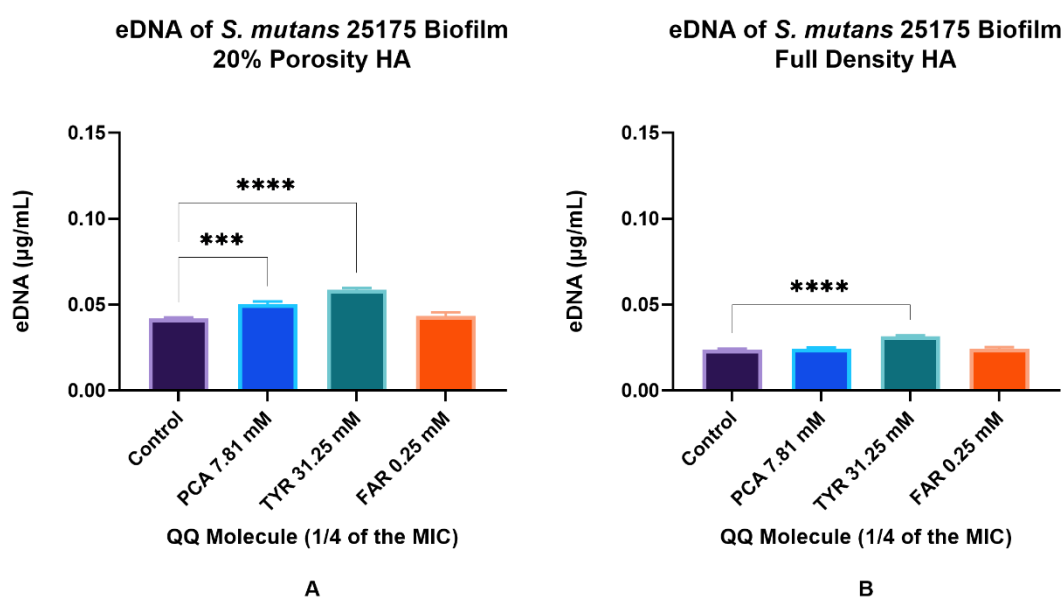


Figure 3.17 The eDNA ($\mu\text{g/mL}$) of *S. mutans* 25175 biofilm formed on A) 20% porosity HA disks or B) full density HA disks when treated with QQ molecules at 1/4 of their MIC. Results are representative of three biological replicates. ($p < 0.0001 = ****$, $p (0.0001 \text{ to } 0.001) = ***$, $p (0.001 \text{ to } 0.01) = **$, $p (0.01 \text{ to } 0.05) = *$).

3.2.5 Protein Quantification of *S. mutans* 25175 Biofilm Formed on HA Disks

For this section, the protein concentration in the *S. mutans* 25175 biofilm formed on full density and 20% porous HA disks were quantified using the Bradford assay

described in Chapter 2. The biofilm collected from the HA disks described in section 3.2.1 was used to quantify the protein concentration of the biofilm. This experiment was repeated independently three times with three replicates each time.

There were no statistically significant changes in the protein concentration of the *S. mutans* 25175 biofilms formed on HA disks (either full density or 20% porosity) when treated with the QQ molecules at the MICs when compared to the untreated control. The results from the Bradford assay for this experiment are shown in Figure 3.18.

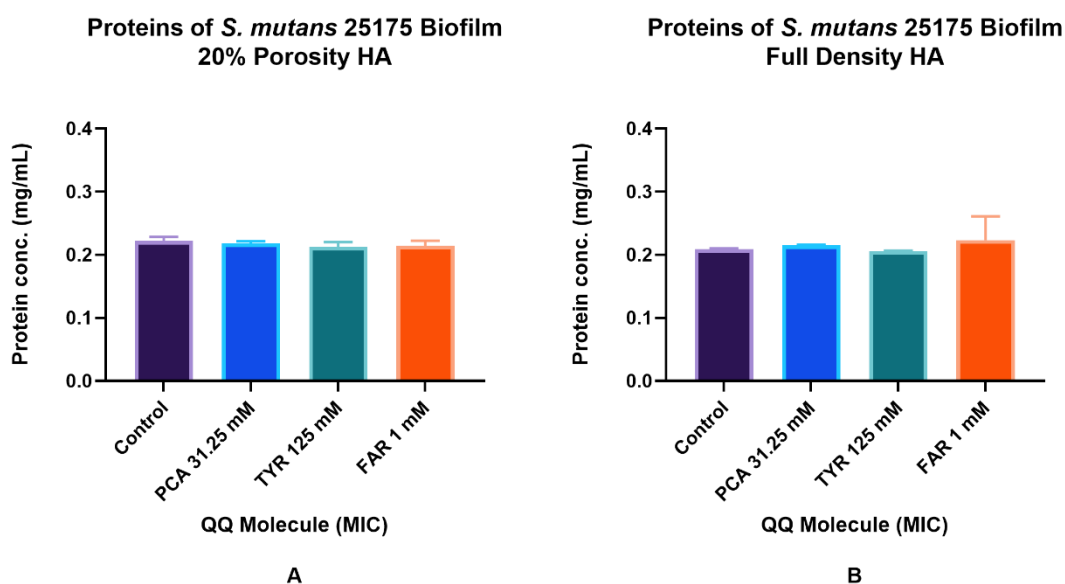


Figure 3.18 The protein concentration (mg/mL) of *S. mutans* 25175 biofilm formed on A) 20% porosity HA disks or B) full density HA disks when treated with QQ molecules at their MIC. Results are representative of three biological replicates. ($p < 0.0001 = ****$, $p (0.0001 \text{ to } 0.001) = ***$, $p (0.001 \text{ to } 0.01) = **$, $p (0.01 \text{ to } 0.05) = *$).

Like the results of the QQ molecules at the MIC, the protein concentration of the biofilms formed on the HA disks (either 20% porosity or full density) at 1/2 of their MICs resulted in no statistically significant changes from the treatments compared to the control. The results are shown in Figure 3.19.

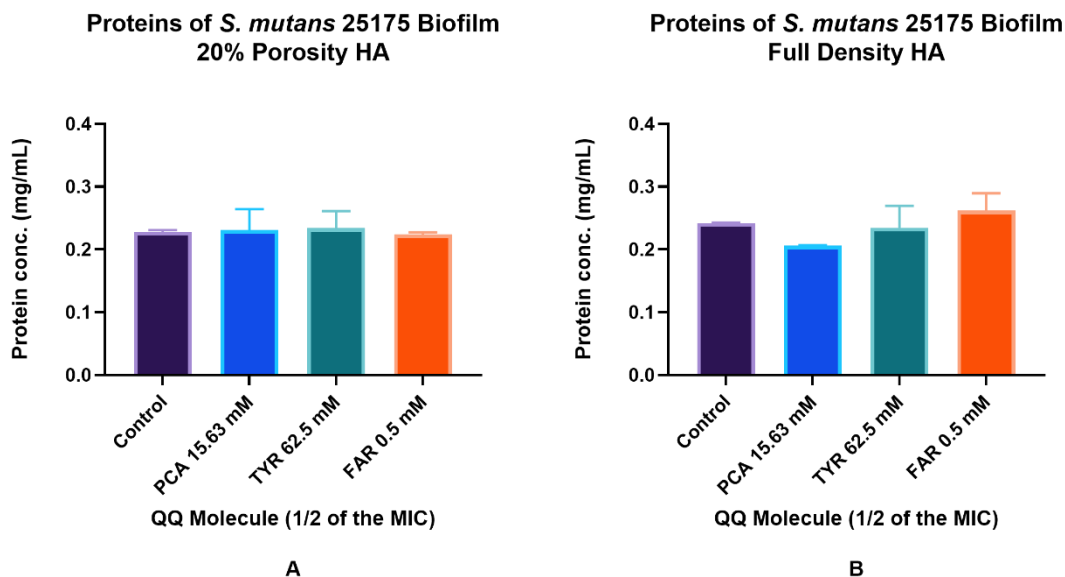


Figure 3.19 The protein concentration (mg/mL) of *S. mutans* 25175 biofilm formed on A) 20% porosity HA disks or B) full density HA disks when treated with QQ molecules at 1/2 of their MIC. Results are representative of three biological replicates. ($p < 0.0001 = ****$, $p (0.0001 \text{ to } 0.001) = ***$, $p (0.001 \text{ to } 0.01) = **$, $p (0.01 \text{ to } 0.05) = *$).

Although there were no statistically significant changes in the protein concentrations of the biofilms when the QQ molecules were at the MICs and 1/2 of the MICs, there was a statistically significant increase in protein concentrations in the biofilms formed on 20% porosity HA disks by both tyrosol and farnesol at 1/4 of their MICs but not my p-coumaric acid. There was a statistically significant decrease in protein concentrations of the biofilms formed on the full density HA

disks when treated with p-coumaric acid and tyrosol at 1/4 of their MICs, but there was no statistically significant change made by farnesol at 1/4 of the MIC on the full density HA disks as shown in Figure 3.20.

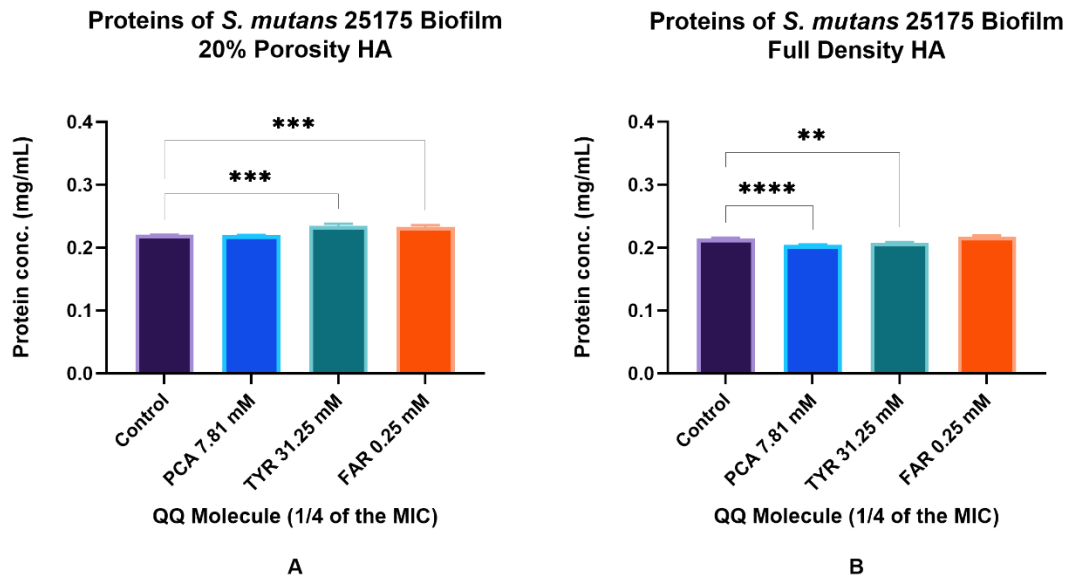


Figure 3.20 The protein concentration (mg/mL) of *S. mutans* 25175 biofilm formed on A) 20% porosity HA disks or B) full density HA disks when treated with QQ molecules at 1/4 of their MIC. Results are representative of three biological replicates. ($p < 0.0001 = ****$, $p (0.0001 \text{ to } 0.001) = ***$, $p (0.001 \text{ to } 0.01) = **$, $p (0.01 \text{ to } 0.05) = *$).

3.2.6 Summary of Section 2 Results

Section 3.2 investigated the effects of QQ molecules p-coumaric acid, tyrosol, and farnesol at their MIC and subinhibitory concentrations (1/2 and 1/4 of the MIC) on the CFUs, carbohydrate concentration, eDNA, and protein concentration of *S. mutans* 25175 biofilm formed on HA disks of either full density or 20% porosity.

For *S. mutans* 25175 biofilm formed on 20% porosity HA disks, there was a decrease in CFUs when treated with the MIC and 1/2 of the MIC of all the QQ molecules but only p-coumaric acid decreased the CFUs in *S. mutans* 25175 biofilm at 1/4 of the MIC. Carbohydrate concentrations were increased by all QQ molecules at their MIC and subinhibitory concentrations except for farnesol that actually decreased the carbohydrate concentration at both subinhibitory concentrations. The eDNA of *S. mutans* 25175 biofilm formed on 20% HA disks elicited both increases and decreases in eDNA when treated with QQ molecules at the MIC and subinhibitory concentrations with p-coumaric acid causing a decrease at the MIC and 1/2 of the MIC, but an increase at 1/4 of the MIC. Tyrosol caused a decrease, no statistically significant change, and an increase (respective of the MIC, 1/2, and 1/4 of the MIC) of eDNA in *S. mutans* 25175 biofilm, while farnesol decreased, increased, and did not changed the eDNA at its MIC, 1/2 of the MIC, and 1/4 of the MIC respectively. The protein concentrations of *S. mutans* 25175 biofilm formed on 20% porosity HA disks was only affected at 1/4 of the MICs of tyrosol and farnesol which caused an increase of eDNA.

For *S. mutans* 25175 biofilm formed on full density HA disks, the same pattern of CFUs was seen as when formed on 20% porosity HA disks. The carbohydrate concentrations were increased by all the QQ molecules at their MICs, while decreased by p-coumaric acid and tyrosol at 1/2 of the MIC and farnesol at 1/4 of the MIC. The eDNA of *S. mutans* 25175 biofilm formed on full density HA disks was only decreased by p-coumaric acid and tyrosol at 1/2 of the MIC and farnesol at the MIC, whereas it was increased by tyrosol at the MIC and 1/4 of the MIC and also by farnesol at 1/2 of the MIC. The protein concentrations of *S. mutans* 25175 biofilm formed on full density porosity HA disks was only decreased by p-coumaric acid and tyrosol at 1/4 of the MIC.

To determine which treatment is best at reduction of *S. mutans* 25175 biofilm formed on HA disks of the full density and 20% porosity when treated with QQ molecules, a mathematical equation can be used to compare the treatments as a whole based on the individual effects of the components of the biofilm by multiplying all the data points together to create a new term 'X'. For this data,

$$X = \text{protein concentration (mg/mL)} * \text{carbohydrate concentration (mg/L)} * \text{eDNA (\mu g/mL)} * \text{CFU (Log CFU/mL)}$$

The treatment with the lowest term (or score X) indicated the best overall treatment since the goal was to reduce the total amount of *S. mutans* 25175 biofilm formed on a HA surface. Table 3.4 indicates that farnesol at 1/2 of MIC was the best treatment to reduce the occurrence of *S. mutans* 25175 biofilm formed on 20% porosity HA disks followed by p-coumaric acid at 1/2 of the MIC and tyrosol at 1/2 of the MIC coming in at 2nd and 3rd places respectively.

TABLE 3.4 SUMMARY OF SECTION 2 RESULTS FOR 20% POROSITY HA DISKS
 Summary of CFU, carbohydrates, eDNA, and proteins in the *S. mutans* 25175 biofilm formed on 20% porosity HA disks and ranked by best treatment as determined by a defined mathematical equation.

HA Disks (20% Porosity)

Treatment	CFU (Log CFU/mL)	Carbohydrate (mg/L)	eDNA (µg/mL)	Protein (mg/mL)	Score (X)	Rank
PCA 31.25 mM	6.5	0.013	0.073	0.22	0.0013	4
PCA 15.63 mM	8.7	0.0092	0.036	0.23	0.00066	2
PCA 7.81 mM	3.0	0.043	0.050	0.22	0.0014	5
TYR 125 mM	6.4	0.013	0.087	0.21	0.0016	6
TYR 62.5 mM	9.1	0.0093	0.053	0.23	0.0010	3
TYR 31.25 mM	20	0.028	0.059	0.23	0.0077	9
FAR 1 mM	6.8	0.020	0.10	0.21	0.0030	7
FAR 0.5 mM	9.5	0.0034	0.058	0.22	0.00043	1
FAR 0.25 mM	20	0.015	0.043	0.23	0.0030	8

For *S. mutans* 25175 biofilm formed on full density HA disks, tyrosol at 1/2 of the MIC was the best at overall reduction of biofilm formation followed by farnesol at the MIC and p-coumaric acid at 1/2 of the MIC as shown in Table 3.5.

TABLE 3.5 SUMMARY OF SECTION 2 RESULTS FOR FULL DENSITY HA DISKS
Summary of CFU, carbohydrates, eDNA, and proteins in the *S. mutans* 25175 biofilm formed on full density HA disks and ranked by best treatment as determined by a defined mathematical equation.

HA Disks (Full Density)						
Treatment	Protein (mg/mL)	Carb (mg/L)	eDNA (µg/mL)	CFU (Log CFU/mL)	Score (X)	Rank
PCA 31.25 mM	0.21	0.0079	0.03	7.0	0.00036	5
PCA 15.63 mM	0.21	0.004	0.02	8.8	0.00014	3
PCA 7.81 mM	0.20	0.024	0.024	3.3	0.00041	7
TYR 125 mM	0.21	0.0077	0.035	7.3	0.0004	6
TYR 62.5 mM	0.23	0.0034	0.017	8.5	0.00011	1
TYR 31.25 mM	0.21	0.014	0.032	18	0.0017	9
FAR 1 mM	0.22	0.0045	0.019	7.2	0.00014	2
FAR 0.5 mM	0.26	0.0061	0.065	9.6	0.00099	8
FAR 0.25 mM	0.22	0.0018	0.024	17	0.00016	4

3.3 Section 3 Cell Culture Results

3.3.1 Introduction to Section 3 Results

The oral cavity is composed of both hard HA surfaces (the teeth) and soft tissue surfaces like the gingiva and tongue. Bacteria in the oral cavity are present on both types of surfaces and when given the opportunity, will colonize the surfaces creating a biofilm in an attempt to survive and thrive in a safe environment. Given the proximity of soft gingiva tissue to the HA surface of the tooth, it can be speculated that bacteria like *S. mutans* could adhere to not only the tooth surface, but also to the surrounding tissue of the gingiva even if the bacteria are unable to cause the same detrimental harm as compared to when they establish themselves on the tooth surface in the form of a biofilm.

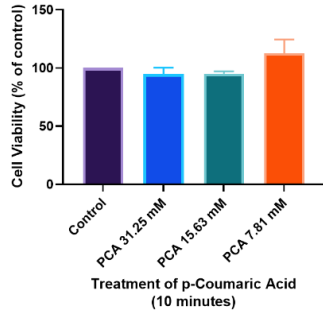
The gingiva surrounding the teeth primarily consist of keratinized epithelial cells and human gingival fibroblast cells. Keratinized epithelial cells are composed of numerous layers of dead squamous cells, which are specially structured to be waterproof and reduce evaporation from underlying tissues. Gingival fibroblasts are of particular importance due to their capability to differentiate into various cell types and generate induced pluripotent stem cells which makes them excellent models for periodontal regeneration, wound healing, toxicology, and cellular biology research. The gingival cells used in this section of research were HGF-1 cell line. The concentrations of the QQ molecules determined to be the MIC and subinhibitory concentrations found in section 1 of this study were used in this section of the research to determine the effects they might have on the tissue cells.

In this section, the toxicity of each QQ molecule on HGF-1 cells was tested at their MIC and subinhibitory concentrations determined in Section 1. The ability of the QQ molecules at their MIC and subinhibitory concentrations to inhibit adherence of *S. mutans* 25175 cells to HGF-1 cells was studied. Finally, the ability of the QQ molecules to prevent *S. mutans* 25175 biofilm formation on HGF-1 cell monolayer was assessed.

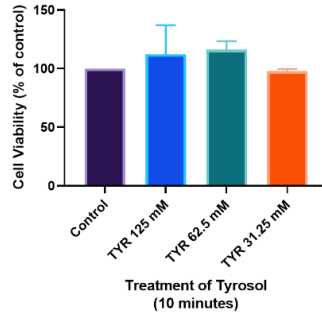
3.3.2 HGF-1 Cellular Viability Assay Results

Earlier in this research, it was found that the QQ molecules p-coumaric acid, tyrosol, and farnesol could prevent or reduce static biofilm formation of *S. mutans* 25175 under certain experimental conditions. As the QQ molecules were successful with *S. mutans* 25175 static biofilm prevention, it was necessary to move to the next stage of research which involved determining if the molecules were toxic to human tissue cells found in the oral cavity. Each QQ molecule's toxicity was tested on HGF-1 cells at their respective MICs and two subinhibitory concentrations (1/2 and 1/4 of the MIC), for 10 minutes, 20 minutes, and 30 minutes of treatment time immediately followed by an MTT assay. The MTT assay was done 3 times with three replicates (n=9) for each of the experimental conditions on the HGF-1 cells to determine the toxicity of the QQ molecules on the human cell line. Figure 3.21 shows the results of the MTT assays.

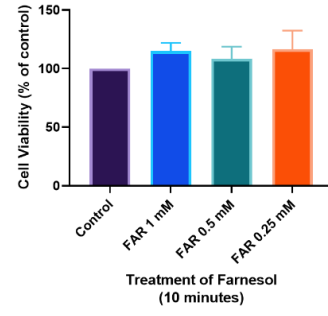
HGF-1 Cell Viability after QQ molecule Treatments



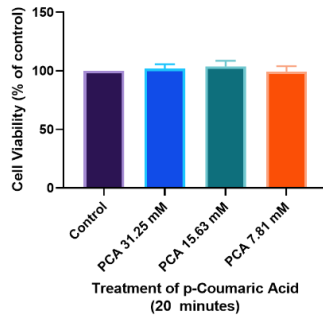
A



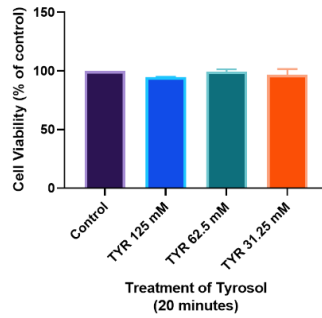
B



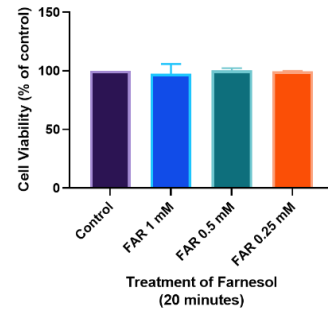
C



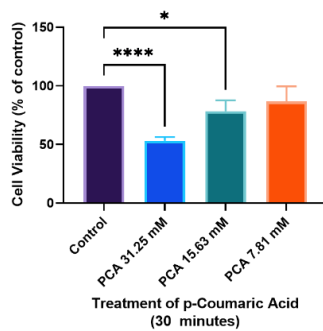
D



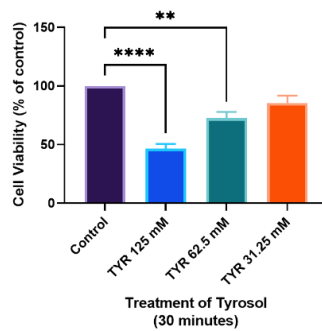
E



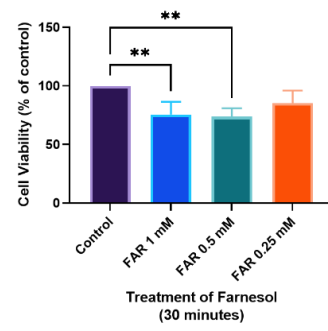
F



G



H



I

Figure 3.21 HGF-1 Cell Viability after QQ molecule Treatments: The cellular viability of HGF-1 cell line when treated with p-coumaric acid, tyrosol, and farnesol at the MIC and subinhibitory concentrations (1/2 and 1/4 of the MIC) for 10 minutes, 20 minutes, and 30 minutes. The data was analysed using GraphPad Prism and a one-way ANOVA was done with multiple comparisons. Each test was done three times with three replicates per test (n=3). The asterisks show the statistically significant data points when compared to the controls. (p < 0.0001 = ****, p (0.0001 to 0.001) = ***, p (0.001 to 0.01) = **, p (0.01 to 0.05) = *).

After 10 minutes of treatment, there was no statistically significant difference in cellular viability between any of the QQ treatments at any concentration and the control. Likewise, there was no statistically significant difference in cellular viability after 20 minutes of treatment with the same concentrations of the QQ molecules. There was, however, a statistically significant difference (p < 0.05) in cellular viability between the treatment of p-coumaric acid, tyrosol, and farnesol at the MIC and 1/2 of the MIC of each molecule after 30 minutes of treatment time as compared to the control. There was no statistically significant difference at the 1/4 of the MIC concentrations of any of the QQ molecules after 30 minutes of treatment.

Based on the results from the MTT cell toxicity assay, the QQ molecules in the concentrations determined to be the MIC, 1/2 of the MIC and 1/4 of the MIC of *S. mutans* 25175 biofilm did not pose statistically significant toxicity to the HGF-1 cells after 10 or 20 minutes of exposure to the molecules or at low concentration (1/4 of the MIC) after 30 minutes of treatment.

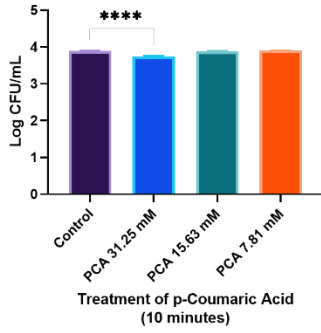
The higher concentrations (the MIC and 1/2 of the MIC) of all three QQ molecules reduced the cellular viability of the HGF-1 cell line after 30 minutes of treatment

time. This data suggests that using higher concentrations of the QQ molecules, the treatment time could not exceed 30 minutes without causing damage to the human tissue cells of the oral cavity. The subinhibitory concentration of 1/4 of the MIC of each of the QQ molecules did not cause statistically significant toxicity effects on HGF-1 cell line which suggests that if a lower concentration of QQ molecules is better at preventing bacterial adhesion to the human cell line then the treatment time could still be 30 minutes.

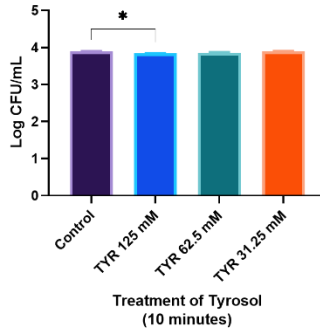
3.3.3 *S. mutans* 25175 Cellular Adherence to HGF-1 Cell Line

S. mutans has many virulence factors that aid in biofilm formation. One of the first obvious virulence factors observed in *S. mutans* is the ability to adhere to firm surfaces. The gingiva of the oral cavity is an abundant surface in the mouth and is in close proximity to the HA surface of the teeth. The ability of *S. mutans* to adhere to the gingiva tissue could give the bacterium a better opportunity to colonize the more desirable tooth surface. Furthermore, *S. mutans* has been found in infants and children with teeth that have not yet erupted indicating that *S. mutans* is able to survive in the oral cavity in the absence of a HA surface and showcasing its ability to withstand the salivary flow of the oral cavity. Therefore, it was necessary to study the ability of *S. mutans* 25175 cells to adhere to HGF-1 cell line. The HGF-1 cell line was grown and treated with the QQ molecules as described in Chapter 2. Each sample of the adherence assay was spot plate on BHI agar plates in triplicate and incubated at 37°C for 24 hours. The colonies of *S. mutans* 25175 were counted and the data were analysed and shown in Figure 3.22.

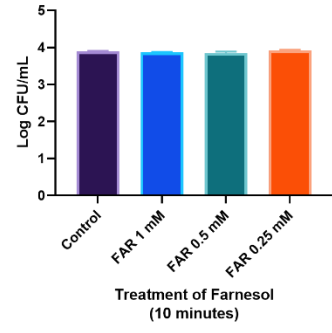
Log CFU/mL of *S. mutans* 25175 attachment to HGF-1 Cell Line Treated with QQ Molecules



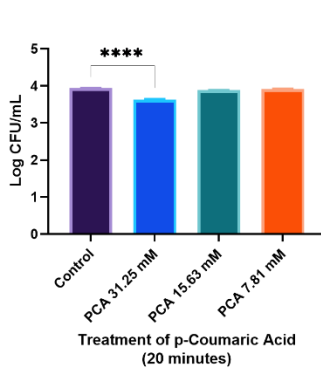
A



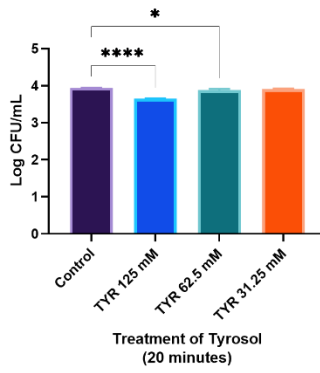
B



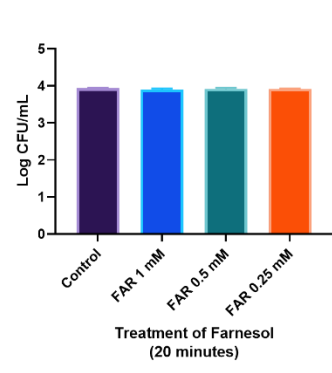
C



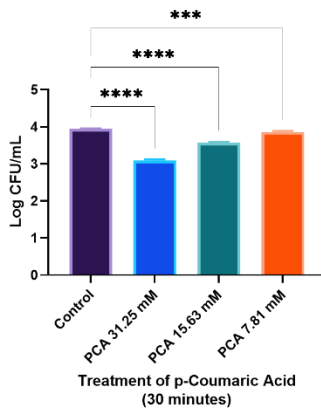
D



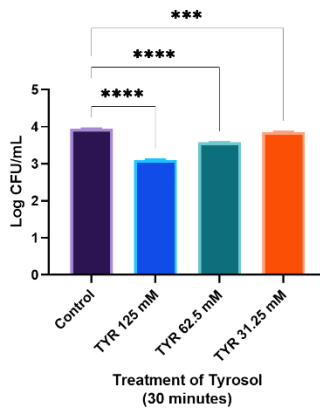
E



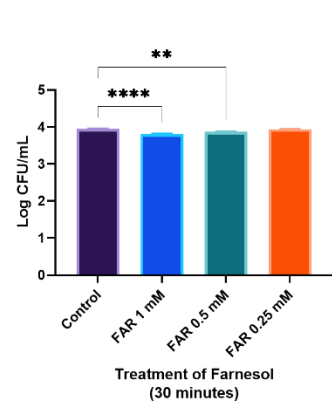
F



G



H



I

Figure 3.22 Log CFU/mL of *S. mutans* 25175 attachment to HGF-1 Cell Line Treated with QQ Molecules: The results from the *S. mutans* 25175 bacterial cell adherence to HGF-1 human tissue culture cell line when treated with the MIC and subinhibitory concentrations (1/2 MIC and 1/4 MIC) of p-coumaric acid (A, D, and G), tyrosol (B, E, and H), and farnesol (C, F, and I) for 10 minutes (A, B, and C), 20 minutes (D, E, and F), and 30 minutes (G, H, and I). Each treatment and condition was done three times with three replicates (n=3). The data was analysed using a one-way ANOVA with multiple comparisons. The asterisks indicate statistically significant results between the treatment and the control when $p < 0.05$. ($p < 0.0001 = ****$, $p (0.0001 \text{ to } 0.001) = ***$, $p (0.001 \text{ to } 0.01) = **$, $p (0.01 \text{ to } 0.05) = *$).

After 10 minutes of treatment, p-coumaric acid and tyrosol at their respective MICs reduced the number of attached *S. mutans* 25175 cells to the HGF-1 cell line. After 20 minutes of treatment time, p-coumaric acid at the MIC and tyrosol at both the MIC and 1/2 of the MIC reduced the attachment of *S. mutans* 25175 cells to the HGF-1 cell line. After 30 minutes of treatment time, all concentration of both p-coumaric acid and tyrosol reduced the *S. mutans* 25175 cells attached to the HGF-1 cell line while farnesol reduced adherence of *S. mutans* 25175 cells to the HGF-1 cell line at the MIC and 1/2 of the MIC. These results show that *S. mutans* 25175 cells are less able to adhere to HGF-1 cells the longer the QQ molecules are allowed to be in contact with the HGF-1 cells up to 30 minutes.

3.3.4 Quantification of *S. mutans* 25175 Biofilm Formation on HGF-1 Cell Line

The ability of *S. mutans* to form biofilms in the oral cavity is necessary for its survival. The ability of QQ molecules to reduce or inhibit biofilm formation on plastic and HA surfaces suggests that they may also be able to reduce *S. mutans* biofilm formation on other surfaces including biotic ones such as HGF-1 cell line.

Section 3.1 demonstrated no change in cellular viability of HGF-1 cells after treatments with the QQ molecules (p-coumaric acid, tyrosol, and farnesol) at their MIC and subinhibitory concentrations against *S. mutans* 25175 biofilm formation after 20 minutes when compared to the control. Additionally, section 3.2 demonstrated the ability for *S. mutans* 25175 to attach to HGF-1 cells despite being treated with QQ molecules at their MIC and subinhibitory concentrations even though successful *S. mutans* 25175 attachment to HGF-1 cells was reduced in some instances. Therefore, it was essential to determine if the attached *S. mutans* 25175 cells could form a biofilm. *S. mutans* 25175 was co-cultured with the HGF-1 monolayer of cells and treated with the QQ molecules and their subinhibitory concentrations. A CV assay (as described in Chapter 2) done after 24 hour incubation quantified the *S. mutans* 25175 biofilm formed on the cell culture monolayer. The biofilm assay was done three times and had three replicates for each test (n=9). Figure 3.23 shows the results from the biofilm CV assay.

S. mutans 25175 Biofilm Formation on HGF-1 Cell Line

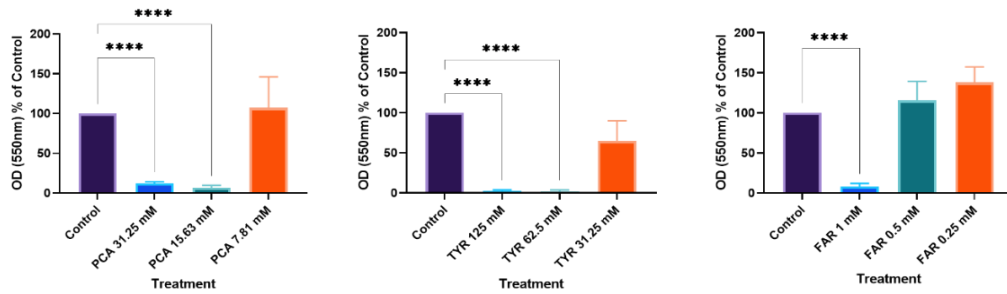


Figure 3.23 *S. mutans* 25175 Biofilm Formation on HGF-1 Cell Line: The percentage (%) of OD (@ A₅₅₀) change in biofilm formation when *S. mutans* 25175 was grown on HGF-1 cell line for 24 hours at 37°C in 5% CO₂ and 95% air when compared to the control (*S. mutans* 25175 biofilm growth on HGF-1 cell line with no QQ treatment). The CV assay was done in triplicate with three repeats per test to ensure reproducibility. The data was analysed in GraphPad Prism by performing a one-way AVOVA with multiple comparisons. The significance was determined if the adjusted p value was $p < 0.0001$ ($p < 0.0001 = ****$).

After 24 hours, there was a statistically significant reduction in *S. mutans* 25175 biofilm formation on the monolayer of HGF-1 cell line when the MIC of each QQ treatment was applied. Additionally, there was a statistically significant reduction in *S. mutans* 25175 biofilm formation at 1/2 of the MIC subinhibitory concentrations with both p-coumaric acid and tyrosol but not with farnesol. *S. mutans* 25175 biofilm formation was not changed with farnesol at 1/2 and 1/4 of the MIC after 24 hours on HGF-1 cell monolayer when compared to the control.

3.3.5 Summary of Section 3 Results

Section 3 investigated preliminary safety and efficacy of QQ molecules and *S. mutans* 25175 biofilm formation in relation to a human tissue cell line of the oral cavity using HGF-1 cell line. This section gave an insight into how these QQ molecules may interact in an *in vivo* environment. The safety of the QQ molecules was determined by performing a cellular toxicity test (MTT) for 10, 20, or 30 minutes using the MIC concentrations (previously determined in Section 1) and two subinhibitory concentrations of the QQ molecules. One of the vital virulence factors that *S. mutans* utilised for successful biofilm formation (adherence) was accessed by counting the number of *S. mutans* 25175 cells that were able to attach to the HGF-1 cell line after treatment with the QQ molecules at their MIC and two subinhibitory concentrations for 10, 20, or 30 minutes. Finally, the ability of QQ molecules to reduce *S. mutans* 25175 formation on a biotic surface was studied by allowing *S. mutans* 25175 to form on HGF-1 cell line when treated with the QQ molecules and two subinhibitory concentrations.

To determine the overall best treatment (including treatment time and concentration of QQ molecules), the data was analysed starting with the MTT toxicity results, followed by the adherence assay results, and finally the biofilm assay results.

First, the results of the MTT toxicity assay were screened and only the treatments without statistically significant reduction in cell viability were considered for further analysis. These treatments included all concentrations of the QQs after 10 and

20 minutes and only the subinhibitory (1/4 of the MIC) of each QQ after 30 minutes of exposure.

Next, the treatments that reduced the *S. mutans* 25175 adherence (Log CFU/mL) to HGF-1 cell line were screened and considered in the next stage of analysis. The treatments that passed this screening included p-coumaric acid 31.25 mM (10 and 20 minutes), tyrosol 125 mM (10 and 20 minutes), and tyrosol 62.5 mM (20 minutes).

These 5 treatments were then analysed on their ability to reduce *S. mutans* 25175 biofilm formation on HGF-1 cell line. All 5 of the treatments reduce *S. mutans* 25175 biofilm formation on HGF-1 cells. To determine which of the 5 treatments performed the best overall, the values from the adherence assay (Log CFU/mL) were multiplied to the values of the biofilm assay (OD @ 550 nm % of control), similar to the mathematical methods adopted in sections 3.1 and 3.2. The results are shown in Table 3.6.

TABLE 3.6 SECTION 3 SUMMARY OF RESULTS

The overall ranking of the top 5 best QQ molecule treatments for disrupting the biofilm formation process of *S. mutans* 25175 in an oral cavity simulated environment. The overall score represents the combination of the QQ treatment to reduce the adherence of *S. mutans* 25175 cells to HGF-1 cell line and subsequent 24-hour biofilm formation.

Rank	Treatment	Overall Score
1	Tyrosol 62.5 mM (20 minutes)	7.7
2	Tyrosol 125 mM (10 minutes)	9.2
3	Tyrosol 125 mM (20 minutes)	9.3
4	p-Coumaric Acid 31.25 mM (10 minutes)	47.5
5	p-Coumaric Acid 31.25 mM (20 minutes)	47.7

This study was interested in the mitigation of *S. mutans* 25175 biofilm formation, therefore the lowest scoring treatment was considered the best when ranked from most effective to least effective. Based on the results from this study, 62.5 mM tyrosol treatment for 20 minutes (ranked #1) was the best overall treatment followed by 125 mM tyrosol for 10 and 20 minutes (ranked #2 and #3 respectively) and 31.25 mM p-coumaric acid for 10 and 20 minutes (ranked #4 and #5 respectively).

Chapter 4 Discussion

The oral health crisis is a silent epidemic that is currently plaguing even the wealthiest of countries (Stephens et al., 2018). Diseases and infections including dental caries and periodontitis are primarily caused by a build-up of opportunistic pathogenic microorganisms including bacteria and fungi that reside in the oral cavity in structures called biofilms (Sims et al., 2019). The current understanding is that daily oral hygiene including brushing twice daily for at least two minutes each time and flossing once a day is the most effective method of removing the daily formation of dental biofilms that, if left to mature and spread, cause irreversible damage to tooth surfaces and surrounding soft tissue of the gingiva (Mayo Clinic, 2021). Preventative measures are the most effective for oral health. Physicians recommend preventative measures that include counselling about diet, oral hygiene, smoking cessation, and fluoride supplementation as well as application of fluoride varnish and regular screening for dental disease (Stephens et al., 2018). Unfortunately, in some cases, physical removal of the daily build-up of dental biofilm is not achievable or not adequately practiced. Some individuals are prone to dental caries and other oral diseases and infections despite their best oral hygiene efforts. This could be caused by genetic predispositions and individual microflora in the oral cavity. Furthermore, daily habits including smoking or diets high in sugar exacerbate these infections and diseases. The rise of antibiotic resistance has been documented for many years. Additionally,

antibiotics have poor permeability in dental biofilms. Therefore, there is a need to find alternatives to the current methods for oral biofilm prevention.

This research investigated the possibility of using three naturally occurring QQ molecules to reduce the instances of dental biofilm formation and subsequent caries formation on tooth surfaces. It is known that caries causing bacteria prefer to live in community biofilms amongst self-secreted EPS in a matrix to avoid detection by the host's immune response and to avoid antibiotic therapy (Berlanga and Guerrero, 2016). This research showed that QQ molecules such as p-coumaric acid, tyrosol, and farnesol could be alternatives or additions to the current gold standard of daily oral hygiene practice and Chlorhexidine.

S. mutans is an initial coloniser of dental biofilms on tooth surfaces and was the chosen organism to test the effects of QQ with the idea that if an initial coloniser can be inhibited from establishing the biofilm, secondary and late coloniser bacterial species would not be able to fill their niche in the maturing biofilm. p-Coumaric acid, tyrosol, and farnesol were chosen in part by their documented ability to disrupt biofilm formation in Gram-negative bacteria and their potential to inhibit biofilm formation in Gram-positive bacteria. This research explored the roles these three QQ molecules had in reducing or preventing the occurrence of eDNA, proteins, carbohydrates, and viable cells within the EPS of the *S. mutans* 25175 biofilm when the biofilm was formed on both abiotic and biotic surfaces.

The first part of this research established the sucrose supplementation necessary for the greatest quantity of biofilm formed after overnight growth. This research found that 1 g/L of sucrose added to the BHI medium resulted in the greatest amount of biofilm attachment. At the same time, it was found that *S. mutans* 25175 (a facultative anaerobe) produced more attached biofilm when grown aerobically despite biofilm forming only on the sides and bottom of the wells and not at the medium-air interface. Next, this research determined the MIC of each QQ molecule necessary to prevent the visible growth of *S. mutans* 25175 in microwells after overnight growth. Those MICs plus subinhibitory concentrations (1/2 and 1/4 of the MIC) were used to treat *S. mutans* 25175 biofilms in subsequent experiments. Subinhibitory concentrations were studied to investigate what effect (if any) lower doses of the QQ molecules would have on biofilm formation. In particular, it was interesting to determine if the QQ molecules produce a hormesis response. Furthermore, the first section investigated the effects of the three QQ molecules (p-coumaric acid, tyrosol, and farnesol) at their respective MIC and subinhibitory concentrations (1/2 and 1/4 of the MIC) on some components of *S. mutans* 25175 biofilm when formed on plastic surfaces such as test tubes or microwell plates. Although there are several components that contribute to a bacterial biofilm, this research focused on the eDNA, total proteins, total carbohydrates, and viable cells within the *S. mutans* 25175 biofilm. The MIC of each QQ molecule was experimentally determined in this research and literature supports the values found in this research. In research done by Esteban-Fernández et al. (2018), the MIC of p-coumaric acid on *S. mutans* was

>1000 µg/mL which corresponds to the MIC that this research produced. p-Coumaric acid is generally found in lower levels in nature (around 0.1 to 8 mg/L) which makes it useful to study the effects of this molecule without killing *S. mutans* cells. Although Esteban-Fernández *et al.* (2018) did not determine the MIC of p-coumaric acid (they did not test concentrations greater than 1000 µg/mL), this research did, and it determined that the MIC of p-coumaric acid on *S. mutans* 25175 is 5,125 µg/mL or 31.25 mM. Souza *et al.*, (2019) also determined the same MIC of tyrosol to be the same that was found in this study (12,430.0 µg/mL). Farnesol has also been studied as an antimicrobial compound for *S. mutans* by Jeon *et al.*, (2011) and the MIC supported the findings of this research (1 mM).

Bacterial biofilms are fluid mosaics of everchanging microcolonies constantly rearranging to overcome challenges at each stage of growth and development. It is difficult to determine the exact proportions of eDNA, proteins, carbohydrates, viable cells, and other components of the EPS within a biofilm because a biofilm is constantly changing and is very dynamic. Some researchers have suggested that the EPS of the biofilm accounts for 50%-90% of the overall dry weight of the biofilm (Saini *et al.*, 2011). Others have similarly suggested that mature bacterial biofilms are about 10% bacterial cells and about 90% EPS (Kostakioti *et al.*, 2013). This research did not investigate the proportions of the biofilm but instead looked at the concentrations of eDNA, carbohydrates, and proteins within the EPS of the biofilm while also calculating the number of viable cells within the *S. mutans* 25175 biofilm formed under static conditions overnight (~18 to 24 hours).

These four components of the *S. mutans* 25175 biofilm have not been studied together, based on the lack of literature, making this research the first of its kind. Therefore, speculation of the possible mechanisms *S. mutans* employs when treated with QQ molecules and other anti-biofilm treatments based on similar literary works will be necessary to attempt to understand the data obtained in this research.

All three QQ molecules reduced the total biomass of *S. mutans* 25175 biofilm formed in microwells at their respective MIC and both subinhibitory concentrations. Although p-coumaric acid at 1/4 of the MIC and farnesol at the MIC did not reduce total biomass, there was still some reduction. Tyrosol at the MIC had the greatest percentage of reduction of overall biomass and was the only QQ molecule to reduce the biofilm biomass at all three concentrations that were tested. The MIC of tyrosol (125 mM) was also the highest MIC compared to the other two QQ molecules' MICs investigated in this study. Studies done by (Arias et al., 2016a) have demonstrated tyrosol's anti-biofilm abilities at concentrations lower than the MIC found in this study suggesting that even at subinhibitory concentrations tyrosol exhibits anti-biofilm capabilities.

When *S. mutans* 25175 biofilm was treated with p-coumaric acid, the eDNA, protein, and viable cell components of the biofilm were reduced by all three concentrations of p-coumaric acid tested while the carbohydrate component of the biofilm was not reduced by any of the concentrations. In this research, when *S. mutans* 25175 was treated with p-coumaric acid there was biomass accumulation in the medium, but the ability of the *S. mutans* 25175 biofilm to

adhere to the surface of the test tubes was visibly reduced which might explain why there was a measurable reduction in eDNA, protein, and viable cells in the adhered biofilm. With that in mind, it would have also been expected to see a statistically significant reduction in carbohydrate concentrations of *S. mutans* biofilm since the overall biomass was suspended in the medium instead of adhering to the available surface, but this was not observed in this research. Instead, the total carbohydrates in the *S. mutans* 25175 biofilm treated with p-coumaric acid was not different from the untreated control.

The importance of eDNA in oral biofilms is understood, but there have been no studies that measure the changes in eDNA of the biofilm when treated with p-coumaric acid at the concentrations used in this study. There have been studies that show eDNA aids *S. mutans* adhering to surfaces in the oral cavity and that without eDNA, *S. mutans* is unable to adhere to surfaces (Serrage et al., 2021). This could explain how when *S. mutans* 25175 biofilm was treated with p-coumaric acid, there was biomass accumulation in the medium, but the biofilm failed to adhere to the surfaces of the test tubes as demonstrated by Figure 3.6.

Like the eDNA in *S. mutans* 25175 biofilm, the protein component of the biofilm was reduced by all three concentrations of p-coumaric acid tested in this research. This research did not study the change in individual proteins, but rather the total protein concentrations in the biofilm because there are over 73 core genes that are only found in *S. mutans* that encode the proteins involved in carbohydrate metabolism and acid resistance (key virulence factors of *S. mutans*) (Lemos et al., 2019). It would be advantageous to have identified the change in

the proteins associated with adhesion, but that was not possible for this research due to the budget and loss of time during the Covid-19 pandemic. However, this research did investigate the fold change in gene expression of *gtfb* which is associated with the production of GtfB proteins that adhere to surfaces and convert dietary sucrose into the glucans that contribute to the carbohydrate component of the EPS. The MIC of p-coumaric acid caused a statistically significant increase in the expression of *gtfb* while the subinhibitory concentrations of p-coumaric acid did not result in a fold change with a statistically significant difference from the control. In order to better understand if these QQ molecules are in fact acting on and disrupting QS pathways within the biofilm, additional experiments can be done. Genetically engineered bacteria are the gold standard when detecting AIPs in Gram-positive bacteria. Plasmids can be developed to detect CSP synthesized by *S. mutans* (Miller and Gilmore, 2020).

Interestingly, there was not a statistically significant reduction in the carbohydrate concentrations in *S. mutans* 25175 biofilm when treated with p-coumaric acid at any of the concentrations as compared to the control despite the reduction in adhered biofilm on the test tube surface. One possible explanation might be that the sulfuric-phenol test employed in this research was flawed. Another explanation might be that despite the reduction of viable cells and proteins that adhered to the sides of the test tubes, there may have been both viable cells and functioning proteins within the biomass suspended in the medium that were able to produce the measurable carbohydrates attached to the walls of the test tubes. p-Coumaric acid may have an effect of the adhesion proteins of *S. mutans* which

prevented the adhesion of the cells to the test tube surface, but not to the functionality of the Gtf proteins that synthesis the glucans for the biofilm.

Although tyrosol has been used as an anti-biofilm agent in other studies, the MIC found in this study was higher (125 mM) than some others who have found that the MIC of tyrosol on *S. mutans* biofilms is around 90 mM (Arias et al., 2016b). Additionally, this is the first study to examine these individual components of the EPS of the *S. mutans* 25175 biofilm collectively. Tyrosol was the only QQ molecule in this study to reduce the overall biomass of the biofilm at all three concentrations. Additionally, tyrosol at its MIC (125 mM) was the treatment that reduced the overall biomass the most out of all the treatments. Like p-coumaric acid, tyrosol also reduced the number of viable cells as well as the eDNA concentration at all three concentrations that were tested. Interestingly, tyrosol, like p-coumaric acid, was able to reduce the protein concentration and have no change on the carbohydrate concentration at the MIC and 1/2 of the MIC but acted inversely at 1/4 of the MIC with the proteins and carbohydrates. This outcome is interesting because when there was no change in the protein concentration, it would be expected that there would also be no change in expression in carbohydrate concentration or even an increase in carbohydrate concentrations since the proteins were not changed, but in fact the carbohydrates decreased significantly. Similar to p-coumaric acid, the *gtfb* gene expression was increased at the MIC of tyrosol but not at the subinhibitory concentrations. Like the treatment of p-coumaric acid, it would have been expected that with an increase in gene expression of *gtfb*, there would have been an increase in

proteins. Additionally, there is a possibility that there was an increase in proteins in the biofilm by *gtfb* but they could have been unable to adhere to the surface and contribute to further biofilm formation.

The use of farnesol as a QQ molecule to prevent biofilm formation was interesting from the start. Farnesol was able to reduce the biomass of the biofilm at all concentrations tested but only at the subinhibitory concentrations. Although methanol was used as the solvent to dilute the concentrated farnesol in, it is possible that at higher concentrations the farnesol was not able to mix as well with the water-based culture media that the *S. mutans* biofilm was cultured in. The biofilm grows on the bottom and sides of the wells but farnesol is oily, less dense, and at higher concentrations will be on the surface of the water-based medium with minimal effect on the developing biofilm at the bottom of the well. However, at lower concentrations, farnesol was able to make a statistically significant impact on the reduction of the biofilm. Like p-coumaric acid and tyrosol, farnesol reduced the number of viable cells in the biofilm at all three concentrations tested in this research. Unlike the other two QQ molecules, farnesol only had a statistically significant impact on the eDNA at the MIC. This is in line with the theory that if there are fewer number of cells in the biofilm, then there is a lower chance that they can contribute to the eDNA of the EPS through secretion or cell lysis. With this in mind, it would have been hypothesised that with the statistically significant reduction of viable cells at the subinhibitory concentrations that there would also be less eDNA in the EPS, but there was no statistically significant difference from the control, only a small decrease in eDNA.

On the other hand, farnesol displayed expected results in regard to the protein and carbohydrate concentrations compared to the expression of *gtfb*. All three concentrations of farnesol caused a statistically significant decrease in *gtfb* gene expression which corresponded to a decrease in all the protein and all the carbohydrate concentrations of the biofilm (the protein concentration of the biofilm was reduced at 1/2 of the MIC of farnesol but not at a statistically significant level). This suggests that farnesol may interact directly with the *gtfb* pathway for synthesising sucrose into glucans for the biofilm. Although Gtfs were not included in the genes that were analysed in a study by Li Cao et al., (2017), other virulence genes in *S. mutans* (*luxS*, *brpA*, *ffh*, *recA*, *nth*, and *smx* genes) were analysed and there was a reduction in gene expression when treated with farnesol (Li Cao et al., 2017). This suggests that farnesol may play a role in reducing the virulence factors associated with biofilm formation and should be studied further.

S. mutans is a primary coloniser of dental biofilm on tooth (HA) surfaces (Lemos et al., 2019b). The ability for *S. mutans* to adhere to HA surfaces is because they overcome challenges such as the acidic environment, salivary flow, and competition by having several virulence factors (Iorgulescu, 2009). The first part of this study investigated the effects the three QQ molecules had on *S. mutans* biofilm formed on plastic surfaces. The next step of studying the effects these three QQ molecules have on *S. mutans* biofilm formation studied whether the results would be similar when the biofilm was formed on HA disks that mimic the natural surface where *S. mutans* would normally form a biofilm. Additionally, this

study investigated the differences of *S. mutans* biofilm forming a biofilm on 20% porosity HA surfaces or full density HA disks since enamel erosion of tooth surfaces can lead to an increase in dental caries incidences (Stephens et al., 2018). These experiments attempted to demonstrate the effectiveness of *S. mutans* biofilm being able to form on a compromised HA surface or a healthy HA surface to try to determine if enamel erosion of tooth surfaces leads to a higher risk of developing dental biofilms than teeth without enamel erosion. Again, this part of the study investigated the eDNA, viable cells, protein, and carbohydrate concentration of *S. mutans* 25175 biofilm when treated with the three QQ molecules at their MIC and subinhibitory concentrations. In previous research, Kim et al., (2018) found that there is a correlation of eDNA and CFUs of *S. mutans* biofilm when formed on HA surfaces. It is worth considering the results found in this study although there were many differences in the research methods including the strain of *S. mutans* used in the study, the sugar concentration in the media, the medium used for culturing the bacteria, and the method of measuring the eDNA in the biofilm.

The viability of cells within the biofilm were reduced by p-coumaric acid at all three concentrations on both the 20% porosity and the full density HA disks which suggests that there was no difference in the QQ's ability to reduce the number of cells within the biofilm despite the differences in surfaces. These results are also the same results that were seen when the biofilm was formed on plastic surfaces, but that is essentially the only similar findings from p-coumaric acid treatments on the biofilms formed on the plastic surfaces. The eDNA concentrations of the

biofilm when formed on the HA disks differed on all occasions except for 1/2 of the MIC of p-coumaric acid. This is interesting because p-coumaric acid appears more capable of reducing the biofilm on 20% porosity disks than full density disks. The eDNA was decreased by the MIC and 1/2 of the MIC on the 20% disks (and increased by 1/4 of the MIC) but the eDNA was unchanged by the MIC and 1/4 of the MIC on the full density disks. In comparison, the eDNA concentration of the biofilm was reduced by all the tested concentrations when the biofilm was formed on plastic surfaces. Although it could be hypothesised that the 20% porosity HA disks would have slightly more surface area and therefore more opportunity for the eDNA to adhere and anchor to than the full density HA disks, the data suggest that this is not the case. The protein concentration of the biofilm formed on HA disks when treated with p-coumaric acid was mainly unchanged. The only exception to this was the 1/4 of the MIC treatment of p-coumaric acid on the full density HA disks. This is not the case for the protein concentrations formed on plastic surfaces. This data suggests that the proteins in the biofilm formed on the HA disks were able to adhere better to the HA surface than plastic surfaces which is notable to acknowledge because after all, this bacterial biofilm is more adept to forming biofilms on tooth (HA) surfaces rather than plastic surfaces and one of *S. mutans* virulence factors is its ability to overcome these stressors from its environment. With the unchanged protein concentrations of the biofilm formed on the HA surfaces, it could be hypothesised that there would also be little to no change in the carbohydrate concentrations of the same biofilms, but in fact, the data show that there was primarily a statistically significant increase

in carbohydrate concentrations of the biofilm. the only exception to this trend was when the biofilm was treated with 1/2 of the MIC of p-coumaric acid on the full density HA disks and the carbohydrate concentration was decreased. This data is not similar to the data when the biofilm was formed on plastic surfaces. There was no change in the carbohydrate concentration of the biofilm formed on plastic surfaces when treated with the p-coumaric acid treatments. this might suggest that because the proteins were able to better adhere and overcome the QQ treatment, the stress response from *S. mutans* was to synthesis more carbohydrates for the biofilm to better protect the integrity of the biofilm and the embodied materials.

Tyrosol at the MIC and 1/2 of the MIC resulted in a statistically significant decrease in viable cells on both types of HA disks but not at 1/4 of the MIC. This differs from the viable cells in the biofilm grown on plastic surfaces where all concentrations of tyrosol caused a reduction of viable cells. In research done by Arias et al., (2016), there was a statistically significant reduction in viable cells at 200 mM on HA disks. That is similar to this study. It also found that the higher the concentrations of tyrosol resulted in fewer viable cells in the biofilm, but this study did not investigate tyrosol concentrations over 125 mM. However, the data from this research supports findings from previous research that suggests that despite the inability for tyrosol to reduce the CFUs in biofilms at concentrations lower than 50 mM, tyrosol does have other anti-biofilm capabilities that, considered together, demonstrate that even live biofilm cells exposed to 50 mM tyrosol had their metabolism reduced, which could compromise their virulence (Arias et al.,

2016b). The 1/4 of the MIC of tyrosol also differed in the other studied components of the biofilm. On the 20% porosity HA disks, there was no statistically significant change in viable cells of the biofilm, but there was a statistically significant increase in the eDNA, protein, and carbohydrate concentrations of the biofilm. This is interesting because it suggests that tyrosol at 1/4 of the MIC might encourage more robust biofilm formation as opposed to the desired outcome of reducing the formation on damaged HA. Similar results were found when the biofilm formed on full density HA disks with an exception of the decrease of proteins. This might suggest that tyrosol was able to impact the ability for the proteins to adhere to the full density HA's surface but caused the proteins that were able to attach to increase the carbohydrate synthesis for the biofilm which was increased in the biofilm on full density disks. The results from the MIC and 1/2 of the MIC of tyrosol regarding the noncellular components of the biofilm resulted in varying outcomes. As somewhat expected, the decrease in viable cells also resulted in a decrease of eDNA in the biofilm formed on 20% porosity HA disks at the MIC of tyrosol while there was no change in protein concentration but an increase in carbohydrate concentrations. Similar results were seen at the MIC of tyrosol on the biofilm formed on full density HA disks apart from the eDNA concentrations of the biofilm which actually increased instead of decreased. This is not what would have been expected when there was a statistically significant decrease in the viable cells of the biofilm. The 1/2 of the MIC of tyrosol on the biofilm produced interesting results that were unlike any results obtained in this study. There was a statistically significant decrease in

viable cells but no change in eDNA concentrations which would have been expected. Additionally, there was no change in protein concentrations but an increase in carbohydrate concentration of the biofilm formed on the 20% porosity HA disks. On the full density HA disks, the decrease in viable cells also resulted in a decrease in eDNA concentrations in the biofilm, but there was no change in the protein concentration of the biofilm but a statistically significant decrease in the carbohydrate concentration when treated with 1/2 of the MIC of tyrosol.

Although farnesol is an effective anti-biofilm reagent, topical farnesol treatments require multiple treatments of high drug concentrations to inhibit oral biofilm growth due to hydrophobicity-related solubility limits and poor biofilm retention (Sims et al., 2019). The shortcomings of farnesol to reduce *S. mutans* biofilm formation on HA disks has been reported in previous literature (Roncari Rocha et al., 2022). The treatment of farnesol on the biofilm formed on HA disks resulted in the same pattern as the treatment of tyrosol where there was a statistically significant decrease in viable cells of the biofilm at the MIC and 1/2 of the MIC of farnesol on both the 20% porosity and the full density HA disks, but there was no change in the number of viable cells when treated with 1/4 of the MIC of farnesol. The concentration of eDNA in the biofilms formed on the HA disks and treated with farnesol were similar on both the 20% porosity disks and the full density disks where there was a decrease in eDNA concentration at the MIC of farnesol, an increase in eDNA concentration at 1/2 of the MIC of farnesol, and no change in eDNA concentrations at 1/4 of the MIC of farnesol. These results were not similar to any of the results seen in the other two QQ molecule treatments. There

is a similarity in the protein concentration of the biofilm formed on 20% porosity HA disks when treated with farnesol as there is when treated with tyrosol. This is not the case with the full density HA disks. There was no change in the protein concentrations of the biofilms formed on full density disks, but there was an increase of carbohydrate concentration on when treated with the MIC and 1/2 of the MIC of farnesol but there was a decrease when treated with 1/4 of the MIC. There was an increase in carbohydrate concentration of the biofilm formed on the 20% porosity disks when treated with the MIC of farnesol which was seen often with the other QQ treatments at their respective MICs, but there was a decrease in carbohydrate concentrations at both 1/2 and 1/4 of the MIC of farnesol. The incidences where there was no change in protein concentrations but a decrease in carbohydrate concentrations at 1/4 of the MIC of the respective QQ molecule occurred with both p-coumaric acid and tyrosol but that was when the biofilm was formed on the full density HA disks, not the 20% porosity HA disks. There was an increase in protein concentration of biofilm formed on the 20% HA disks when treated with 1/4 of the MIC of farnesol but there was a decrease in carbohydrate concentration. This was not demonstrated in any other treatment. Improvements for the application of farnesol as an anti-biofilm treatment could be enhanced by encapsulating farnesol in a nanoparticle delivery system as described by Roncari Rocha et al., (2022). Farnesol has been found to be an effective anti-microbial agent against *S. mutans* biofilm formation in the oral cavity when delivered using nanoparticle delivery systems (Horev et al., 2015). Additionally, farnesol could be used synergistically with other antimicrobials to prevent or reduce *S. mutans*

biofilm formation on HA surfaces as was suggested in a study done by Rocha et al., (2018).

In the oral cavity, the HA surface of the tooth is negatively charged and positively charged molecules found in saliva and gingival crevicular fluid such as salivary glycoproteins, statherin, histatin, proline-rich proteins, and alpha-amylase attach to the surface of the tooth to form the acquired salivary pellicle. Some bacterial components such as Gtfs have also been found in the acquired salivary pellicle (Seneviratne et al., 2011). Because saliva was not used as a medium in this research and subsequently a salivary pellicle was not formed on the HA disks, it is plausible that the negatively charged cellular membrane of *S. mutans* could have prevented the attachment of the bacterial cells to the HA disks instead of the QQ molecules used in this study. This could explain why there was a statistically significant decrease in viable cells found in the *S. mutans* biofilm formed on the HA disks in this study. Additionally, this may explain why there was only two incidences of a statistically significant decrease in the protein concentrations found in the biofilm attached to the HA disks. Furthermore, if it is assumed that Gtf proteins were able to attach to the HA disks due to the electrostatic chemistry, it may explain the reason for the increase of carbohydrate concentrations found in the majority of biofilms attached to the HA disks. Repeating this research using saliva as a medium would afford the opportunity for a salivary pellicle to form on the HA disks and would advance the knowledge obtained from this study.

Within the oral cavity, there are both hard and soft tissue surfaces that give rise to the opportunity for microorganisms to colonise and form biofilms. Pathogenic biofilms formed on teeth can spread to the surrounding soft tissue of the gingiva and cause further infections such as gingivitis (Stephens et al., 2018). Furthermore, infections of the soft tissues surrounding the teeth can also cause damage to the tooth surface (Bowen et al., 2018). The oral cavity is a warm, moist environment where bacteria, fungi, and other microorganisms can thrive. The oral cavity has a built-in self-cleaning mechanism through chemical buffer systems via the saliva such as bicarbonate, phosphate, and protein that through salivary flow, waste and debris are cleared from the oral cavity (Iorgulescu, 2009.). The self-cleaning mechanism of the oral cavity is good at what it does, but it is not sufficient. That is why pathogenic microorganisms are able to persist and thrive in the oral cavity. This is also a reason why studying the effects of QQ molecules on biofilms that adhere to soft tissues in the oral cavity are also important.

The three QQ molecules in this study were effective in reducing *S. mutans* 25175 biofilm formation on abiotic surfaces such as plastic and HA. The QQ molecules were then investigated to determine their ability to reduce *S. mutans* 25175 biofilm formation on a biotic surface. First, it was necessary to determine if the QQ molecules in this study were toxic to HGF-1 cells which are found in the oral cavity. All three QQ molecules showed the same results with the MTT assay. After 10 and 20 minutes all three concentrations of each QQ molecule (the MIC and subinhibitory concentrations) did not produce a statistically significant change in the viability of the cells as well as 1/4 of the MIC of each QQ molecule

after 30 minutes. However, after 30 minutes, the MIC and 1/2 of the MIC resulted in a statistically significant decrease in the viability of the HGF-1 cells.

The ability of p-coumaric acid to prevent the adhesion of the bacterial cells to the HGF-1 cells was determined by counting the number of viable cells that were able to adhere to the cell line after 10, 20, or 30 minutes. p-Coumaric acid was able to decrease the number of cells that adhered to the HGF-1 cell line after 10, 20, and 30 minutes at the MIC and also at 1/2 and 1/4 of the MIC after 30 minutes. Despite their ability to adhere to the HGF-1 cells, the bacterial cells were only successful in forming a biofilm at 1/4 of the MIC after overnight incubation. The two higher concentrations of p-coumaric acid reduced the bacterial biofilm on the HGF-1 cell line. Although *S. mutans* is an oral pathogen that has an affinity for hard surfaces, studies suggest that there is some attachment of *S. mutans* cells to soft tissues of the oral cavity such as the gingiva (Wang et al., 2013). This research demonstrated that QQ molecules such as p-coumaric acid can reduce the adhesion of *S. mutans* cells to HGF-1 cells suggesting that by inhibiting the bacteria to adhere to the soft tissue surrounding the tooth, it could decrease the likelihood of *S. mutans* spreading to the hard surface of the tooth. Similar results were recorded by (Esteban-Fernández et al., 2018) regarding p-coumaric acid's ability to prevent *S. mutans* adhesion to fibroblast cells.

Tyrosol was also able to reduce the bacterial cells from adhering to the HGF-1 cells lines at the MIC after 10, 20, and 30 minutes. Additionally, 1/2 of the MIC of tyrosol reduced the adherence after 20 and 30 minutes and 1/4 of the MIC of tyrosol reduced the adherence after 30 minutes. Similar to p-coumaric acid, both

the MIC and 1/2 of the MIC of tyrosol were able to reduce the bacterial biofilm formed on the HGF-1 cell line. Although there is no literature suggesting that tyrosol inhibits *S. mutans* ability to adhere to soft tissue in the oral cavity, a study showed that purified extracts such as ethanol, ethyl acetate and chloroform from mushrooms such as *Antrodia camphorata* demonstrated similar inhibition abilities like the ones in this study using tyrosol and farnesol (Lien et al., 2014).

Farnesol was only able to reduce the adherence of bacterial cells to the HGF-1 cells line at the MIC and 1/2 of the MIC after 30 minutes. Both of these results also reduced the viability of the HGF-1 cells so although they were able to reduce the number of bacterial cells that adhered to the cell line, they would not be suitable treatments at these concentrations. Farnesol was only able to reduce the amount of *S. mutans* biofilm formed on HGF-1 cell lines at the MIC.

While dental caries is a polymicrobial disease, selective targeting of *S. mutans* in dental biofilms is viewed as a suitable approach for its prevention. This is primarily because the synthesis of insoluble glucans from sucrose by *S. mutans* is central for the formation of a stable biofilm matrix that facilitates bacterial colonisation of the tooth surface and, at the same time, serves as a diffusion barrier helping to maintain the acidic environment where cariogenic bacteria thrive (Lemos et al., 2019b). Based on the data from this research, all three QQ molecules were able to reduce *S. mutans* 25175 biofilm formation on both biotic and abiotic surfaces at their respective MICs to some degree and had statistically significant impact on important components of the EPS. p-Coumaric acid, tyrosol, and farnesol at the MICs and some subinhibitory concentrations found in this research suggest

that they may be an alternative to conventionally used anti-biofilm treatments without adverse effects on the tissues.

Chapter 5 Conclusion

Biofilms and their complexity pose a serious threat to the environment, industry, and human health. Virulence factors including biofilm formation initiated by QS aid microorganisms in the construction of impenetrable fortresses that protect them from conventional therapies. Interrupting or inhibiting QS among microorganisms without killing them in a targeted approach via QQ is one method proposed to combat biofilm formation and subsequent infection or disease. This approach offers a promising solution to prevent biofilm formation and subsequent diseases and infections.

The bacterium *S. mutans* is a primary coloniser of dental biofilms on tooth surfaces that creates an ideal environment for subsequent colonisation of other bacterial species that result in acidification and erosion of the enamel surface that can lead to painful carious lesions. *S. mutans* utilises the AIP QS pathway to transition from the planktonic state of being to the attached, biofilm lifestyle. Existing in a biofilm is advantageous for *S. mutans* and enables the bacterium to multiply and evade host responses and anti-biotic treatments. The use of QQ techniques suppresses *S. mutans*' ability to communicate effectively resulting in no biofilm formation or impeded integrity of the successful biofilm. This research studied the effects of three QQ molecules (p-coumaric acid, tyrosol, and farnesol) at the MIC and subinhibitory concentrations on the eDNA, proteins,

carbohydrates, and viable cells of *S. mutans* 25175 biofilm formed on plastic, HA, and HGF-1 cell line.

Section one of this research investigated the effects the QQ molecules had on *S. mutans* biofilm formed on plastic surfaces. The data collected from the studies in this section conclude that tyrosol was the QQ molecule that reduced the biofilm the most when formed on plastic surfaces. Unlike p-coumaric acid and farnesol, tyrosol reduced *S. mutans* biofilm formed on plastic surfaces at its MIC and both subinhibitory concentrations (1/2 and 1/4 of the MIC). Although p-coumaric acid and farnesol were successful in reducing certain measured components of the biofilm, when the data were normalised and compared to one another, tyrosol had the lowest score indicating that it reduced biofilm formation more than the other two QQ molecules. Another conclusion drawn from the data in section one indicated that p-coumaric acid and tyrosol increase *gtfb* expression of *S. mutans* biofilm at their MICs, but farnesol decreases *gtfb* expression at all three concentrations that were tested in this research. These data suggest that the QQ molecules act on the specific QS pathways necessary for GtfB production and biofilm formation. More research into other virulence genes and protein production is necessary to fully understand the mechanisms these three QQ molecules can disrupt in *S. mutans* which may also provide clues to how these QQ molecules can disrupt other species of microbial biofilms.

Section two of this research studied the effects of the three QQ molecules' ability to prevent *S. mutans* biofilm formation biofilm on full density and 20% porosity HA disks by measuring the individual components of the biofilm (eDNA,

carbohydrates, protein, and viable cells) that adhered to the HA disks. It was hypothesised that there would be a difference in biofilm formation on the full density HA disks in comparison to the 20% porosity HA disk, but there was not sufficient evidence to support this and further studies on this topic should be done. There was not a consensus that one QQ molecule prevented *S. mutans* biofilm formation on either type of HA disk; however, each of the QQ molecules were among the top 3 performers for each type of disk. The biofilms formed on 20% porosity disks were reduced by 1/2 of the MIC of farnesol (#1), p-coumaric acid (#2), and tyrosol (#3). The biofilm formed on full density HA disks were reduced by 1/2 of the MIC of tyrosol (#1) and p-coumaric acid (#3) and by the MIC of farnesol (#2). These results suggest that subinhibitory concentrations of QQ molecules should be studied further for their role in anti-biofilm formation.

Section three of this research studied the effects that the QQ molecules have on bacterial cell adherence and biofilm formation on human tissue. The results conclude that tyrosol out performed the other two QQ molecules, taking the top three places when the treatments were normalised and ranked for their ability to reduce the number of viable cells that adhered to the HGF-1 cell line and to prevent biofilm formation.

Overall, this research studied four major individual components of *S. mutans* 25175 biofilm at the same time (eDNA, proteins, carbohydrates, and viable cells) and the effects that followed treatment with the QQ molecules p-coumaric acid, tyrosol, and farnesol at their MICs and subinhibitory concentrations. This research concluded that these three QQ molecules can aid in the reduction of *S.*

mutans biofilm formation and are effective anti-biofilm agents. Special attention should be given to tyrosol in future studies due to its consistent ability to reduce *S. mutans* biofilm formation on a variety of surfaces.

Chapter 6 Future Work

The limited duration of PhD research frequently leaves numerous questions unanswered, and the novel findings during PhD research opens the door to new and exciting questions. This research showed just how dynamic the characteristics of a single species biofilm can be when formed on three different surfaces. Additionally, this research showed how different the effects of three QQ molecules can be on different components the EPS of a single species biofilm formed on the various substrates. This research studied the effects of only a select few components (eDNA, carbohydrates, proteins, and viable cells) of the biofilm but did not exhaust all the known components such as metal ions, divalent cations, lipids, and humic substances which could hold crucial information for drug development and targeted therapy using QQ molecules.

This research studied *S. mutans* 25175 using only BHI medium that was supplemented only with sucrose. Studying this organism in a medium more closely related to the oral cavity such as real or artificial saliva and various sugar sources could be beneficial in closing the gap between laboratory settings and real-life applications.

Dental biofilms are typically multispecies biofilms with primary, secondary, and late colonisers that occupy available niches within the biofilm and contribute to the detrimental effects of acidification and demineralisation of the tooth surface. This research studied the effects of QQ molecules on a single species biofilm (*S.*

mutans, a primary coloniser). Further research involving multispecies biofilms and the effects QQ molecules have on the species in tandem would greatly benefit dental biofilm research efforts. Only three QQ molecules were used in this research because of promising results from previous studies despite there being a vast array of other existing QQ molecules (e.g., cinnamaldehyde, furanone, paraoxonase, 3-oxo-C12-(2-aminocyclohexanone), and many others) and antimicrobial compounds that could potentially provide better biofilm reduction capabilities.

The research done in this project allowed *S. mutans* biofilm to be established on a limited number of surfaces including polystyrene plastic, HA, and monolayer cell line surfaces. The use of real teeth as a substrate for *S. mutans* biofilm to form on instead of HA disks could provide additional information on the ability of the QQ molecules used in this study to inhibit attachment and biofilm formation. The findings can potentially provide useful information regarding the responses based on the differences between the model system (HA disks) and the real system (teeth). This may help in the choice of model systems in future works in this line of research. Furthermore, differences in the response of teeth from different age groups and genders might reveal novel information on the biofilm preventing strategies. The biofilms in this study were formed under static conditions which is not representative of the oral cavity which suggests that the use of a flow-cell model would more accurately mimic *in vivo* conditions. Additionally, the inclusion of clinical trials or animal studies could demonstrate the effects of the QQ molecules *in vivo*.

This research was not able to identify the specific mechanisms of interaction including how the QQ molecules interact in the quorum sensing system in *S. mutans* of which there are three or more possibilities within the two different quorum sensing systems that *S. mutans* utilises.

There are many genes including *gtfC*, *gtfD*, *luxS*, *comX*, *comFA*, *celA*, and *cglA* that respond to QS molecules in *S. mutans* that are activated when a quorum is reached that aid in the formation of the biofilm. This research only looked at one gene that encodes the GtfB proteins that are responsible for glucan synthesis from dietary sucrose leaving the door open to additional genetic and molecular biology work in the future as it relates to QQ capabilities. A comprehensive genomic study will increase the knowledge significantly, opening avenues for further and extended research in this area.

Protein quantification of individual proteins within a biofilm was not done in this study but should be encouraged in future work for a better understanding of the contributions of specific proteins and the effects QQ molecules have on their quantity and functionality. In this context, proteomics investigations are of interest.

Chapter 7 References

- Abisado, R.G. et al. (2018). Bacterial Quorum Sensing and Microbial Community Interactions. *mBio*, 9 (3). Available from <https://doi.org/10.1128/mBio.02331-17>.
- Abu Khweek, A. and Amer, A.O. (2018). Factors Mediating Environmental Biofilm Formation by *Legionella pneumophila*. *Frontiers in Cellular and Infection Microbiology*, 8. Available from <https://doi.org/10.3389/fcimb.2018.00038>.
- Agnihotry, A., Fedorowicz, Z. and Nasser, M. (2016). Adhesively bonded versus non-bonded amalgam restorations for dental caries. *Cochrane Database of Systematic Reviews*. Available from <https://doi.org/10.1002/14651858.CD007517.pub3>.
- Al-Omari, A. et al. (2014). Oral antibiotic therapy for the treatment of infective endocarditis: a systematic review. *BMC Infectious Diseases*, 14 (1). Available from <https://doi.org/10.1186/1471-2334-14-140>.
- Andrews, J.M. (2001a). Determination of minimum inhibitory concentrations. *Journal of Antimicrobial Chemotherapy*, 48 (suppl_1). Available from https://doi.org/10.1093/jac/48.suppl_1.5.
- Arias, L.S. et al. (2016a). Activity of tyrosol against single and mixed-species oral biofilms. *Journal of Applied Microbiology*, 120 (5), 1240–1249. Available from <https://doi.org/10.1111/jam.13070>.

Banthia, R., Chandki, R. and Banthia, P. (2011). Biofilms: A microbial home. *Journal of Indian Society of Periodontology*, 15 (2). Available from <https://doi.org/10.4103/0972-124X.84377>.

Barbosa, J.O. et al. (2016). Streptococcus mutans Can Modulate Biofilm Formation and Attenuate the Virulence of Candida albicans. *PLOS ONE*, 11 (3). Available from <https://doi.org/10.1371/journal.pone.0150457>.

Beitelshees, M., Hill, A., Jones, C. and Pfeifer, B., 2018. Phenotypic Variation during Biofilm Formation: Implications for Anti-Biofilm Therapeutic Design. *Materials*, 11(7), p.1086.

Bowen, W.H. and Koo, H. (2011). Biology of <i>Streptococcus mutans</i>-<i>Derived Glucosyltransferases: Role in Extracellular Matrix Formation of Cariogenic Biofilms. *Caries Research*, 45 (1). Available from <https://doi.org/10.1159/000324598>.

Bowen, W.H. et al. (2018). Oral Biofilms: Pathogens, Matrix, and Polymicrobial Interactions in Microenvironments. *Trends in Microbiology*, 26 (3), 229–242. Available from <https://doi.org/10.1016/j.tim.2017.09.008>.

Breton, C. et al. (2006). Structures and mechanisms of glycosyltransferases. *Glycobiology*, 16 (2). Available from <https://doi.org/10.1093/glycob/cwj016>.

Cao Li et al. (2017). Farnesol inhibits development of caries by augmenting oxygen sensitivity and suppressing virulence-associated gene expression in *Streptococcus mutans*. *Journal of Biomedical Research*. Available from <https://doi.org/10.7555/JBR.31.20150151>.

Castillo Pedraza, M.C. et al. (2017). Extracellular DNA and lipoteichoic acids interact with exopolysaccharides in the extracellular matrix of *Streptococcus mutans* biofilms. *Biofouling*, 33 (9), 722–740. Available from <https://doi.org/10.1080/08927014.2017.1361412>.

Chenicheri, S. et al. (2017). Insight into Oral Biofilm: Primary, Secondary and Residual Caries and Phyto-Challenged Solutions. *The Open Dentistry Journal*, 11 (1). Available from <https://doi.org/10.2174/1874210601711010312>.

Cohen, B.A. (2013). Oral Cavity. *Pediatric Dermatology*. Elsevier. Available from <https://doi.org/10.1016/B978-0-7234-3655-3.00009-6>.

Cukkemane, N. et al. (2014). Identification and characterization of a salivary-pellicle-binding peptide by phage display. *Archives of Oral Biology*, 59 (5), 448–454. Available from <https://doi.org/10.1016/j.archoralbio.2014.02.006>.

Dave, P. et al. (2020). Survey of Saliva Components and Virus Sensors for Prevention of COVID-19 and Infectious Diseases. *Biosensors*, 11 (1). Available from <https://doi.org/10.3390/bios11010014>.

di Lorenzo, F. et al. (2020). The Structure of the Lipid A of Gram-Negative Cold-Adapted Bacteria Isolated from Antarctic Environments. *Marine Drugs*, 18 (12). Available from <https://doi.org/10.3390/md18120592>.

Díaz-Garrido, N. et al. (2020). Competition and Caries on Enamel of a Dual-Species Biofilm Model with *Streptococcus mutans* and *Streptococcus sanguinis*. *Applied and Environmental Microbiology*, 86 (21). Available from <https://doi.org/10.1128/AEM.01262-20>.

Dong, Y.-H., Wang, L.-H. and Zhang, L.-H. (2007). Quorum-quenching microbial infections: mechanisms and implications. *Philosophical Transactions of the Royal Society B: Biological Sciences*, 362 (1483), 1201–1211. Available from <https://doi.org/10.1098/rstb.2007.2045>.

Donlan, R.M. (2002). Biofilms: Microbial Life on Surfaces. *Emerging Infectious Diseases*, 8 (9). Available from <https://doi.org/10.3201/eid0809.020063>.

Esteban-Fernández, A. et al. (2018). Inhibition of Oral Pathogens Adhesion to Human Gingival Fibroblasts by Wine Polyphenols Alone and in Combination with an Oral Probiotic. *Journal of Agricultural and Food Chemistry*, 66 (9). Available from <https://doi.org/10.1021/acs.jafc.7b05466>.

Federle, M.J. (2009). Autoinducer-2-Based Chemical Communication in Bacteria: Complexities of Interspecies Signaling. *Bacterial Sensing and Signaling*. Basel: KARGER, 18–32. Available from <https://doi.org/10.1159/000219371>.

Flemming, H.-C. and Wingender, J. (2010). The biofilm matrix. *Nature Reviews Microbiology*, 8 (9). Available from <https://doi.org/10.1038/nrmicro2415>.

Fong, J.N.C. and Yildiz, F.H. (2015). Biofilm Matrix Proteins. *Microbiology Spectrum*, 3 (2). Available from <https://doi.org/10.1128/microbiolspec.MB-0004-2014>.

Fuqua, C., Parsek, M.R. and Greenberg, E.P. (2001). Regulation of Gene Expression by Cell-to-Cell Communication: Acyl-Homoserine Lactone Quorum

Sensing. *Annual Review of Genetics*, 35 (1), 439–468. Available from <https://doi.org/10.1146/annurev.genet.35.102401.090913>.

Giordano, D. (2020). Bioactive Molecules from Extreme Environments. *Marine Drugs*, 18 (12). Available from <https://doi.org/10.3390/md18120640>.

Grande, R. et al. (2015). NF- κ B mediated down-regulation of collagen synthesis upon HEMA (2-hydroxyethyl methacrylate) treatment of primary human gingival fibroblast/*Streptococcus mutans* co-cultured cells. *Clinical Oral Investigations*, 19 (4). Available from <https://doi.org/10.1007/s00784-014-1304-4>.

Graves, D.T., Corrêa, J.D. and Silva, T.A. (2019). The Oral Microbiota Is Modified by Systemic Diseases. *Journal of Dental Research*, 98 (2). Available from <https://doi.org/10.1177/0022034518805739>.

Gu, Y. et al. (2020). Effects of Exogenous Synthetic Autoinducer-2 on Physiological Behaviors and Proteome of Lactic Acid Bacteria. *ACS Omega*, 5 (3), 1326–1335. Available from <https://doi.org/10.1021/acsomega.9b01021>.

Guan, C. et al. (2020). Effect of Rubusoside, a Natural Sucrose Substitute, on *Streptococcus mutans* Biofilm Cariogenic Potential and Virulence Gene Expression In Vitro. *Applied and Environmental Microbiology*, 86 (16). Available from <https://doi.org/10.1128/AEM.01012-20>.

Holland, T.L. et al. (2016). Infective endocarditis. *Nature Reviews Disease Primers*, 2 (1). Available from <https://doi.org/10.1038/nrdp.2016.59>.

Horev, B. et al. (2015). pH-Activated Nanoparticles for Controlled Topical Delivery of Farnesol To Disrupt Oral Biofilm Virulence. *ACS Nano*, 9 (3), 2390–2404. Available from <https://doi.org/10.1021/nn507170s>.

<https://www.webmd.com/oral-health/picture-of-the-teeth#1>. (no date).

Humphrey, S.P. and Williamson, R.T. (2001). A review of saliva: Normal composition, flow, and function. *The Journal of Prosthetic Dentistry*, 85 (2), 162–169. Available from <https://doi.org/10.1067/mpr.2001.113778>.

Ibáñez de Aldecoa, A.L., Zafra, O. and González-Pastor, J.E. (2017). Mechanisms and Regulation of Extracellular DNA Release and Its Biological Roles in Microbial Communities. *Frontiers in Microbiology*, 8. Available from <https://doi.org/10.3389/fmicb.2017.01390>.

Iorgulescu, G. (2009). Saliva between normal and pathological. Important factors in determining systemic and oral health. *Journal of medicine and life*, 2 (3), 303–7.

Ito, T., Maeda, T. and Senpuku, H. (2012). Roles of Salivary Components in *Streptococcus mutans* Colonization in a New Animal Model Using NOD/SCID.e2f1^{-/-} Mice. *PLoS ONE*, 7 (2), e32063. Available from <https://doi.org/10.1371/journal.pone.0032063>.

Jamal, M. et al. (2018). Bacterial biofilm and associated infections. *Journal of the Chinese Medical Association*, 81 (1). Available from <https://doi.org/10.1016/j.jcma.2017.07.012>.

Kaplan, J.B. (2010). Biofilm Dispersal: Mechanisms, Clinical Implications, and Potential Therapeutic Uses. *Journal of Dental Research*, 89 (3). Available from <https://doi.org/10.1177/0022034509359403>.

Kawada-Matsuo, M., Oogai, Y. and Komatsuzawa, H. (2016). Sugar Allocation to Metabolic Pathways is Tightly Regulated and Affects the Virulence of *Streptococcus mutans*. *Genes*, 8 (1). Available from <https://doi.org/10.3390/genes8010011>.

Kim, M., Jeon, J. and Kim, J. (2018). *Streptococcus mutans* extracellular DNA levels depend on the number of bacteria in a biofilm. *Scientific Reports*, 8 (1), 13313. Available from <https://doi.org/10.1038/s41598-018-31275-y>.

Koo, H. et al. (2002). Effects of Compounds Found in Propolis on *Streptococcus mutans* Growth and on Glucosyltransferase Activity. *Antimicrobial Agents and Chemotherapy*, 46 (5). Available from <https://doi.org/10.1128/AAC.46.5.1302-1309.2002>.

Kostakioti, M., Hadjifrangiskou, M. and Hultgren, S.J. (2013). Bacterial Biofilms: Development, Dispersal, and Therapeutic Strategies in the Dawn of the Postantibiotic Era. *Cold Spring Harbor Perspectives in Medicine*, 3 (4), a010306–a010306. Available from <https://doi.org/10.1101/cshperspect.a010306>.

Lane, N. (2015). The unseen world: reflections on Leeuwenhoek (1677) 'Concerning little animals.' *Philosophical Transactions of the Royal Society B:*

Biological Sciences, 370 (1666). Available from
<https://doi.org/10.1098/rstb.2014.0344>.

Lemos, J.A. et al. (2013). Streptococcus mutans: a new Gram-positive paradigm? Microbiology, 159 (Pt_3). Available from
<https://doi.org/10.1099/mic.0.066134-0>.

Lemos, J.A. et al. (2019). The Biology of Streptococcus mutans. Microbiology Spectrum, 7 (1). Available from <https://doi.org/10.1128/microbiolspec.GPP3-0051-2018>.

Li, X. et al. (2000). Systemic Diseases Caused by Oral Infection. Clinical Microbiology Reviews, 13 (4), 547–558. Available from
<https://doi.org/10.1128/CMR.13.4.547-558.2000>.

Lien, H.-M. et al. (2014). Antimicrobial Activity of Antrodia camphorata Extracts against Oral Bacteria. PLoS ONE, 9 (8), e105286. Available from
<https://doi.org/10.1371/journal.pone.0105286>.

Limoli, D.H., Jones, C.J. and Wozniak, D.J. (2015). Bacterial Extracellular Polysaccharides in Biofilm Formation and Function. Microbiology Spectrum, 3 (3). Available from <https://doi.org/10.1128/microbiolspec.MB-0011-2014>.

Lindh, L. et al. (2014). Salivary Pellicles. 30–39. Available from
<https://doi.org/10.1159/000358782>.

Lister, J.L. and Horswill, A.R. (2014). Staphylococcus aureus biofilms: recent developments in biofilm dispersal. *Frontiers in Cellular and Infection Microbiology*, 4. Available from <https://doi.org/10.3389/fcimb.2014.00178>.

Luo, Y. et al. (2021). Mechanisms and Control Strategies of Antibiotic Resistance in Pathological Biofilms. *Journal of Microbiology and Biotechnology*, 31 (1). Available from <https://doi.org/10.4014/jmb.2010.10021>.

Majumdar, S. and Pal, S. (2016). Quorum sensing: a quantum perspective. *Journal of Cell Communication and Signaling*, 10 (3), 173–175. Available from <https://doi.org/10.1007/s12079-016-0348-4>.

Matsumoto-Nakano, M. (2018). Role of Streptococcus mutans surface proteins for biofilm formation. *Japanese Dental Science Review*, 54 (1), 22–29. Available from <https://doi.org/10.1016/j.jdsr.2017.08.002>.

Mayo Clinic Staff. (2021). Oral health: A window to your overall health. *Healthy Lifestyle Adult health*.

McBrayer, D.N., Cameron, C.D. and Tal-Gan, Y. (2020). Development and utilization of peptide-based quorum sensing modulators in Gram-positive bacteria. *Organic & Biomolecular Chemistry*, 18 (37), 7273–7290. Available from <https://doi.org/10.1039/D0OB01421D>.

Miklasińska-Majdanik, M. et al. (2018). Phenolic Compounds Diminish Antibiotic Resistance of Staphylococcus Aureus Clinical Strains. *International Journal of Environmental Research and Public Health*, 15 (10), 2321. Available from <https://doi.org/10.3390/ijerph15102321>.

Miller, C. and Gilmore, J., 2020. Detection of Quorum-Sensing Molecules for Pathogenic Molecules Using Cell-Based and Cell-Free Biosensors. *Antibiotics*, 9(5), p.259.

Monnet, V. and Gardan, R. (2015). Quorum-sensing regulators in Gram-positive bacteria: 'cherchez le peptide .' *Molecular Microbiology*, 97 (2), 181–184.

Available from <https://doi.org/10.1111/mmi.13060>.

Montanaro, L. et al. (2011). Extracellular DNA in Biofilms. *The International Journal of Artificial Organs*, 34 (9). Available from

<https://doi.org/10.5301/ijao.5000051>.

Mukherjee, S. and Bassler, B.L. (2019). Bacterial quorum sensing in complex and dynamically changing environments. *Nature Reviews Microbiology*, 17 (6), 371–382. Available from <https://doi.org/10.1038/s41579-019-0186-5>.

Muras, A. et al. (2018). Inhibition of *Streptococcus mutans* biofilm formation by extracts of *Tenacibaculum* sp., a bacterium with wide-spectrum quorum quenching activity. *Journal of Oral Microbiology*, 10 (1), 1429788. Available from <https://doi.org/10.1080/20002297.2018.1429788>.

Nakano, K., Nomura, R. and Ooshima, T. (2008). *Streptococcus mutans* and cardiovascular diseases. *Japanese Dental Science Review*, 44 (1). Available from <https://doi.org/10.1016/j.jdsr.2007.09.001>.

National Cancer Institute. (2021). Oral Cavity .

<https://www.cancer.gov/publications/dictionaries/cancer-terms/def/oral-cavity>.

Nguyen, T., Roddick, F. and Fan, L. (2012). Biofouling of Water Treatment Membranes: A Review of the Underlying Causes, Monitoring Techniques and Control Measures. *Membranes*, 2 (4). Available from <https://doi.org/10.3390/membranes2040804>.

Nomura, R. et al. (2007). Repeated bacteraemia caused by *Streptococcus mutans* in a patient with Sjögren's syndrome. *Journal of Medical Microbiology*, 56 (7). Available from <https://doi.org/10.1099/jmm.0.47186-0>.

Nomura, R. et al. (2020). Potential involvement of *Streptococcus mutans* possessing collagen binding protein Cnm in infective endocarditis. *Scientific Reports*, 10 (1), 19118. Available from <https://doi.org/10.1038/s41598-020-75933-6>.

O'Toole, G.A. (2011). Microtiter Dish Biofilm Formation Assay. *Journal of Visualized Experiments*, (47). Available from <https://doi.org/10.3791/2437>.

Okshevsky, M. and Meyer, R.L. (2015). The role of extracellular DNA in the establishment, maintenance and perpetuation of bacterial biofilms. *Critical Reviews in Microbiology*, 41 (3). Available from <https://doi.org/10.3109/1040841X.2013.841639>.

Paluch, E. et al. (2020). Prevention of biofilm formation by quorum quenching. *Applied Microbiology and Biotechnology*, 104 (5). Available from <https://doi.org/10.1007/s00253-020-10349-w>.

Pandit, A. et al. (2020). Microbial biofilms in nature: unlocking their potential for agricultural applications. *Journal of Applied Microbiology*, 129 (2). Available from <https://doi.org/10.1111/jam.14609>.

Passos da Silva, D. et al. (2017). An Update on the Sociomicrobiology of Quorum Sensing in Gram-Negative Biofilm Development. *Pathogens*, 6 (4), 51. Available from <https://doi.org/10.3390/pathogens6040051>.

Phumat, P. et al. (2018). Effects of *Piper betle* fractionated extracts on inhibition of *Streptococcus mutans* and *Streptococcus intermedius*; *Drug Discoveries & Therapeutics*, 12 (3), 133–141. Available from <https://doi.org/10.5582/ddt.2018.01021>.

Pierrat, X. and Persat, A. (2017). Flipping the switch. *eLife*, 6. Available from <https://doi.org/10.7554/eLife.31082>.

Pijning, T., Gangoiti, J., te Poele, E., Börner, T. and Dijkhuizen, L., 2021. Insights into Broad-Specificity Starch Modification from the Crystal Structure of *Limosilactobacillus Reuteri* NCC 2613 4,6- α -Glucanotransferase GtfB. *Journal of Agricultural and Food Chemistry*, 69(44), pp.13235-13245.

Rainey, K. et al. (2019). Glycosyltransferase-Mediated Biofilm Matrix Dynamics and Virulence of *Streptococcus mutans*. *Applied and Environmental Microbiology*, 85 (5). Available from <https://doi.org/10.1128/AEM.02247-18>.

Rao, X., Lai, D. and Huang, X., 2013. A New Method for Quantitative Real-Time Polymerase Chain Reaction Data Analysis. *Journal of Computational Biology*, 20(9), pp.703-711.

Rehman, Z.U. and Leiknes, T. (2018). Quorum-Quenching Bacteria Isolated From Red Sea Sediments Reduce Biofilm Formation by *Pseudomonas aeruginosa*. *Frontiers in Microbiology*, 9. Available from <https://doi.org/10.3389/fmicb.2018.01354>.

Ren, Z. et al. (2016). Molecule Targeting Glucosyltransferase Inhibits *Streptococcus mutans* Biofilm Formation and Virulence. *Antimicrobial Agents and Chemotherapy*, 60 (1). Available from <https://doi.org/10.1128/AAC.00919-15>.

Renner, L.D. and Weibel, D.B. (2011). Physicochemical regulation of biofilm formation. *MRS Bulletin*, 36 (5), 347–355. Available from <https://doi.org/10.1557/mrs.2011.65>.

Rocha, G.R. et al. (2018). Effect of tt-farnesol and myricetin on in vitro biofilm formed by *Streptococcus mutans* and *Candida albicans*. *BMC Complementary and Alternative Medicine*, 18 (1), 61. Available from <https://doi.org/10.1186/s12906-018-2132-x>.

Roncari Rocha, G. et al. (2022). Nanoparticle carrier co-delivery of complementary antibiofilm drugs abrogates dual species cariogenic biofilm formation in vitro. *Journal of Oral Microbiology*, 14 (1). Available from <https://doi.org/10.1080/20002297.2021.1997230>.

Roy, R. et al. (2018). Strategies for combating bacterial biofilms: A focus on anti-biofilm agents and their mechanisms of action. *Virulence*, 9 (1), 522–554. Available from <https://doi.org/10.1080/21505594.2017.1313372>.

Rutherford, S.T. and Bassler, B.L. (2012). Bacterial Quorum Sensing: Its Role in Virulence and Possibilities for Its Control. *Cold Spring Harbor Perspectives in Medicine*, 2 (11), a012427–a012427. Available from <https://doi.org/10.1101/cshperspect.a012427>.

Sahni, K. and Khashai, F. (2016). Exploring Mechanisms of Biofilm Removal. *Dentistry*, 06 (04). Available from <https://doi.org/10.4172/2161-1122.1000371>.

Saini, R., Saini, S. and Sharma, S. (2011). Biofilm: A dental microbial infection. *Journal of Natural Science, Biology and Medicine*, 2 (1), 71. Available from <https://doi.org/10.4103/0976-9668.82317>.

Senadheera, D. and Cvitkovitch, D.G. (2008). Quorum Sensing and Biofilm Formation by *Streptococcus mutans*. *Bacterial Signal Transduction: Networks and Drug Targets*. New York, NY: Springer New York. Available from https://doi.org/10.1007/978-0-387-78885-2_12.

Seneviratne, C.J., Zhang, C.F. and Samaranayake, L.P. (2011). Dental plaque biofilm in oral health and disease. *The Chinese journal of dental research : the official journal of the Scientific Section of the Chinese Stomatological Association (CSA)*, 14 (2), 87–94.

Serrage, H.J. et al. (2021). Understanding the Matrix: The Role of Extracellular DNA in Oral Biofilms. *Frontiers in Oral Health*, 2. Available from <https://doi.org/10.3389/froh.2021.640129>.

Sims, K.R. et al. (2019). Enhanced design and formulation of nanoparticles for anti-biofilm drug delivery. *Nanoscale*, 11 (1), 219–236. Available from <https://doi.org/10.1039/C8NR05784B>.

Souza, J.A.S. et al. (2019). Antimicrobial Activity of Compounds Containing Silver Nanoparticles and Calcium Glycerophosphate in Combination with Tyrosol. *Indian Journal of Microbiology*, 59 (2). Available from <https://doi.org/10.1007/s12088-019-00797-y>.

Steinberg, D., Poran, S. and Shapira, L. (1999). The effect of extracellular polysaccharides from *Streptococcus mutans* on the bactericidal activity of human neutrophils. *Archives of Oral Biology*, 44 (5). Available from [https://doi.org/10.1016/S0003-9969\(99\)00014-X](https://doi.org/10.1016/S0003-9969(99)00014-X).

Stephens, M.B., Wiedemer, J.P. and Kushner, G.M. (2018). Dental Problems in Primary Care. *American family physician*, 98 (11), 654–660.

Stewart, P.S. (2002). Mechanisms of antibiotic resistance in bacterial biofilms. *International Journal of Medical Microbiology*, 292 (2). Available from <https://doi.org/10.1078/1438-4221-00196>.

Takenaka, S., Ohsumi, T. and Noiri, Y. (2019). Evidence-based strategy for dental biofilms: Current evidence of mouthwashes on dental biofilm and gingivitis. *Japanese Dental Science Review*, 55 (1). Available from <https://doi.org/10.1016/j.jdsr.2018.07.001>.

Taylor, P.W., Stapleton, P.D. and Paul Luzio, J. (2002). New ways to treat bacterial infections. *Drug Discovery Today*, 7 (21). Available from [https://doi.org/10.1016/S1359-6446\(02\)02498-4](https://doi.org/10.1016/S1359-6446(02)02498-4).

Tiwari, M. (2011). Science behind human saliva. *Journal of Natural Science, Biology and Medicine*, 2 (1), 53. Available from <https://doi.org/10.4103/0976-9668.82322>.

Torabi, S. and Soni, A. (2022). *Histology, Periodontium*.

Turovskiy, Y. et al. (2007). Quorum Sensing: Fact, Fiction, and Everything in Between. Available from [https://doi.org/10.1016/S0065-2164\(07\)62007-3](https://doi.org/10.1016/S0065-2164(07)62007-3).

Uppsala University (2014). Very low concentrations of heavy metals, antibiotics contribute to resistance. *ScienceDaily*. ScienceDaily, 7 October 2014. <www.sciencedaily.com/releases/2014/10/141007111231.htm>.

Vadakkan, K. et al. (2018). Quorum sensing intervened bacterial signaling: Pursuit of its cognizance and repression. *Journal of Genetic Engineering and Biotechnology*, 16 (2). Available from <https://doi.org/10.1016/j.jgeb.2018.07.001>.

Veloz, J.J., Alvear, M. and Salazar, L.A. (2019). Antimicrobial and Antibiofilm Activity against *Streptococcus mutans* of Individual and Mixtures of the Main Polyphenolic Compounds Found in Chilean Propolis. *BioMed Research International*, 2019. Available from <https://doi.org/10.1155/2019/7602343>.

Wanasathop, A. and Li, S. (2018). Iontophoretic Drug Delivery in the Oral Cavity. *Pharmaceutics*, 10 (3). Available from <https://doi.org/10.3390/pharmaceutics10030121>.

Wang, L. et al. (2015). Bacterial growth, detachment and cell size control on polyethylene terephthalate surfaces. *Scientific Reports*, 5 (1). Available from <https://doi.org/10.1038/srep15159>.

Wang, Y. et al. (2013). Inhibition of attachment of oral bacteria to immortalized human gingival fibroblasts (HGF-1) by tea extracts and tea components. *BMC Research Notes*, 6 (1), 143. Available from <https://doi.org/10.1186/1756-0500-6-143>.

Whitchurch, C.B. (2002). Extracellular DNA Required for Bacterial Biofilm Formation. *Science*, 295 (5559). Available from <https://doi.org/10.1126/science.295.5559.1487>.

Whiteley, M., Diggle, S.P. and Greenberg, E.P. (2017). Progress in and promise of bacterial quorum sensing research. *Nature*, 551 (7680), 313–320. Available from <https://doi.org/10.1038/nature24624>.

Whitman, W.B., Coleman, D.C. and Wiebe, W.J. (1998). Prokaryotes: The unseen majority. *Proceedings of the National Academy of Sciences*, 95 (12). Available from <https://doi.org/10.1073/pnas.95.12.6578>.

Wood, T.K., Knabel, S.J. and Kwan, B.W. (2013). Bacterial Persister Cell Formation and Dormancy. *Applied and Environmental Microbiology*, 79 (23). Available from <https://doi.org/10.1128/AEM.02636-13>.

Xu, R.-R. et al. (2018). An Update on the Evolution of Glucosyltransferase (Gtf) Genes in Streptococcus. *Frontiers in Microbiology*, 9. Available from <https://doi.org/10.3389/fmicb.2018.02979>.

Yadav, M.K. et al. (2020). Microbial biofilms and human disease: A concise review. *New and Future Developments in Microbial Biotechnology and Bioengineering: Microbial Biofilms*. Elsevier. Available from <https://doi.org/10.1016/B978-0-444-64279-0.00001-3>.

Yang, Y. and Tal-Gan, Y., 2019. Exploring the competence stimulating peptide (CSP) N-terminal requirements for effective ComD receptor activation in group 1 *Streptococcus pneumoniae*. *Bioorganic Chemistry*, 89, p.102987.

Yousra Turki et al. (2017). Biofilms in bioremediation and wastewater treatment: characterization of bacterial community structure and diversity during seasons in municipal wastewater treatment process. *Environmental Science and Pollution Research*, 24 (4). Available from <https://doi.org/10.1007/s11356-016-8090-2>.

Zhang, L. et al. (2020). Sensing of autoinducer-2 by functionally distinct receptors in prokaryotes. *Nature Communications*, 11 (1), 5371. Available from <https://doi.org/10.1038/s41467-020-19243-5>.

Zhang, Q. et al. (2017). Structure-Based Discovery of Small Molecule Inhibitors of Cariogenic Virulence. *Scientific Reports*, 7 (1), 5974. Available from <https://doi.org/10.1038/s41598-017-06168-1>.

Zhang, W. et al. (2015). Extracellular matrix-associated proteins form an integral and dynamic system during *Pseudomonas aeruginosa* biofilm development. *Frontiers in Cellular and Infection Microbiology*, 5. Available from <https://doi.org/10.3389/fcimb.2015.00040>.

Appendix

A) MIC for QQ molecules on *S. mutans* 25175 biofilm formed in 96-well plates.

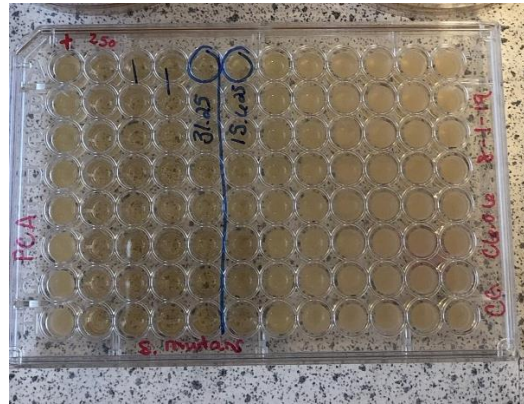


Figure 1: The MIC of p-coumaric acid on *S. mutans* 25175 biofilm

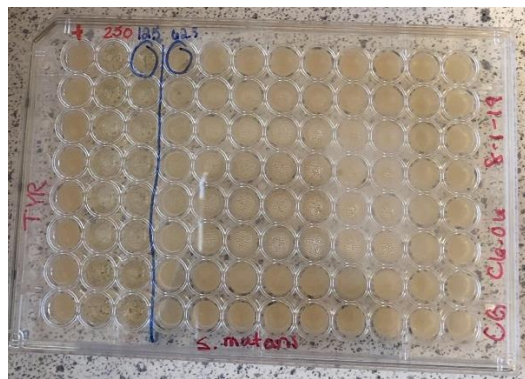


Figure 2: The MIC of tyrosol on *S. mutans* 25175 biofilm

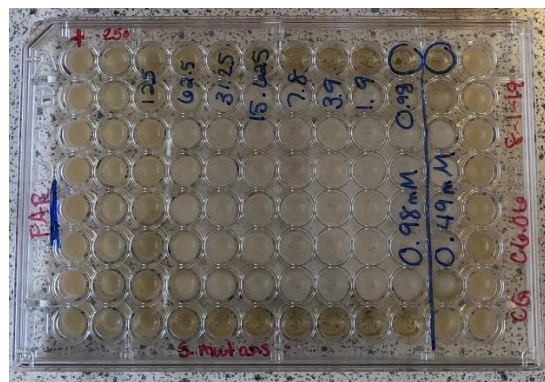


Figure 3: The MIC of farnesol on *S. mutans* 25175 biofilm

B) Standard Curves

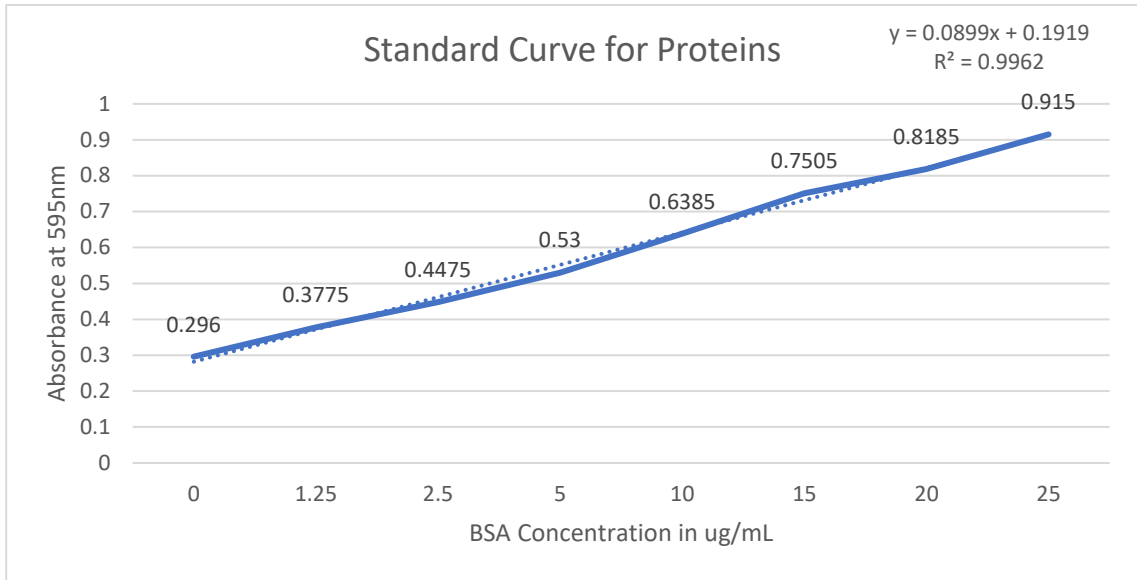


Figure 4: Bradford assay standard curve for proteins

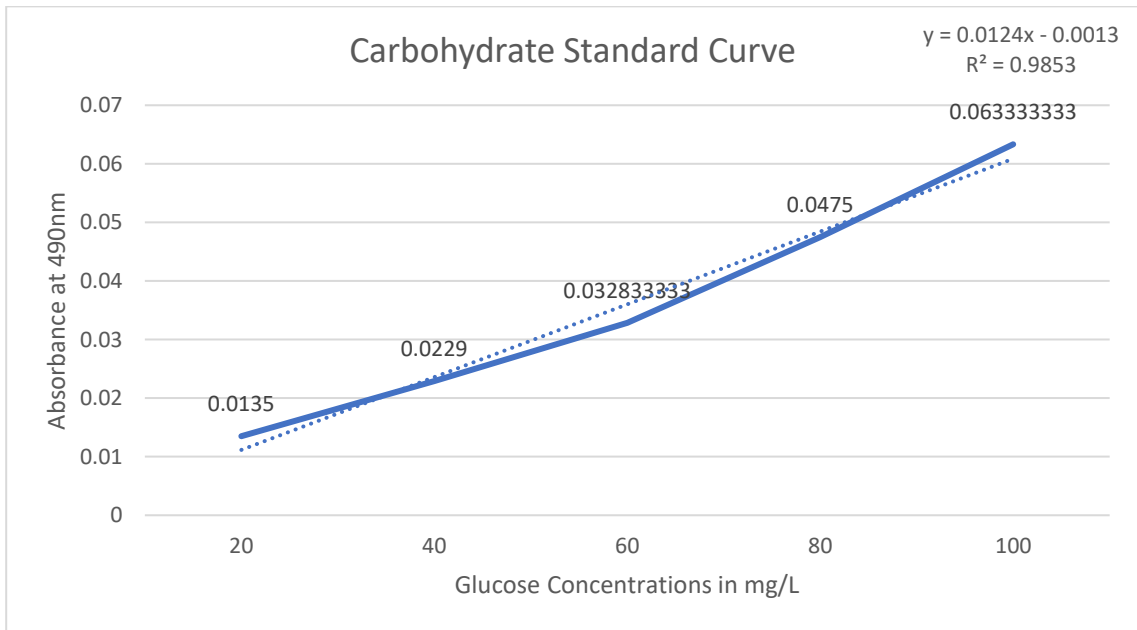


Figure 5: Phenol-sulfuric acid assay standard curve for carbohydrates